Universidad de Huelva

Departamento de Ingeniería Química, Química Física y Ciencias de los Materiales

Novel organoclay/isocyanate-based modification of bitumen for the development of high-performance composites

Memoria para optar al grado de doctor
presentada por:

Francisco José Ortega Bravo

Fecha de lectura: 12 de julio de 2017

Bajo la dirección de los doctores:

Francisco Javier Navarro Domínguez

Moisés García Morales

Huelva, 2017

UNIVERSITY OF HUELVA

Department of Chemical Engineering, Physical Chemistry and Materials Science

Ph.D. Thesis

NOVEL ORGANOCLAY/ISOCYANATE-BASED MODIFICATION OF BITUMEN FOR THE DEVELOPMENT OF HIGH-PERFORMANCE COMPOSITES

Francisco José Ortega Bravo

2017

UNIVERSITY OF HUELVA

Department of Chemical Engineering, Physical Chemistry and Materials Science

Ph.D. Thesis

NOVEL ORGANOCLAY/ISOCYANATE-BASED MODIFICATION OF BITUMEN FOR THE DEVELOPMENT OF HIGH-PERFORMANCE COMPOSITES

Francisco José Ortega Bravo

Doctoral Programme in Chemical Processes and Products

Supervised by:

Prof. Dr. Francisco Javier Navarro Domínguez

Prof. Dr. Moisés García Morales

2017

Universidad de Huelva
Escuela de Doctorado

AUTORIZACIÓN PARA LA DEFENSA DE LA TESIS DOCTORAL EMITIDA POR EL DIRECTOR Y EL TUTOR Y POR LA COMISIÓN ACADÉMICA DEL PROGRAMA DE DOCTORADO

DATOS DEL DOCTORANDO:

Apellidos y nombre: Ortega Bravo, Francisco José	NIF/NIE/Pasaporte: 48954932F	Nacionalidad: Español
Dirección a efectos de notificaciones: C/ Hermano Palomo; Blq.: 28, 2º A, 21006, Huelva		
Teléfono: 650517894	EMAIL: francisco.ortega@diq.uhu.es	

DATOS DE LA TESIS DOCTORAL:

Título: Novel organoclay/isocyanate-based modification of bitumen for the development of high-performance composites
Programa Oficial de Doctorado al que se adscribe y órgano responsable: Procesos y productos químicos; Dpto. de Ingeniería Química, Química Física y Ciencias de los Materiales
Línea de investigación a la que se adscribe y órgano responsable: Caracterización y procesado de productos derivados del petróleo; Dpto. de Ingeniería Química, Química Física y Ciencias de los Materiales
Rama de Conocimiento **(marcar casilla)**: ☐ Arte y Humanidades ☐ Ciencias ☐ Ciencias de la Salud ☐ Ciencias Sociales y Jurídicas ☐ Ingeniería y Arquitectura

A CUMPLIMENTAR POR EL DIRECTOR Y POR EL TUTOR DE LA TESIS DOCTORAL: (en caso de que el Director y Tutor sean la misma persona, no es necesario cumplimentar los campos relativos al Tutor ni se precisa la firma de éste).

Director/es:	**Tutor/es:**
Dr./Dra.: Fco. Javier Navarro Domínguez	Dr./Dra.:
Dr./Dra.: Moisés García Morales	Dr./Dra.:
Dr./Dra.:	Dr./Dra.:
como Director/Tutor de la Tesis Doctoral antes indicada **AUTORIZA** LA DEFENSA DE LA MISMA.	

En Huelva a, _____ de _____ de 2017

Firma del/los Director/es de la Tesis Doctoral

Fdo.: Fco. Javier Navarro Domínguez Fdo.: Moisés García Morales Fdo.:

Firma del/los Tutor/es de la Tesis Doctoral

Fdo.: Fdo.: Fdo.:

A CUMPLIMENTAR POR LA COMISIÓN ACADÉMICA DEL PROGRAMA DE DOCTORADO:

Cumplidos los criterios de calidad aprobados para este Programa de Doctorado por el Comité de Dirección de la Escuela de Doctorado de la Universidad de Huelva y una vez valorada la Tesis Doctoral presentada por el Doctorando y haber incorporado éste las modificaciones y/o cambios que esta Comisión Académica le pudiera haber indicado, **se AUTORIZA** en reunión de fecha _____ **LA DEFENSA** de la misma.

En Huelva a, _____ de _____ de _____

Firma y sello del Presidente de la Comisión Académica

Fdo. _____

ACKNOWLEDGEMENTS

This Thesis, which has enriched me so much in a multitude of aspects of my life, on both professional and personal levels, would not have been possible without the help and contribution from all the people around me, my colleagues, my friends, and above all, my family, who have made me become the person I am now. Amongst them, those who first saw some potential in me and offered me the opportunity to take on this challenging undertaking, relying on me and providing me with the guidelines and tools to pave my own path in pursue of the accomplishment of this Thesis, Professors Dr. Fco. Javier Navarro Domínguez and Dr. Moisés García Morales. For all of this, I first want to express my gratitude to both you, thank you two for your blind trust and support.

Undoubtedly, neither could such a work have been possible without the help and support from the rest of people from the Research Centre for Technology of Chemical Products and Processes (Pro2TecS), who have shared their valuable time and knowledge with me. Special mention deserve Professors Dr. Fco. José Martínez, Dr. Pedro Partal, Dr. J. M. Franco and Dr. Concepción Valencia; my colleagues, Dr. Mª. Ángeles Izquierdo, Dr. Rubén Sánchez, Mr. Muhammad A., Dr. Luis A. García, Dr. A.A. Cuadri, and Dr. J.E. Martín; and in general, those in the shared office, on the third floor of the Dept. of Chemical Engineering. Thank you all for your help and support.

I am also greatly grateful to Prof. Dr. Tony McNally, from the International Institute for Nanocomposites Manufacturing (IINM), at the University of Warwick (U.K.), for his always fruitful and keen contributions to my work, as well as for kindly allowing me to stay at the IINM and use its facilities. Special thanks go to a person who become a great friend, and largely facilitated things for me, my colleague Mr. Jaipal Gupta, for his inestimable help during my stay at the IINM.

Unforgettable are also all those moments I have lived with my friends, all of whom have somehow contributed to smooth the path for the completion of this work. Rubén and Esther, great, unconditional friends and a paramount support at any time. Luis V., Alberto, Cristina and Margarita, by my side when needed. Chan and Rocío C., whom I thank their talks and company. Gema, a trustworthy friend. Luis C., a knowledgeable friend about life. Lourdes and José, a companionable couple that provides

inherent affection. And last but not least, the person who has faithfully accompanied me, helped me out and put up with me along this entire process, my “sister-in-arms”, Rocío G. Thank you all for your company and support.

Definitely, I have to reserve my finest words to the most important people, those who are and have always been there unconditionally, my family. First, and above all, I have to thank my parents, whose support, efforts and teachings have made me the person I am. My father, Domingo, for having been by my side; and specially my mother, María, who has given it all to provide me with everything. My uncle, Pepe, and my aunt, Paqui, who have always cared about me like my parents. My faithful cousins, Andrés and Mariana, like siblings for me. And finally, a person who will always be with me, my grandmother, Pepa (1915-2017), who did her best to take care of me ever since the very first moment of my life, like a mother, with unlimited fondness and support. This Thesis is dedicated to her loving memory.

AGRADECIMIENTOS

Esta tesis, que tanto me ha enriquecido en multitud de aspectos de mi vida, a nivel tanto profesional como personal, no habría sido posible sin la ayuda y participación de todas las personas de mi entorno, mis compañeros, mis amigos, y sobre todo, mi familia, que han hecho de mí la persona que soy. De entre todos ellos, aquellos que en primer lugar vieron un cierto potencial en mí y me ofrecieron la oportunidad de emprender este proyecto, confiando en mí y dándome las pautas y herramientas con las que establecer mi propio camino hacia la compleción de esta Tesis, los Profesores Dr. Fco. Javier Navarro Domínguez y Dr. Moisés. Por todo ello, en primer lugar, quiero expresar mi gratitud a ambos, gracias a los dos por vuestra confianza y apoyo.

Sin duda alguna, este proyecto tampoco habría sido posible sin la ayuda y el apoyo del resto de las personas del Centro de Investigación en Tecnologías de los Procesos y Productos Químicos (Pro2TecS), quienes han compartido su valioso tiempo y conocimiento conmigo. Mención especial merecen los Profesores Dr. Fco. José Martínez, Dr. Pedro Partal, Dr. J M. Franco y Dra. Concepción Valencia; mis compañeros, Dra. Mª. Ángeles Izquierdo, Dr. Rubén Sánchez, D. Muhammad A., Dr. Luis A. García, Dr. A.A. Cuadri, y Dr. J.E. Martín; y en general, todos aquellos con los que he compartido espacio en la Sala Común de la tercera planta del Dpto. de Ingeniería Química. Gracias a todos por vuestra ayuda y apoyo.

He de agradecer también al Prof. Dr. Tony McNally, del International Institute for Nanocomposites Manufacturing (IINM), en la Universidad de Warwick (Reino Unido), por sus siempre efectivas y provechosas contribuciones al presente trabajo, así como por amablemente permitirme usar las instalaciones del IINM. Agradezco especialmente a mi compañero Jaipal Gupta su inestimable ayuda durante mi estancia en el IINM, resultando ser un gran amigo que hizo que todo fuese mucho más fácil para mí.

Inolvidables son también todos aquellos momentos vividos con mis amigos, que de una forma u otra han contribuido a facilitar el trayecto hacia la compleción de este proyecto. Rubén y Esther, grandes amigos incondicionales y un apoyo fundamental en todo momento. Luis V., Alberto, Cristina y Margarita, a mi lado cuando los he necesitado. Chan y Rocío C., a quienes agradezco sus conversaciones y compañía. Gema, una

amiga en la que se puede confiar. Luis C., un amigo instruido en la vida. Lourdes y José, una pareja que profesa afecto innato. Y por último, pero no por ello menos relevante, la persona que fielmente me ha acompañado, ayudado y sufrido durante todo este proceso, mi hermana de espíritu y lucha, Rocío G. Gracias a todos por vuestra compañía y apoyo.

Definitivamente, he de reservar mis palabras más especiales para las personas más importantes, aquellas que están y siempre han estado ahí incondicionalmente, mi familia. Primero, y por encima de todo, he de dar las gracias a mis padres, cuyo apoyo, esfuerzo y enseñanzas han hecho de mí la persona que soy. Mi padre, Domingo, por haber estado a mi lado, y especialmente mi madre, María, que lo ha dado todo para que no me faltara nada. Mi tío Pepe, y mi tía Paqui, que siempre se han preocupado por mi como unos padres. Mis fieles primos, Andrés y Mariana, unos hermanos para mí. Y finalmente, una persona que siempre estará conmigo, mi abuela, Pepa (1915-2017), que cuidó de mí de la mejor forma posible desde el primer momento de mi vida, como una madre, con cariño y apoyo ilimitados. Esta Tesis está dedicada a su memoria.

CONTENTS

Novel organoclay/isocyanate-based modification of bitumen for the development of high-performance composites

INTRODUCTION 1

1. Research Summary 3

2. Research Background 9

3. Research Objectives 12

4. Research Structure 13

LITERATURE REVIEW 15

1. Introduction 17

2. Bitumen nomenclature 19

3. Bitumen production 21

4. Bitumen manufacture 23

4.1. Air blowing 26

4.2. Solvent de-asphalting 27

4.3. Residue from visbreaking 27

5. Bitumen composition 28

6. Bitumen fractionation 30

6.1. Saturates 33

6.2. Aromatics 33

6.3. Resins 34

6.4. Asphaltenes 34

7. Association Models for Asphaltenes 36

7.1. The Yen model 36

7.2. The Yen-Mullins Model 37

7.3. Oligomer-like model 40

7.4. Supramolecular assembly model 43

8. Molecular structural models of bitumen 45

8.1. Colloidal model 45

8.2. Dispersed Polar Fluid (DPF) Model 47

8.3. Nanoaggregate-based Models 48

8.4. Modern Colloidal Model 50

9. Rheology fundamentals 51

9.1. Introduction 51

9.2. Classification of materials 53

9.3. Newtonian fluid behaviour 56

9.4. Non-Newtonian fluid behaviour 56

9.4.1. Shear-thinning fluid behaviour 57

9.4.2. Bingham plastic or viscoplastic behaviour 59

9.4.3. Shear-thickening or dilatant fluid behaviour 59

9.4.4. Time-dependent fluid behaviour- 60

10. Rheology of bitumen and structure-property relations 68

10.1. Steady state shear flow 68

10.2. Linear viscoelasticity 69

10.2.1. Newtonian-to-viscoelastic transition: α-relaxation 73

10.2.2. Viscoelastic-to-elastic transition: β-relaxation 74

11. Bitumen Modification 75

11.1. Polymer-based modification 79

11.1.1. Polymer modification mechanism 82

11.2. Isocyanate-based modification 84

11.2.1. Manufacture of isocyanates 84

11.2.2. The chemistry of isocyanates 85

11.2.3. Isocyanate-bitumen reactive interaction 92

11.3. Clay-based modification 94

11.3.1. Classification and structural properties of clays 95

11.3.2. Organo-modification of layered silicates 99

11.4. Bituminous Composites 105

11.4.1. Nanocomposite formation.....106

11.4.2. Types of nanocomposite structures.....112

11.4.3. Rheology of bituminous nanocomposites.....115

11.4.4. Properties of bituminous nanocomposites.....127

12. Bibliography.....133

MATERIALS AND METHODS.....153

1. Materials.....155

1.1. Bitumen.....155

1.2. Modifying agents.....155

1.2.1. Cloisite® 20A.....156

1.2.2. Polymeric MDI (4,4'-diphenylmethane diisocyanate)..157

2. Processing of samples.....158

2.1. Processing devices for bitumen modification.....158

2.2. Processing sequences.....159

2.2.1. Bitumen modification.....159

2.2.2. Reactive modification of Cloisite® 20A.....163

3. Technological characterization.....163

3.1. Penetration Test.....163

3.2. Ring and ball (R&B) softening point test.....164

4. Chemical Characterization.....166

4.1. Thin Layer Chromatography-Flame Ionization Detector analysis.....166

4.2. Fourier Transform Infrared Spectroscopy (FTIR).....167

5. Microstructural Characterization.....169

5.1. Atomic Force Microscopy (AFM).....169

5.2. X-ray Diffraction (XRD).....171

5.3. Optical Microscopy.....173

6. Thermal analysis 175

6.1. Modulated Differential Scanning Calorimetry (MDSC) 175

6.2. Thermogravimetric Analysis (TGA) 176

7. Rheological Characterization 178

7.1. Rheometers 178

7.2. Rheological tests 180

7.2.1. Steady-state viscous flow tests 180

7.2.2. Oscillatory shear tests 180

8. Bibliography 182

RESULTS AND DISCUSSION 185

1. Block 1 (article 1): 187

Thermo-mechanical behaviour and structure of novel bitumen/nanoclay/MDI composites 187

1.1. Abstract 187

1.2. Introduction 188

1.3. Experimental 191

1.3.1. Materials 191

1.3.2. Modified Binders 193

1.3.3. Modified Cloisite 20A® 194

1.4. Tests and Measurements 195

1.5. Results and Discussion 197

1.5.1. Effect of single addition of MDI and nanoclay on rheological properties 197

1.5.2. Combined effect of MDI and nanoclay on composite rheological properties 202

1.5.3. Chemical modification and microstructure of the nanoclay, bitumen and composites 206

1.6. Conclusions 215

1.7. References 216

2. Block 2 (article 2): 222

Effect of shear processing on the linear viscoelastic behaviour and microstructure of bitumen/montmorillonite/MDI ternary composites 222

2.1. Abstract 222

2.2. Introduction 223

2.3. Experimental 226

2.3.1. Materials 226

2.3.2. Processing devices and sequence for bitumen modification 227

2.3.3. Rheological Measurements and Material Characterisation 229

2.4. Results and Discussion 230

2.4.1. Linear viscoelastic behaviour 230

2.4.2. Linear and non-linear viscoelastic behaviour 238

2.4.3. Effect of shear processing 242

2.4.4. Differential scanning calorimetry and chemical composition 247

2.5. Conclusions 255

2.6. References 256

3. Block 3 (article 3): 264

Physico-chemistry control of the linear viscoelastic behaviour of bitumen/montmorillonite/MDI ternary composites: effect of the modification sequence 264

3.1. Abstract 264

3.2. Introduction 265

3.3. Experimental 268

3.3.1. Materials 268

3.3.2. Sample Processing 269

3.3.3. Characterization 272

3.4. Results and Discussion 274

3.4.1. Linear viscoelastic behaviour of the binary and ternary composites 274

3.4.2. Morphological and microstructural characterization. Physico-chemistry behind the linear viscoelastic behaviour observed 278

3.5. Conclusions 291

3.6. References 292

CONCLUSIONS 297

LIST OF PUBLICATIONS 307

LIST OF TABLES 347

LIST OF FIGURES 351

Chapter 1

INTRODUCTION

Novel organoclay/isocyanate-based modification of bitumen for the development of high-performance composites

1. Research Summary

Bitumen, by-product resulting from the vacuum distillation of crude oil, consists of a complex mixture of organic and inorganic compounds, comprising mainly aliphatic, aromatic and naphthenic hydrocarbons. Even though its composition greatly depends on the crude source and the refining process, it can be subjected to a basic characterization by its separation into two main fractions: maltenes and asphaltenes, normally described according to bitumen solubility in n-alkanes. Maltenes, in turn, can also be subdivided into saturates, aromatics and resins, showing in that order, increasing degrees of complexity, aromaticity, heteroatom content and molecular weight. Asphaltenes, on the other hand, correspond to solid black particles characterized by polar aromatic ring systems with highly condensed planar and heteroatom polar functional groups, constituting the most polar fraction of bitumen, and playing a major role in its viscoelastic properties. Accordingly, this classification leads to the general characterisation of bitumen on the basis of the so-called SARAs fractions.

Amongst bitumen properties, waterproofing, ductility, adhesiveness, and resistance to weathering and chemicals have favoured its development for a wide range of applications, mainly in the fields of pavement construction and roofing membrane manufacture. However, bitumen properties and mechanical behaviour are highly influenced by temperature, which may lead to several problems such as thermal cracking and rutting. Furthermore, external agents, mainly oxygen diffusion and UV radiation, may also induce ageing processes on bitumen, increasing its thermal susceptibility, and eventually provoking its premature failure.

In an attempt to overcome such issues, bitumen has normally been modified by the use of different types of additives, commonly polymers like SBS,

EVA, etc., which when added to bitumen and properly mixed improve its mechanical properties, decreasing its thermal susceptibility. However, many different problems arise from bitumen/polymer mutual thermodynamic incompatibility, which tends to provoke an eventual phase separation in such mixtures, with the subsequent loss of improvement in properties. Thus, specific technical conditions are usually required during manufacture to achieve suitable polymer dispersions in bitumen.

Interestingly, chemical modification by means of reactive polymers has shown to be an effective way to noticeably enhance bitumen properties. One of these reactive agents, polymeric MDI (a blend of diphenylmethane diisocyanate and its higher homologues) has allowed improving the thermorheological behaviour of the resulting products for different applications.

On the other hand, another kind of material, layered silicates (clays), has attracted the interest of both polymer and bitumen modifications, given the enhancement it may provoke on their properties when interacting at the nanometre scale. Nanoclays are naturally occurring minerals, mostly consisting of alumina-silicates with a layered structure, inherently inorganic. Nevertheless, when subjected to ion-exchange reactions with quaternary ammonium salts with alkyl chains, some clays might be rendered organophilic, thus, resulting compatible for their dispersion in clay layers within bitumen or polymers to produce nanocomposites.

Targeting at high performance materials for civil engineering applications, the optimisation of processing conditions that allow for the delamination of clay layers and production of tailored nanocomposites, with associated benefits in properties and characteristics, requires information on their rheological properties.

Accordingly, in this work, a further approach has been taken by preparing ternary bituminous composites consisting of an organically-modified montmorillonite clay, Closite 20A®, along with a reactive isocyanate-based oligomer, polymeric MDI. These two additives have been used to modify bitumen, both separately and jointly, resulting in binary and ternary systems that were studied in a twofold perspective. On the one hand, the influence exerted by different processing variables, such as shear and time, on the end thermo-mechanical properties. And on the other hand, the effects of those variables when combined with the reactivity of isocyanate groups in polymeric MDI. Thus, investigation has focused on factors behind the formation of a nanoreinforced structure in bitumen/clay binary systems, giving rise to a nanocomposite with improved thermo-mechanical performance, and to what extent the reactivity of isocyanate groups in ternary systems influenced such structure and performance. To proceed so, systems were subjected to a wide range of rheological tests, complemented by thermal, microstructural, and chemical studies, which allowed characterising the microstructural properties of the resulting composites and the chemical changes they underwent as a consequence of isocyanate-involved reactions, including the reactivity associated to each phase (bitumen and clay). Consequently, a deeper insight has been taken into bitumen/clay nanocomposites, and to the best of our knowledge, a first approach into the characterisation of isocyanate-modified bituminous/clay composites, and the influence of some major controlling variables on their end properties.

Resumen de la Investigación

El betún, subproducto de la destilación al vacío del crudo de petróleo, está constituido por una mezcla compleja de compuestos orgánicos e inorgánicos, principalmente de hidrocarbonos alifáticos, aromáticos y nafténicos. Aunque su composición depende en gran medida del origen del crudo y del proceso de refino utilizado, ésta se suele definir en base a la solubilidad en n-alcanos, resultando en la separación en maltenos y asfaltenos. Los maltenos, a su vez, pueden subdividirse en saturados, aromáticos y resinas, en orden creciente de complejidad, aromaticidad, contenido en heteroátomos y peso molecular. Los alfaltenos, por otra parte, corresponden a partículas sólidas caracterizadas por sistemas de anillos aromáticos polares con grupos funcionales planos, altamente condensados, y polares con heteroátomos, constituyendo así la fracción más polar del betún, e influyendo en gran medida en sus propiedades viscoelásticas. Así, esta clasificación define la caracterización composicional general del betún en base a las denominadas fracciones SARAs.

Entre las propiedades del betún, la impermeabilidad, ductilidad, adhesividad, y la resistencia a la climatología y a agentes químicos han favorecido su desarrollo para un amplio rango de aplicaciones, principalmente en los terrenos de la pavimentación y de las membranas impermeabilizantes. Sin embargo, la temperatura influye en gran medida sobre dichas propiedades y el comportamiento mecánico del betún, lo que puede producir problemas, como deformaciones y grietas. Asimismo, la acción de agentes externos, principalmente la difusión de oxígeno y la radiación UV, pueden inducir procesos de envejecimiento, incrementando su susceptibilidad térmica, provocando finalmente su fallo prematuro.

Con objeto de superar tal problemática, el betún se ha modificado tradicionalmente con diversos aditivos, generalmente polímeros como el SBS, EVA, etc., que cuando se mezclan adecuadamente mejoran sus propiedades mecánicas, disminuyendo su susceptibilidad térmica. No obstante, la existencia de cierta incompatibilidad termodinámica entre ambos puede conllevar a la separación de las fases, con el consiguiente deterioro de la mejora obtenida en las propiedades. De esta forma, el establecimiento de una adecuada dispersión del polímero en el betún generalmente requiere el uso de condiciones técnicas específicas.

En este sentido, la modificación química por medio de polímeros reactivos ha mostrado ser una técnica efectiva para la mejora de las propiedades del betún. Entre dichos compuestos, el MDI polimérico (una mezcla de diisocianato de difenilmetano y homólogos superiores) ha permitido obtener mejoras significativas en las propiedades termorreológicas de los productos resultantes para diferentes tipos de aplicaciones.

Por otra parte, otro tipo de material, los silicatos laminados (arcillas), ha centrado el interés de la modificación de polímeros y betunes, dada la mejora que puede producir en sus propiedades cuando interacciona a escala nanométrica. Las nanoarcillas son minerales naturales inorgánicos, principalmente constituidos por aluminosilicatos con una estructura laminada. No obstante, algunas nanoarcillas se pueden modificar mediante reacciones de intercambio iónico con sales de amonio cuaternario, permitiendo su conversión en organofílicos, lo que favorece su compatibilidad con el betún y los polímeros, y la separación de sus capas para producir nanocomposites.

Así, la producción de materiales de alto rendimiento para aplicaciones de ingeniería civil implica la optimización de las condiciones de procesado,

de tal forma que posibiliten la separación de las capas de aluminosilicatos, permitiendo la producción de nanocomposites con características específicas, lo que requiere información sobre las propiedades reológicas.

De esta forma, en este trabajo se ha abordado la modificación del betún mediante la preparación de composites bituminosos ternarios con una montmorillonita organomodificada , Cloisite 20A®, y un oligómero reactivo de base isocianato, MDI polimérico. Estos dos aditivos se usaron por separado y conjuntamente, resultando en sistemas binarios y ternarios, estudiándose sus efectos desde una perspectiva dual. Por una parte, la influencia ejercida por diferentes variables de procesado, como la cizalla y el tiempo, sobre las propiedades termo-mecánicas finales. Y por otra parte, los efectos de estas variables en combinación con la reactividad de los grupos isocianato del MDI polimérico. Así, la investigación se ha enfocado en los factores que influyen en la formación de una estructura nanoreforzada en sistemas binarios betún/arcilla, para dar lugar a nanocomposites con un comportamiento termo-mecánico mejorado; y en el nivel de influencia que ejerce la reactividad de los grupos isocianato en sistemas ternarios sobre dicha estructura y el comportamiento del material. Para ello, los sistemas se sometieron a numerosos ensayos reológicos, complementados por estudios térmicos, micro-estructurales y químicos, que posibilitaron caracterizar las propiedades micro-estructurales de los composites resultantes, y los cambios químicos derivados de la reactividad de los isocianatos, incluyendo su interacción con cada una de las fases (betún y arcilla) Por tanto, ello constituye una profundización en el conocimiento sobre los nanocomposites de betún y arcilla, y de cuanta constancia se tiene, una primera incursión en la caracterización de composites de betún y arcilla modificados con isocianatos, y en la

influencia que ejercen algunas de las principales variables de procesado sobre sus propiedades finales.

2. Research Background

Current world's industrial and technical development demands materials that provide the best possible performance and durability specifications without compromising sustainability, as well as cost-effectiveness. Bitumen, as an organic material with an ample variety of uses in engineering and building-related applications, mainly providing waterproofing, moisture resistance and corrosion protection, has also been required to fulfil, performance-wise, increasingly greater demanding characteristics (e.g. adhesion, temperature sensitivity, friction properties, oxidation resistance, aging resistance and durability). Besides these requirements, bitumen nature makes it prone to undergo several temperature-related problems, such as thermal cracking and rutting; and ageing processes, mainly as a consequence of oxygen diffusion and UV radiation, which further increase its thermal susceptibility, and may lead to premature failure.

In order to overcome those drawbacks and to enhance bitumen properties, different approaches have been followed, like its simple oxidization, which provokes the alteration of its chemical characteristics, causing some hardening, and so, increasing its suitability for waterproofing and high temperature application. However, the enhancement provided by this type of modification is generally insufficient to satisfy requirements imposed by current industry. This has hence led to the application of further procedures that principally involve the use of additives. In this sense, any compound, in order to be suitable as a modifying agent, should be easily blended with bitumen, yielding a bituminous system highly stable on storage, and

viscous enough at in-service temperatures to avoid its mechanical degradation. With that aim, various resins, rubbers, polymers, sulphur, metal complexes, fibres and chemical agents have been used for bitumen modification. Amongst them, polymers have largely become the most widely used additives for the modification of bitumen, having SBS and EVA as major exponents. This, though, does not mean that polymer modification lacks shortcomings, especially those concerning processing conditions and high-temperature storage stability, associated to two crucial operations in bitumen applications. Such issues find their foundation in an inherent thermodynamic incompatibility between phases (polymer and bitumen), in some cases attributed to a difference in density, which ultimately tends to promote their separation.

Minimization of their degree of incompatibility has been addressed by means of different procedures, including the chemical modification of the polymer to increase its affinity with bitumen, or the addition of a third component in the system that somehow acts as a compatibilizer. Even though those measures have been effective to some extent, there still exists a certain degree of phase instability, with some tendency to fail in high temperature applications, accompanied by other problems like polymer degradation or aging. Eventually, high cost, technical limitations, and certain lack of performance lead to unfulfilled requirements for bitumen application.

In a different approach, reactive polymers, e.g. MDI and random terpolymers of ethylene (RET), have also been used for bitumen modification, and contrarily to other types of polymers, they noticeably improve high temperature properties, contrasting with poor performance in the low temperature range though. They may also provoke some problems

like bitumen gelation, associated to an excess of reactivity, which renders modified bitumen unworkable.

In recent years, nevertheless, nanotechnology, which had already gained attention in other areas of science and technology, has gradually been incorporated into the field of modified bitumen. The use of nanotechnology, and hence nanomaterials, offers a superior insight into the possibilities of bitumen modification, as phenomena associated to the atomic and molecular levels are used to influence or control materials' macroscopic properties. For that purpose, some materials exhibiting nanoscale characteristics, such as clays, have been added to bitumen, providing noticeable enhancements at very low dosages, if compared to other types of additives. Furthermore, clays are naturally occurring materials, which translates to high cost-effectiveness and sustainability.

Bearing that in mind, several attempts have been made in the use of clays as a third component in polymer-modified bitumens, acting somehow as a compatibilizer between both phases, as it helps reduce the density difference between them. In this regard, obtaining significant enhancements in properties with the use of clay requires the structural modification at the nanometre scale, and thus, clay delamination, which is difficult to achieve in the presence of polymers like SBS. Only slight improvements have been obtained in low temperature properties, unlike aging resistance and storage stability, which may result significantly enhanced.

On account of this, and envisaging a new pathway for further progress in bitumen modification, the present work constitutes a different incursion into that field by jointly using a clay and a reactive polymer (an isocyanate-based oligomer termed polymeric MDI) for the modification, pursuing to

combine the nanoscale tailoring capabilities of the former (physical modification) with the reactivity of the latter (chemical modification). This opens a new modification path in which clay nanoscale characteristics can be used to promote the reactive effects of polymeric MDI and its interaction with bitumen, cooperating synergistically to maximize the degree of modification and improvement in a wider range of properties and conditions.

3. Research Objectives

The present Thesis is mainly focused on the development of an initial approach for the formulation of isocyanate modified clay/bitumen composites with enhanced thermo-mechanical properties by means of the addition to neat bitumen of an organically-modified clay, Cloisite® 20A, and an isocyanate-based oligomer, polymeric 4,4', diphenylmethane diisocyanate (polymeric MDI).

With that aim, a first step on the study of ternary bituminous composites consists on the evaluation of the effects that both individual and joint addition of those two additives exert on bitumen's properties and performance, in order to elucidate the mechanisms behind such modification.

In the preparation of composites, shear constitutes a paramount variable for the adequate dispersion of clay, which results a determinant factor for the end structural properties and performance of composites. Therefore, a second goal is targeted at assessing the influence on the composites' end properties of the type of processing, which is directly related to the shear applied. Moreover, given the use of a reactive additive, the effects of shear on reactive processes arising from such an additive also constitute a further relevant goal to investigate.

Finally, with a view to complement and optimize the group of crucial variables controlling the end properties of a given ternary bituminous composite formulation, the influence of processing time, both in presence and in absence of the reactive additive; and the order of addition of both additives to neat bitumen are also targeted as major goals to evaluate in this work.

4. Research Structure

The present work is organized into five chapters, each focused on a specific topic and all of them interrelated to make up the backbone of the entire investigation. Accordingly, every chapter is briefly described as follows:

Chapter 1. Introduction, which provides a necessary background to frame the present study into high performance requirements of bitumen industry, accompanied by a summary of the development of the investigation and its main goals.

Chapter 2. Literature review, comprising a wealth of information on the industry of bitumen, its production and its physico-chemical characterization, complemented by the description of the main additives used for bitumen modification, emphasizing those related to isocyanates and clays. Main rheological properties of the resulting modified bitumens are also outlined.

Chapter 3. Materials and methods, which includes the description of the materials used, the processing sequences followed for the preparation of the different systems studied, and a full classification of equipment utilized for the rheological, thermal and microstructural characterization of such systems.

Chapter 4. Results and discussion, this part of the work is further divided into three blocks, each corresponding to an article published in a high impact peer-review scientific journal and focusing on different aspects of the work carried out. Thus, Block 1 refers to the evaluation of the effects associated to the individual and combined addition of the modifying agents to bitumen. Block 2, on the other hand, comprises the study of the influence of shear on the bituminous systems' end properties, involving both a physical and chemical perspective. And, finally, Block 3, relates to the evaluation of two additional processing variables, corresponding to the order of addition of the modifying agents, and the duration of processing, assessing their effects on the systems' performance.

Chapter 5. Conclusions, which gathers the most remarkable facts derived from the experimental results obtained in this research.

Chapter 2

LITERATURE REVIEW

Novel organoclay/isocyanate-based modification of bitumen for the development of high-performance composites

1. Introduction

Bitumen is the oldest known engineering material and as such, it has been used from the earliest times as an adhesive, sealant and waterproofing agent. Its formation stems from the degradation of organic material incorporated and preserved in sediments. After its migration out of source rocks, petroleum accumulates in reservoirs at depth. These oil-stained reservoirs may be affected by active tectonic activities, for instance, those related to the formation of mountains, and can release their stored bitumen through cracks and faults. Bitumen may then find its way to surface and seepage may occur, appearing through fractures or with water flow in the form of natural bitumen and mineral matter. Impregnated reservoirs may also be outcropping at the surface through uplifts. These sources are not restricted to single seepages, but enclose an area where bitumen can be extracted at many locations (Connan and de Velde 2010).

Historically, bitumen was first used as a hafting material and for coating basketry, during the Hummalian period, 180,000 years ago in the El Kowm Basin in Syria, where it was applied to stick flint implements to the handles of various tools in a way that persisted until Neolithic time. Further on in time, its use as a building mortar and coating of waterproof structures was incorporated in architecture by the Sumerians, whose empire existed from around 3500 BC to approximately 2000 BC, in areas where abundant resources were available. Among others, bitumen was applied on the outside of buildings (e.g. rooftops and other structures such as the ritual bath at Mohendjo-Daro), in the interior of rooms (such as the bathrooms at the Mari palace), and in reed mats, which were coated with bitumen and used as flooring or to waterproof roofs.

Even the Bible cites examples such as in Genesis, Noah's ark is "pitched within and without with pitch", and Moses' juvenile adventure is in "an ark of bulrushes, daubed with slime and with pitch". More perplexing are the descriptions of the building of the Tower of Babel, which state that "they used bricks for stone and bitumen for mortar" (Connan 1999).

Bitumen was also extensively used to seal pottery and for the caulking of ships, as bitumen coating protected the ships against mechanical damage and waterproofed the hull. Nevertheless, this bituminous coating was not permanent and ships often had to be recaulked during their travels.

Medical uses have also been reported, with bitumen acting as a remedy for various illnesses (trachoma, leprosy, gout, eczema, asthma ...), as a disinfectant or as an insecticide (Connan 1999). Another well-studied historical application was for the embalming of mummies by the Egyptians.

As for road construction, the first mention of use of bitumen dates back to Nabopolassar, King of Babylon (625–604 BC): a bitumen-containing mortar cemented both the foundation made of three or more courses of burnt bricks and the stone slabs put on top. It is also believed that his oldest son and successor, Nebuchadnezzar, was an able exponent of the use of bitumen, because there is also evidence that he used the product for waterproofing the masonry of his palace and as a grout for stone roads.

Besides these uses, bitumen is attested in numerous examples of small artefacts: beads, spindle whorls, stoppers, as a black pigment for the painting and decoration of pots, bowls, etc. (Lesueur 2009).

The ancient uses of "natural" bitumen, natural deposits consisting of natural bitumen and mineral matter undoubtedly continued in those

inhabited parts of the world where deposits were readily available. However, there seems to have been little development of usage elsewhere.

Bitumen essentially disappeared from the pavements until the early 19th century, when the rediscovered European sources of natural bitumen, in the form of an asphaltic limestone, in Seysselin France and Val de Travers in Switzerland, with bitumen contents of 8 wt.% and 12 wt.%, respectively, led to the development of the modern applications for this material. The reference material for paving applications in the USA at the beginning of the 20th century were mostly the Trinidad Lake asphalt, containing 39 wt.% bitumen, 33 wt.% emulsified water and 27 wt.% mineral matter in the form of colloidal clay, and to a lesser extent, the Bermudez Pitch Lake asphalt from Venezuela, with 64 wt.% bitumen, 30 wt.% water, 4 wt.% insoluble organic matter and 2 wt.% dispersed mineral matter (Lesueur 2009). Both of which constitute some of the largest natural bitumen deposits in the World. The use of natural bitumen in road construction started to decay in the 1910s with the advent of vacuum distillation, which made it possible to obtain artificial bitumen from crude oil, and nowadays, paving grade bitumen is almost exclusively obtained as the vacuum residue of petroleum distillation.

2. Bitumen nomenclature

Petroleum bitumen is known by different names throughout the world.

The nomenclature for bituminous materials has been handed down from antiquity and the derivation of the modern terms asphalt and bitumen is difficult to determine with certainty. Ancient writings often consist of vague descriptions of materials, as for example, asphalt, pitch or bituminous earth, and lacked essential technical detail such as the form or

composition of the materials which would aid in identifying the types of materials used.

It is widely believed that the term "bitumen" originated in Sanskrit, in which "jatu" means pitch and "jatu-krit" means pitch creating. The terms referred to the pitch produced by some resinous trees. The Latin equivalent is claimed by some to be originally "gwitu-men" (pertaining to pitch) and by others to be "pitxu-men" (bubbling pitch), which was subsequently shortened to "bitumen", then passing via French into English.

Even today, the meanings of the words bitumen, tar, asphalt and pitch vary between users.

Another semantic confusion arises from the difference in meaning of the word "asphalt" in Europe and North America. In Europe, asphalt is typically used to refer to a mixture of bitumen and mineral aggregate, e.g. rolled asphalt, mastic asphalt, Gussasphalt, etc. However, in North America, the term "asphalt" is used for bitumen, "asphalt concrete" means asphalt road surface and "asphalt binder" refers to bitumen binder.

The term "bitumen" in Europe is synonymous with the term "asphalt", or "asphalt binder" used in North America.

In this document, the term bitumen will be used in the European sense throughout, in accordance with the current European specifications (EN 12597), which define bitumen as a *"virtually involatile, adhesive and waterproofing material derived from crude petroleum, or present in natural asphalt, which is completely or nearly completely soluble in toluene, and is very viscous or nearly solid at ambient temperatures*".

3. Bitumen production

Estimations indicate a current world production of bitumen of nearly 100 Million tonnes, with more than 250 applications, mostly within the frame of paving and roofing. In this regard, around 85 % of the production is essentially used as a binder for mineral aggregates in asphalt pavements for roads, airports, etc. Another 10 % of the bitumen production is allocated for the roofing industry in shingles, cold applied roll roofing, hot applied built up roofing, etc. The rest of the production, roughly accounting for a 5 % of the total, is related to a wide range of small volume applications, such as water pipe coating, paints, waterproofing and sealing materials (Asphalt Institute and Eurobitume 2015).

Crude oil is a natural mixture of hydrocarbons, generally in the liquid state, which may also include compounds of sulphur, nitrogen, oxygen, metals and other elements. Hydrocarbons are molecules that contain only the elements of carbon and hydrogen. According to the dominant type of hydrocarbon chains, crude oil is commonly classified as: paraffin base, naphthenic base, aromatic base, mixed base (Hsu and Robinson 2007; Lesueur 2009).

Paraffinic crude oil contains paraffin wax and practically no asphalt or naphthenes. Paraffins are saturated hydrocarbons, straight or branched chains but without any ring structures. The paraffin series of hydrocarbons is characterized by the rule that the carbon atoms are connected by a single bond and the other bonds are saturated with hydrogen atoms. The general formula for paraffins is C_nH_{2n+2} (Hsu and Robinson 2007).

Naphthenic crude oil contains mainly (by volume) naphthenes and other aromatic hydrocarbons completely without paraffin. Naphthenes are defined as saturated hydrocarbons with one or more rings and these

hydrocarbons may have one or more paraffinic side chains. It is a closed group of saturated ring of the general formula C_nH_{2n} (Hsu and Robinson 2007).

Aromatic crude oil has an unsaturated ring compound having a basic 6-carbon-atom ring with either a hydrogen atom or a chain joined to each carbon atom. The aromatic group of the general formula is C_nH_{2n-6}. The aromatic series of hydrocarbons are chemically and physically very different from the paraffin base and naphthenic base crude oil. Aromatic hydrocarbons contain a benzene ring which is unsaturated but very stable and frequently behaves as a saturated compound (Hsu and Robinson 2007).

Generally, paraffin base crude oil is not suitable for the production of bitumen, because of the lack of a sufficient amount of asphaltenes. Nevertheless, paraffin crude oil mixed with the naphthenic crude oil can be the basis for the production of bitumen; whilst aromatic crude oil is more suitable for chemical reagents. Therefore, naphthenic and naphthenic-paraffinic base crude oils are the best for bitumen production.

Another way to classify crude oils is by their density: light, medium, heavy and extra heavy. Some crude oils, such as those in the original Pennsylvanian oil fields of the U.S.A., consist mainly of paraffin. Others, such as the heavy Mexican and Venezuelan crude oils, are predominantly naphthenic and rich in bitumen. Russian crude oil is mixed-base (paraffinic and naphthenic), and consequently, has less asphaltenes and more resins. Heavy crude oils tend to be more aromatic/naphthenic, whereas lighter crude oils are more paraffinic. Light crude oil (e.g. Nigeria Bonny) is a low-viscous material with low density, and so, it tends to produce higher amount of light fractions, such as gasoline, kerosene and gas oil, than a heavy crude

oil. Usually, it may also have a small amount of paraffin, requiring some oxidation when used for bitumen.

Heavy/extra heavy crude oil (e.g. Boscan Venezuela) is a very viscous material with a high specific density. This type of crude oil presents a high sulphur content, which can be found in organic and inorganic compounds, and may exert a negative influence on bitumen properties. Moreover, it contains less light fractions and more naphthenic and aromatic hydrocarbons if compared to a light crude oil, as well as more heteroatoms of nitrogen, sulphur, oxygen and heavy metals. For these reasons, the processing of heavy oil requires special manufacturing techniques.

As a result, the appropriate selection of crude oil for bitumen production depends on the specific gravity, carbon and sulphur contents, as well as those of wax and asphaltene.

4. Bitumen manufacture

Currently, bitumen is essentially obtained from crude oil by distillation. As crude oil is a complex mixture of hydrocarbons differing in molecular weight and, consequently, in boiling range, it has to be separated, purified, blended and, sometimes, chemically or physically changed before being used (Read and Whiteoak 2003).

Not every crude oil yields sufficient amounts of bitumen, and only about one tenth of the available petroleum is found suitable. As a rule of thumb, the heavier the crude oil, the higher its bitumen yield (Read and Whiteoak 2003; Lesueur 2009).

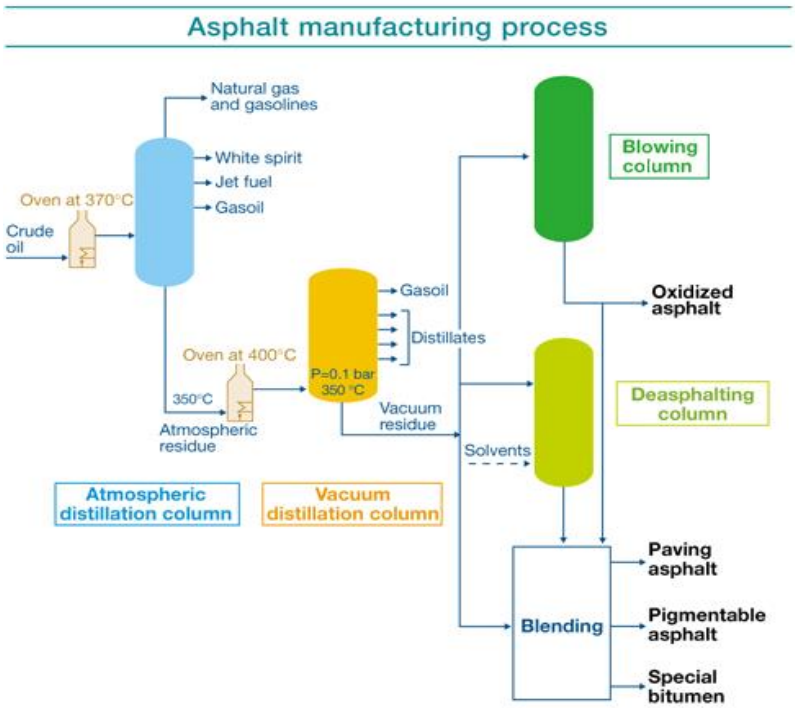

Fig. 2.1. Bitumen manufacturing process

The typical distillation process, as illustrated in Fig. 2.1, consists on a fractional distillation at atmospheric pressure, which allows separating the light components; followed by a vacuum distillation, in order to remove the last traces of lighter fractions, avoiding any unwanted thermal transformation of the compounds. Crude oil is heated up to 350 – 380 ºC and passed into the lower part of a distillation column operating at a pressure slightly above atmospheric. The material entering the column is a mixture of liquid and vapour, with the liquid comprising the higher boiling point fractions, and the vapour the lower boiling point ones. Thus, the lightest fractions will remain as vapour and are taken from the top of the distillation column; heavier fractions, which will remain as liquids, are taken off the column as side-streams; and the heaviest fractions, also remaining as liquids, leave the column at the base. The lightest fractions obtained from the crude distillation process include propane and butane,

both of which are gases under atmospheric conditions. Naphta, a slightly heavier material used as a feedstock for gasoline production and the chemical industry, is obtained moving down the column. The following one is kerosene, mainly used for aviation fuel, and further down the column, gas oil, a heavier fraction used as a fuel for diesel engines and central heating. Finally, the heaviest fraction produced from crude oil distillation is the so-called long residue, a complex mixture of high molecular weight hydrocarbons that requires further processing before it can be used as a feedstock for bitumen manufacture.

In a second step, the long residue is further refined at a slightly higher temperature (350 – 425 °C) but under vacuum, with pressures ranging 1 – 10 kPa (0.01 – 0.1 bars) in order to avoid cracking or thermal decomposition, which would occur at higher temperatures under atmospheric pressure conditions. The products of this distillation correspond to gas oil, distillates and short residue, also called "straight-run" bitumen, which corresponds to an equivalent atmospheric cut-point of typically 500 °C, and its properties depend on the crude origin and operating conditions (temperature and pressure). The resulting material might be further used as a feedstock in the manufacture of several other grades of bitumen. Generally, refineries manufacture only two grades of bitumen, a soft one and a hard one, and the intermediate grades are obtained by blending. Nevertheless, new vacuum distillation columns with structured packing internals have allowed obtaining harder grades by distillation, sometimes referred to as special bitumens, a concept which tends to include another product known as multigrade bitumen, which exhibits a wider operating temperature range and can be obtained not only through new refining processes, but also through acid modification.

Depending on the specification grade requirements, the vacuum residue can be used either directly, further processed, or used as a component of blended bitumen, in which products with different viscosities are blended in suitable proportions to satisfy final specifications.

In case of further processing, several processes can be applied to modify bitumen properties, such as penetration, stiffness or viscosity, in order to meet the required technical specification for a certain application.

4.1. Air blowing

This process, developed in the late 19th century, consists on an oxidation of bitumen by passing air through it at a volumetric flow rate of 85 – 140 m^3/min (Asphalt Institute and Eurobitume 2015) for a few hours at 240 – 320 °C (Read and Whiteoak 2003). A catalyst, such as copper sulphate, zinc, ferric or alumina chloride, boric acid or phosphorous pentoxide, can also be used to increase the speed of reaction and improve temperature susceptibility of the product (Lesueur 2009). The application of this process involves the development of oxidation, dehydrogenation and polymerization reactions, provoking an increase in the apparent molecular weight and polarity of bitumen, accompanied by a rise in the asphaltenic fraction (Read and Whiteoak 2003). This ultimately results in a reduction in penetration, along with a greater softening point and lower thermal susceptibility. The end properties of the resulting material, called "air-blown" or "oxidized" bitumen, depend on the crude origin (or the soft bitumen) and the operating conditions, especially blowing temperature and time. It remains the best process to make very hard bitumens, especially for waterproofing. For paving applications, however, air-blown bitumens were discarded because they were too susceptible to cracking. In certain cases, bitumen is subjected to a process termed semi-blowing or air rectification,

in which a limited amount of air blowing is applied in order to make minor adjustments to bitumen's physical properties (Read and Whiteoak 2003; Asphalt Institute and Eurobitume 2015). The resulting bitumen, so-called "semi-blown" or "air-rectified" bitumen, is predominantly used in paving applications, although other uses are also possible, such as roofing, industrial coatings and the production of polymer modified binders and bitumen emulsions (Asphalt Institute and Eurobitume 2015).

4.2. Solvent de-asphalting

This process developed in the 1930s as an alternative for vacuum distillation, proved to be less industrially successful, although it remains the preferred method for recovering lubricants, with bitumen as a by-product (Lesueur 2009).

The process is carried out under supercritical conditions by mixing the vacuum residue with 3 to 10 times its volume of liquefied propane, butane, isobutene or pentane to separate asphaltene-type fractions from residue (Lesueur 2009; Asphalt Institute and Eurobitume 2015). Then, the system is left to settle and bitumen is recovered as the solvent-free precipitate, which can be blended to produce a specific grade bitumen; whilst the other stream, deasphalted oil, is used for producing lubricating oil base stocks (Asphalt Institute and Eurobitume 2015).

4.3. Residue from visbreaking

Bitumen can also be obtained as a residue from a visbreaking unit. The visbreaking process is a mild thermal cracking operation by which the viscosity of residues or heavy oils can be reduced to meet specifications.

During visbreaking, operation conditions are optimised so that long paraffinic side chains attached to aromatic rings, considered the primary

cause of the high pour point and viscosity in residue streams, are broken off and subsequently transformed to form shorter molecules with lower viscosity and pour point (Asphalt Institute and Eurobitume 2015). Temperatures applied range from 455 to 510 ºC, under pressures between 0.3 and 2 MPa (3 – 20 bars), with residence times of 1 – 3 min. These short residence times are the main factor behind the concept of being a mild thermal reaction, as reactions are not allowed to proceed completely (Speight 2014). When used for bitumen production, the residue is subjected to vacuum distillation to remove the distillate fractions, which are further treated for the production of fuels (mainly naphtha and gas oils). Finally, a hard material is generally obtained as a residue from vacuum distillation, which can then be used as a blending component for bitumen production (Asphalt Institute and Eurobitume 2015).

5. Bitumen composition

The chemical composition amongst bitumens is quite similar, with some variations depending upon factors such as the source of crude oil from which it originates, the manufacturing process applied during refining and blending, and ageing.

In general, bitumen can be described as a complex chemical mixture of molecules that are predominantly hydrocarbons with a small amount of structurally analogous heterocyclic species and functional groups containing sulphur, nitrogen and oxygen atoms. Sulphur and nitrogen hetero-atoms occur largely in stable ring configurations, with the former being generally the most present polar atom in the form of sulphides, thiols and, to a lesser extent, sulfoxides; whilst the latter, nitrogen, not as common, being typically found in the form of pyrrolic structures, such as those in pyrrole, indole and carbazole compounds; or in pyridinic

structures, forming amphoteric species such as 2-quinolones. In the case of oxygen, it is mainly present in functional groups in the form of ketones, phenols and, to a lesser extent, carboxylic acids and esters (Read and Whiteoak 2003; Asphalt Institute and Eurobitume 2015). Bitumen also contains trace quantities of metals such as vanadium, nickel, iron, magnesium and calcium, which occur in the form of inorganic salts and oxides or in porphyrin-like structures. Elementary analysis of bitumens manufactured from a variety of crude oils shows the following composition (Read and Whiteoak 2003):

- Carbon 82 – 88 wt.%
- Hydrogen 9.8 – 10.8 wt.%
- Sulphur 0.9 – 6.6 wt.%
- Oxygen 0.4 – 1.0 wt.%
- Nitrogen 0.2 – 1.2 wt.%
- Nickel 10 – 139 ppm
- Vanadium 7 – 1590 ppm
- Iron 5 – 147 ppm
- Manganese 0.1 – 3.7 ppm
- Calcium 1 – 335 ppm
- Magnesium 1 – 134 ppm
- Sodium 6 – 159 ppm

Hence, the sum of carbon and hydrogen contents corresponds to a total concentration of hydrocarbons generally greater than 90 wt.%, with an hydrogen-to-carbon molar ratio (H/C) around 1.5, resulting in a value which is intermediate between that of aromatic structures (H/C = 1 for benzene) and that of saturate alkanes (H/C ≈ 2). The data also show that, according to the concentration of polar atoms, functional groups generally

do not amount for more than a few 0.1 mol/L for straight-run bitumens, although this value may increase as a consequence of ageing.

The composition of bitumen, especially concerning the content of molecules with hetero-atoms, is certainly of great importance in relation to its physico-chemical properties. The presence of sulphur, nitrogen, oxygen or metals in some molecules makes them slightly polar, conferring on them the ability to form molecular associations, and defining how these develop within bitumen and with other materials. Thus, despite the minimal heteroatomic content normally present in bitumen, these atomic species greatly influence its properties and performance (Asphalt Institute and Eurobitume 2015).

6. Bitumen fractionation

The physico-chemical properties of the species present in bitumen largely define the configuration of its internal structure. As reported in the literature (Petersen et al. 1994; Read and Whiteoak 2003), typical number-average molecular weight values for bitumen fall within the range of 600 – 1500 g/mol, depending on the experimental procedure applied (Domin et al. 1999). In accordance with the proportion of polar atoms, this yields an average ratio of 1 – 3 polar atoms per bitumen molecule.

Nevertheless, current techniques are not capable of providing accurate information on bitumen's molecular composition within the entire range of molecular weight distributions (Domin et al. 1999), nor is it easily attainable to relate these to the properties of bitumen, resulting extremely laborious and impractical. Thus, a different approach is applied when analysing and studying bitumen composition. It is generally subjected to a separation into different chemical families of fractions, based upon their size and solubility in polar, aromatic or non-polar solvents.

Several methods are available for the fractionation of bitumen (Read and Whiteoak 2003):

- Solvent extraction
- Chromatography
- Adsorption by finely divided solids and removal of non-adsorbed solution by filtration
- Molecular distillation, used in conjunction with one of the above techniques.

Solvent extraction and chromatography are the most used techniques. The former is relatively fast, but the quality of the separation provided is generally poorer than that resulting from chromatography, where solvent effect is combined with selective adsorption. Analogously, simple adsorption methods lack the effectiveness of column chromatography-based techniques, in which an eluting solution, used to remove an adsorbed substance by washing, is constantly re-exposed to fresh adsorbent and to different equilibrium conditions as it moves down the column. As for molecular distillation, its lengthiness and limitations in terms of the extent of which type of high molecular weight components of bitumen can be affected render it undesirable.

Therefore, chromatographic techniques have been the most widely used ones for defining bitumen constitution. In fact, such techniques were used on bitumen as early as 1908, and have evolved to become the current reference method, the elution-adsorption liquid chromatography on active alumina with solvents of increasing polarity and aromaticity (Lesueur 2009). The characterization of bitumen based on chromatographic separations describe the composition in terms of weight percent concentrations of operationally defined fractions. The method, initially

proposed by Corbett (Corbett 1969), firstly uses n-heptane to precipitate asphaltenes out of solution, separating bitumen into two broad chemical groups called asphaltenes and maltenes. Then, a chromatographic separation of the remaining material is carried out, leading to a further subdivision into resins, aromatics and saturates, which provides the composition of bitumen in terms of the relative quantity of the so-called SARA fractions for Saturates, Aromatics, Resins and Asphaltenes (Corbett 1969; Read and Whiteoak 2003; Lesueur 2009).

Another widely used chromatographic experiment set-up is the coupling between thin layer liquid chromatography on silica gel and a flame ionization detector (IATROSCAN) (Eckert 2001; Masson et al. 2001; Lesueur 2009), using a set of solvents such as n-heptane, a 80/20 toluene/n-heptane blend and a 95/5 blend of methylenedichloride/methanol for the separation of saturates, aromatics and resins, respectively.

It is worth noting that changing any component of the experiment set-up, such as the type of eluant or the stationary phase, may significantly affect the yield of each fraction (Wallace et al. 1987; Agrawala and Yarranton 2001; Goual and Firoozabadi 2002; Speight 2004; Goual 2012; Speight 2014), and hence, experimental conditions should be maintained and applied equally when comparing the chemical composition of various bitumens in order to obtain consistent results.

Elaborating on the composition of each of these four broad chemical families (SARAs), all of them show some common features and overall properties amongst bitumens, despite their variability in relation to the crude origin and the experiment set-up.

6.1. Saturates

This fraction, which usually amounts for 5 – 15 wt.% of bitumen, is made up of straight and branch chain aliphatic hydrocarbons, along with alkyl-naphthenes and some alkyl-aromatics (Speight 2014), with a hydrogen-to-carbon ratio of 1.9 and only traces of heteroatoms (Lesueur 2009). It constitutes a non-polar viscous oil that is colourless or straw in colour, and liquid at room temperature, as its glass transition temperature is located at around -60 ºC (Masson et al. 2002). The number-average molecular weight range for this faction is comprised between 470 - 880 g/mol (Lesueur 2009), with a solubility parameter laying between 15 and 17 $MPa^{0.5}$ (Speight 2014) and a density at 20 °C of 0.9 g/cm^3 (Corbett 1969), approximately.

6.2. Aromatics

They are called naphthene aromatics, and represent 30 – 45 wt.% of bitumen, which establishes them as the most abundant constituents in bitumen, together with the resins. At room temperature, they form a yellow to red liquid (Corbett 1969), slightly more viscous than that constituted by saturates, due to a higher glass transition temperature centred at around −15 °C (Masson et al. 2002). The compounds consist of non-polar carbon chains with a slightly aliphatic carbon skeleton and a majority of unsaturated ring systems (aromatics), resulting in a hydrogen-to-carbon ratio of 1.5 and a number-average molecular weight in the order of 570 – 980 g/mol (Lesueur 2009). Their solubility parameter falls between 17 and 18.5 $MPa^{0.5}$ (Speight 2014), along with a density, at 20 °C, of 0.99 g/cm^3 (Corbett 1969).

6.3. Resins

The amount of this fraction, also called polar aromatics, differs depending on the type of solvent used in the separation, which can lead to the retention and incorporation of a part of this fraction into the asphaltenes. Generally, resins represent up to 30 – 45 wt.% of bitumen and unlike saturates and aromatics, which are oily liquids at room temperature, they form a black solid or semisolid (Corbett 1969), given their main glass transition temperature located at around 20 ºC (Masson et al. 2002). As for composition, resins consist of compounds containing fused aromatic rings in their structure, similarly to asphaltenes but with less condensed aromatic rings, most probably involving 2 – 4 fused rings, which leads to a hydrogen-to-carbon ratio of approximately 1.40 (Koots and Speight 1975), along with a number-average molecular weight ranging between 780 – 1400 g/mol (Lesueur 2009). Their solubility parameter lies between 18.5 and 20 $MPa^{0.5}$ (Speight 2014), with a density, at 20 °C, close to 1.07 g/cm^3 (Corbett 1969).

6.4. Asphaltenes

Asphaltenes, which generally represent between 5 and 25 wt.% of bitumen (Corbett 1969; Read and Whiteoak 2003; Tanaka et al. 2004), are constituted by the most aromatic of the heaviest components in bitumen. This fraction has been the focus of continuous and intensive study, given its critical influence on bitumen's properties, as well as its implications in all aspects of crude oil utilization and processing (Mullins et al. 2007b).

Alphaltenes are currently defined as the constituents of a bitumen (or a petroleum fluid) that are insoluble in light n-alkanes, normally n-pentane or n-heptane (ASTM International 2012), but soluble in aromatics, such as toluene. The concept of solubility regarding asphaltenes has to be

understood from a perspective of not generating a precipitate, as asphaltene molecules in solution tend to aggregate to form basic aggregates, so-called "nanoaggregates", which have traditionally been described as micelles though (see section 8.1, "*Colloidal model*").

Depending on the n-alkane used for the extraction of asphaltenes, the insoluble fraction obtained will vary, and heavy resins may co-precipitate with asphaltenes (Agrawala and Yarranton 2001; Speight 2004; Goual 2012), bringing about the modification of the asphaltene content. Generally, alkanes with low carbon numbers lead to higher asphaltene contents (Lesueur 2009).

Asphaltenes are solid at room temperature (Read and Whiteoak 2003; Goual 2012), forming a black powder (Corbett 1969), and are largely responsible for the black colour of bitumen. They display a broad glass transition region in the normally investigated temperature range, being discernible a main glass transition at 70 ºC, whilst another one, less relevant, is located at 0 ºC (Masson et al. 2002). Their solubility parameter is comprised between 17.6 and 21.7 $MPa^{0.5}$ (Speight 2014) and their density, at 20 °C, is close to 1.15 g/cm^3 (Corbett 1969).

A paramount aspect of the characterization of asphaltenes has been the determination of a representative molecular weight for its constituents, in an attempt to relate this parameter to the properties of the fraction. However, the search for that value has been pretty much a matter of controversy, as discrepancies in the results have arisen amongst different techniques applied. In recent years, improvements in measuring techniques and new findings on the chemical properties of the asphaltenes have shed some light on this issue, yielding an estimated value for the number-average molecular weight of 750 g/mol, with most of the population

between 500 and 1000 g/mol (Agrawala and Yarranton 2001; Mullins 2008; Mullins 2010; Goual et al. 2011; Mullins et al. 2012; Goual 2012; Wu et al. 2014). The variations observed in this parameter, which was thought to reach values larger than 1000 g/mol (Dickie and Yen 1967; Speight 1970; Moschopedis et al. 1976; Speight, J. G. et al. 1985; Wiehe and Liang 1996), or much greater in certain cases (Dickie and Yen 1967; Moschopedis et al. 1976; Herod et al. 2007), stemmed from an incomplete understanding of the asphaltenes' molecular structure and intermolecular interactions.

As a result of so many years of research trying to disclose the molecular characterization behind the asphaltenes, several structural models have been proposed and developed over time to adapt to ongoing discoveries.

7. Association Models for Asphaltenes

7.1. The Yen model

At early stages of asphaltene study, a primitive model accounting for the information available was defined, namely the "Yen model" (Dickie and Yen 1967), providing a general frame for the macrostructure of the asphaltenic fraction, in which the asphaltene molecule would correspond to the unit sheet, consisting of a condensed polycyclic aromatic nucleus surrounded by aliphatic chains. Each asphaltene sheet would then tend to associate into larger structures due to electrostatic interactions between the aromatic centres, leading to stacked sheets or particles, which in turn may also interact with the aromatic areas from molecules in the vicinity, increasing the degree of association to several groups of stacked sheets, the so-called "micelle".

7.2. The Yen-Mullins Model

By the time the Yen model was developed, numerous properties of the asphaltenes, such as the size of the polycyclic aromatic nucleus, number of fused rings, aggregation numbers for individual molecules, molecules stacks and aggregates, and even the most basic characteristic, the molecular weight, were still mostly uncertain, rendering the model basically phenomenological. Nevertheless, advances in petroleum science allowed defining the pathway for the clarification of some of the issues, including the molecular weight of asphaltenes, but lack of consensus was still predominant, thwarting any development of structure-function relationships. Yet, progress in measuring techniques led to an increasing knowledge in asphaltene science, which favoured a progressively broader acceptance of some of the properties determined for asphaltenes. This, hence, established the basis for the constitution of an updated Yen model, which materialized into the so-called "modified Yen model" or "Yen-Mullins" model (Mullins 2010).

This model maintains general concepts of the Yen model, with the inclusion of a redefined and more specific description of the asphaltenes, for which the molecular structure is a key factor. It encompasses the main properties observed for the asphaltenic fraction, along with the proposed hierarchical organization of its structures and how these are structurally and energetically related. In this vein, the fundamental and predominant molecular architecture of the asphaltene is considered to consist of a single, moderate-sized polycyclic aromatic hydrocarbon (PAH) ring system with alkane substituents located at the periphery (Mullins 2010). As for its compositional properties, and according to bitumen's general composition, heteroatoms are mostly located in the asphaltenic fraction, mainly within

the PAH (Speight 2004; Mullins 2010), with nitrogen present in pyrrolic and pyridinic structures; sulphur in tiophenic ones; and oxygen in phenolic structures, although it can appear in several other groups, as described in section 6, "*Bitumen fractionation*".

As a consequence of such a distribution of heteroatoms, the PAH ring system is suitable for polarization, defining the zone of the asphaltene molecules where attractive electrostatic interactions between molecules may appear. In this regard, non-specific electrostatic interactions (dispersive or London interactions) are assumed to drive the association of asphaltene molecules (Mullins 2010; Redelius and Soenen 2015). As a part of dispersive interactions, a contribution that becomes significant, especially for large aromatic systems like those in asphaltenes (Hunter and Sanders 1990a; Grimme 2008), corresponds to π-π interactions (Hunter and Sanders 1990a; Buenrostro-gonzalez et al. 2001; Tanaka et al. 2004; Andreatta et al. 2005a; Grimme 2008; Lu et al. 2008; Mullins 2010; Redelius and Soenen 2015; Wei et al. 2015), arising from the delocalized π electrons, such as in the case of charge transfer complexes, which may also be present in asphaltenes by means of porphyrin molecules or metal organic molecules (Mullins 2010; Redelius and Soenen 2015). Moreover, electronegative elements like nitrogen and oxygen are liable to undergoing some charge separation, further enhancing the π-π interaction, as well as providing locations for polar and hydrogen bonding interactions (Lu et al. 2008; Mullins 2010; Redelius and Soenen 2015), which are additional contributors to the types of interactions that asphaltene molecules may exhibit.

By contrast, alkane substituents at the periphery are thought to bring about some steric hindrance between the outermost regions of the molecules at a

certain intermolecular distance (Buenrostro-gonzalez et al. 2001; Rogel 2002; Eyssautier et al. 2011). Hence, this alkane shell is assumed to impose some physical constrain for intermolecular interaction, unless orientation and distance of the molecules involved allow attractive forces in the core of the molecules (PAH ring system) to be effective enough to lead to association.

As indicated, the molecular structure of asphaltenes has been assumed to consist of a PAH core and a shell of alkyl substituents, which geometrically resembles a cylinder with a high diameter-to-height ratio, i.e. disk-shaped geometry, and is widely supported in the literature (Rogel 2002; Tanaka et al. 2004; Mullins 2010; Eyssautier et al. 2011; Mullins et al. 2012; Evdokimov and Fesan 2016). This molecular structure, also referred to as core-shell model, owing to the different compositional layers that make it up (Eyssautier et al. 2011), is liable to interact electrostatically with molecules from the surroundings and provoke its association. In such a case, attractive dispersion forces (Van der Waals interaction) at the nucleus have to overcome steric effects from the shell, so that cores from the molecules involved can approach one another and reach a stable state of association. Among the above-mentioned possible types of attractive electrostatic interaction that may arise, the aromatic properties of the asphaltenic molecule core hint at π-π interaction as the major driving force for association (Hunter and Sanders 1990b; Buenrostro-gonzalez et al. 2001; Rogel 2002; Tanaka et al. 2004; Andreatta et al. 2005a; Grimme 2008; Lu et al. 2008; Wei et al. 2015).

Thus, asphaltene molecules may undergo association into structures of increasing size and complexity, starting from dimers, followed by trimmers and so on up to greater states of association through further interaction with

other asphaltene molecules (Evdokimov and Fesan 2016). This increasingly complex variety of structures might be framed into a hierarchical organization in which the asphaltene molecule constitutes the basic unit, followed by the so-called "nanoaggregate", made up of asphaltene stacks, and further degrees of aggregation, corresponding to clusters and flocculates, the highest structural order (Tanaka et al. 2004; Mullins 2010; Mullins et al. 2012).

7.3. Oligomer-like model

Asphaltene molecules have been assumed to associate with other asphaltene molecules due to electrostatic interactions that mainly arise at the fused aromatic ring system (PAH), with "π-π interaction" as their major contributor. This association presumably leads to asphaltene stacking, forming the so-called nanoaggregates, and those may further associate into clusters and flocculates.

Nevertheless, disparities related to the types of interaction involved in the process of association (not only limited to the presence of "π-π stacking") (Murgich 2002; Andersen et al. 2005; Gray et al. 2011) and the possible influence exerted by external conditions and other molecules from the surroundings (e.g. resins, solvents, surfactants, etc.) (Murgich and Strausz 2001; Agrawala and Yarranton 2001; Gray et al. 2011) have led to additional approaches that attempt to give a different vision for such a process. One of these association schemes finds its basis in the analogy with linear polymerization, assuming oligomerization-like association reactions for the constitution of large asphaltene entities (Agrawala and Yarranton 2001), which unlike polymers, are non-covalently linked to one another. Correspondingly, associating molecules are classified depending on their bonding properties into two types, "propagators" and

"terminators". The former correspond to molecules containing multiple active sites for interaction with other molecules; whilst the latter (terminators) are ideally assumed to have only one site available for interaction, so that upon linking, no further association is possible.

In contrast with previous models, in which asphaltene molecules were the only constituents of the aggregates, this scheme attributes some properties of asphaltene aggregates to the joint presence of resins and asphaltenes in them (Yarranton et al. 2007). Hence, in the case of asphaltenes, which have been shown to contain multiple heteroatoms and an aromatic cluster, all being possible sources of electrostatic interaction, their molecules are considered to be capable of interacting with themselves and with resins, and thus, they are mainly treated as propagators, although some may behave as terminators. Resins, on the other hand, mostly correspond with terminators, given their lower number of functional groups, which results in fewer active sites for interaction.

As a result, propagators (mainly asphaltenes) are eligible to interact with either other propagators or terminators (principally resins), although showing a greater preference for interaction with the latter, increasing the size of the resulting aggregate; whilst terminators will only interact with propagators or with aggregates, leading the oligomerization-like process to termination (Agrawala and Yarranton 2001; Yarranton et al. 2007).

In addition to that model for asphaltene aggregation, a different work, which followed the descriptive framework proposed by the Yen-Mullins model, applied high-Q ultrasonics spectroscopy to investigate the aggregation process and the relations between structure and function that control stability of asphaltene aggregates (Andreatta et al. 2005b). Similarly to the Yen-Mullins model, asphaltenes are assumed to be

characterized by an island-like structure with a single fused aromatic core, which contains most of the heteroatomic content, and peripheral alicyclic and alkane substituents. Van der Waals forces and charge separation, mainly acting within the polyaromatic core, drive the intermolecular attractive interactions; whilst steric repulsion is attributed to the shell of alkanes. Hence, both interactions are involved in the intermolecular association of asphaltenes and, given the different nature of each of the two dominions, they are also a major controlling factor of the interaction with the surrounding medium and so, the asphaltene solubility. In fact, results showed that asphaltenes from different sources present comparable aggregation properties (Andreatta et al. 2005b), implying that both attractive and repulsive interaction forces have to be balanced, independently of the specific structural features of the molecules. This approach somehow complements the Yen-Mullins model by including some concepts from the oligomerization model proposed, which are adapted to further develop the role of polydispersity in the asphaltene aggregation and the nanoaggregate stability.

Thus, different sizes of the asphaltene structures correspondingly relates to several degrees of solubility in toluene, and so, to different behaviours in the aggregation process. Smaller molecules, characterized by a greater solubility and low energy sites for association, are viewed as "chain terminators", whilst larger ones, with a lower solubility and sites with greater energy, are considered "chain propagators". The latter tend to associate strongly, forming large aggregates, however, when linking to the so-called "chain terminators", the remaining sites will have low energy, preventing further growth of the aggregate and providing stability. Accordingly, size polydispersity of the molecules that make up aggregates

allows balancing their growth and hence, their solubility in aromatic solvents, ensuring the stability of the system.

7.4. Supramolecular assembly model

A deeper knowledge on the characterization of asphaltene behaviour tends to provoke discrepancies among the myriad of interpretations that struggle to relate experimental observations to the molecular and structural characteristics.

In that line, and complementarily to the previous approaches, in which asphaltene association either is comparable to an oligomerization-like process or follows the trends of the Yen-Mullins model, accompanied by the concepts of molecular size polydispersity and solubility in relation to the aggregate stability in solvents, a more complete association scheme was proposed, in an attempt to account for the variety of properties observed for asphaltene aggregates. It finds its foundations in the supramolecular chemistry, a domain of chemistry that focuses on molecular assemblies made up of smaller units or components linked together by non-covalent interactions, and that has lately been gaining relevance in several other fields of knowledge, such as materials science or biology.

In the context of asphaltene association, this approach, referred to as supramolecular assembly model (Gray et al. 2011), brings some concepts from supramolecular chemistry to provide a new structural and compositional view for asphaltene aggregates, as well as an interpretation for the interaction mechanisms and forces behind their association, for which molecular recognition and host-guest interactions in three dimensional porous networks are considered the main driving interaction forces; whilst π-π stacking is relegated from the forefront of the interaction

scheme to just an additional contributing factor to the formation of aggregates.

Thus, in contrast with the aggregation schemes related to the Yen model, and similarly to the oligomerization-like model, the supramolecular assembly model suggests that several types of electrostatic interactions, such as hydrogen bonding, acid-base interactions or π-π stacking, act cooperatively and simultaneously in the asphaltene aggregates to provide a greater degree of structural stability and interaction strength than each interaction force individually. Aggregates are thought to correspond to at least ternary complexes consisting of host, gest, and solvent molecules, which following the guidelines of the oligomerization-like model, in the case of host molecules (e.g. asphaltenes), these are viewed as having multiple sites for interaction, analogously to propagators, and may increase the extension of the supramolecular assembly. Guest molecules would refer to alkyl aromatics and naphtenes with fewer sites for interaction; and solvent molecules or low-molecular-weight species, on the other hand, might be similar to terminators, provided that they only have one active site for interaction with the rest of molecules in the aggregate.

Structurally, unlike the Yen model and its disk-like geometry with an alkylic shell, the resulting asphaltene aggregates will presumbly exhibit functional groups on the outside of the supramolecular assembly, suitable to further interact with other functional groups in molecules from the surroundings.

Finally, due to the variety of dimensions and properties of the molecules involved in the formation of the supramolecular assemblies (i.e. aggregates), these would be characterized by a wide range of sizes and

shapes, also dependent on the concentration and temperature conditions, resulting in a highly polydispersed population.

8. Molecular structural models of bitumen

The study of the state and solution behaviour of asphaltenes in several solvents has derived in a wealth of experimental data, later organized and represented in the form of models, as those described above, trying to give explanation to the properties observed in well-known conditions and solvents, and to predict or estimate them in others not yet well understood. In this regard, such a myriad of models and information ultimately aims at a common target issue, which refers to reaching a better, if not fully, comprehension of asphaltene behaviour in its natural media (e.g. crude and petroleum oils, bitumen or vacuum residua). Although there exists increasingly ample knowledge on property-composition relations for asphaltenes and other fraction compounds, their molecular structural organization and possible molecular interactions and arrangements are indeed still a point of contention, especially in the case of bitumen.

8.1. Colloidal model

Traditionally, the molecular organization of bitumen has been regarded as a colloidal system (Nellensteyn 1924; Pfeiffer and Saal 1940; Saal and Labout 1940), in which asphaltenes are dispersed in maltenes in the form of micelles, which consist of associated asphaltene molecules surrounded by a shell of resin molecules that act as peptizing agents, creating a solvation layer that stabilizes asphaltenes from aggregation. The medium environing those micelles is constituted by molecules of lighter resins, aromatics and saturates, with a progressive transition in composition between them in that order, as distance to the nucleus of the micelles increases.

According to this model, the content of resins in relation to asphaltene defines the colloidal behaviour of any bitumen. The presence of enough resin and aromatic molecules to solvate completely the asphaltene molecules leads to fully peptized asphaltenes, and so, micelles with high mobility within bitumen. This type of bitumen configuration, depicted in Fig. 2.2(a), is referred to as "SOL".

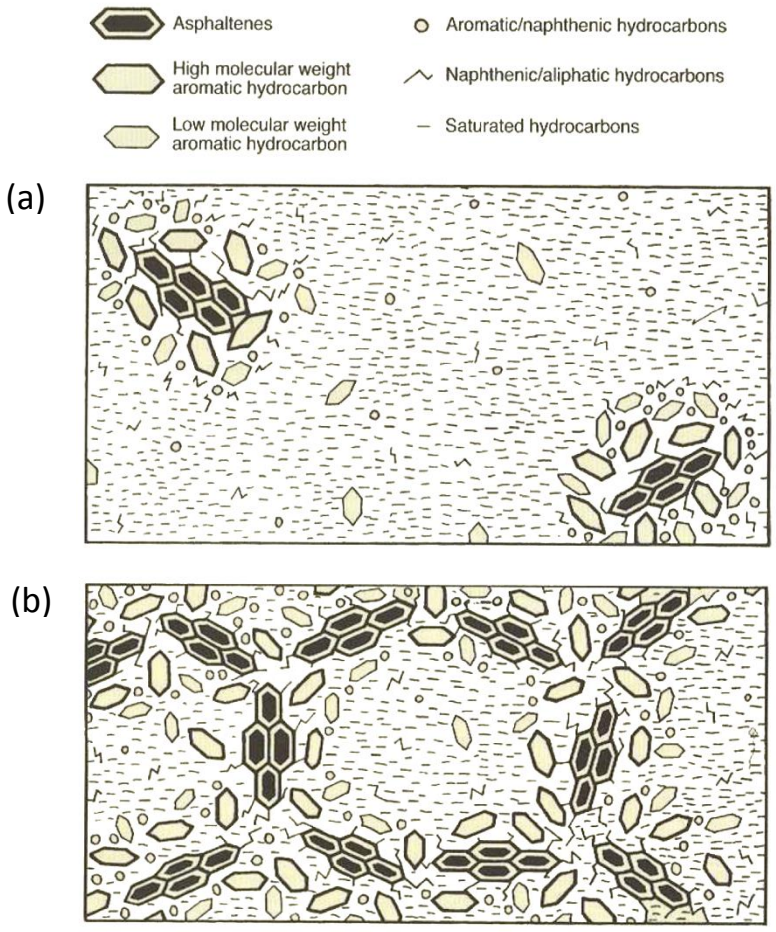

Fig. 2.2. Schematic representation of the molecular organization in (a) SOL type bitumen and; (b) GEL type bitumen (Read and Whiteoak 2003).

In the case of an insufficient quantity of resin and aromatic molecules to ensure the complete peptization of asphaltene molecules, further association of asphaltenes may take place, giving rise to a type of loosely

packed or open structure of linked micelles with maltenic compounds filling its internal spaces, as illustrated in Fig. 2.2(b), which is known as "GEL" type.

Notwithstanding, most bitumens are characterized by structures and properties in-between those two types.

It can then be assumed that the degree of peptization of the resin and aromatic fractions greatly influences the properties of bitumen, especially concerning its rheological behaviour, and its dependency with temperature. In this regard, properties of GEL type bitumens exhibit lower temperature dependence, although generally a certain transition to SOL type structure takes place when bitumen is heated up to high temperatures, due to a decrease in the interactions between asphaltenes and micelles, hence modifying the rheological properties of the system, represented by a reduction in viscosity. Moreover, changes in the content of saturates might also affect the balance of the interactions between asphaltenes/micelles and their state of aggregation, leading to an increase or reduction in GEL character and, inversely, in temperature dependence.

8.2. Dispersed Polar Fluid (DPF) Model

The Colloidal model has proved to be very useful for the explanation and description of bitumen's properties, as well as its thermal and rheological behaviour. However, recent interaction and association models (described in section 7, "*Association Models for Asphaltenes*"), accompanied by experimental data in various types of solvent media, even in crude oils and bitumen, have led to slightly different interpretations for the organization of molecules in asphaltene-containing systems, as well as their role in the stability of such systems.

One interpretation (Redelius 2006) for the description of bitumen's molecular organization is based on the idea that its stability arises from the continuum of increasingly high polar molecules that constitute it, which allows mutual solubility of the successive fractions in bitumen (Redelius 2006). Complementarily, polarity, as a component of molecular solubility, is assumed to be responsible for the elasticity of bitumen and the dependency of its complex rheological behaviour with temperature. Thus, at low temperatures, the strength of polar interactions between molecules is higher than their thermal energy, providing enough structural stability to maintain the viscoelastic response of bitumen. However, as temperature is raised, thermal energy does so, eventually overcoming the strength of polar interactions, which reduces the elastic component of the rheological response, resulting in Newtonian behaviour at sufficiently high temperatures. Bitumen structure is then defined on the basis of a thermodynamic solubility model, viewed as a homogeneous mixture made up of a continuum of molecules, whose interaction properties make every group of them that pertain to a specific bituminous fraction act as a solubilizer of the molecules of the closest fraction in the polarity classification. As a consequence, mutual solubility of molecules implies that any mixture of bituminous fractions will be stable as long as continuity in the polarity of the fractions involved is maintained, and so, the model does not contemplate the formation of any micellar structure or any other molecular association that may resemble such a structure.

8.3. Nanoaggregate-based Models

In contrast to the previous model of molecular co-solubilisation, most structural interpretations for bitumen, supported either by experimental data from different techniques (Mullins et al. 2007a; Eyssautier et al.

2012c; Eyssautier et al. 2012a; Painter et al. 2015b) or by molecular mechanics (Murgich and Strausz 2001; Painter et al. 2015b; Mousavi et al. 2016), agree that asphaltene molecules self-aggregate to form aggregates, generally referred to as nanoaggregates. However, discrepancies arise as to whether there exists any relevant interaction between those asphaltene nanoaggregates and resin molecules, and if so, the role of such an interaction.

In that regard, some authors (Eyssautier et al. 2011; Eyssautier et al. 2012a; Eyssautier et al. 2012b) state that no interaction exists between resins and asphaltenes in bitumen, indicating that colloidal suspensions of asphaltene nanoaggregates are also formed in model solvents in absence of resins, where nanoaggregate stability against coalescence is ensured by the steric repulsion of the surrounding alkyl substituents, and thus, this organization would be similar to that of asphaltenes in bitumen (Mullins et al. 2007a; Eyssautier et al. 2012c).

Notwithstanding, other authors do accept the existence of some interaction between asphaltene and resins, which would not act as peptizing agents, but would involve a certain degree of selectivity and specificity in the interaction (Murgich and Strausz 2001), and may lead somehow to a greater population of smaller-sized asphaltene aggregates (Mullins 2010). They also point out that the presence of resins in nanoaggregates, although minimal, might be related to a fraction of the heaviest resins or lightest asphaltenes, with the bulk of resins not being present in the majority of nanoaggregates (Mullins et al. 2007a; Mullins 2010).

Accompanying those descriptions of the asphaltene-resin interaction in bitumen, some recent work on that issue provides a combined and complementary view for the stability of asphaltenes in bitumen (Mousavi

et al. 2016). This model is in agreement with the existence of molecular clusters containing associated asphaltenes as the core structure, similarly to the nanoaggregate description, with the presence in the surroundings of molecules corresponding to the rest of bituminous fractions, i.e. lighter resins, aromatics and saturates. It is also mentioned that given the molecular likeness between resins and asphaltenes, their aromatic dominions may interact through Van der Waals and π- π interaction forces, resulting energetically favoured, as this indeed reduces the asphaltene stacking intermolecular distance, increasing the energetic stability and the dispersive character of the structures formed. Aliphatic side chains in asphaltene molecules are shown to further stabilize those structures.

Nevertheless, such an asphaltene-resin interaction is favoured by an appropriate spatial disposition of the asphaltene stacked molecules, with enough active sites available for binding, and more importantly, by an adequate ratio resin-asphaltene, as resin-asphaltene interactions are promoted at concentrations of resins higher than those of asphaltenes.

8.4. Modern Colloidal Model

Concepts from previous models can be combined into a modern colloidal representation of bitumen, in which both mutual solubility and structural associations would be involved to ensure the stability of the molecular arrangements.

The basic structures are hence constituted by clusters of asphaltene nanoaggregates (asphaltene stacked molecules), which interact with resins, contributing to their stability in the rest of fractions, i.e. aromatics and saturates (as proposed by the DPF model), although some molecules of these could also be entrapped within the colloidal structure, similarly to the supramolecular assembly model. These colloidal assemblies are subjected

to further interactions, both attractive and repulsive, and depending on external factors, such as temperature, pressure or solvents, charge unbalance may arise leading to their association into larger fractal aggregates, as indicated by the Yen-Mullins model, entrapping some molecules from the maltenic environment. The aggregates formed, with greater effective volumes, influence the hydrodynamics of the surrounding medium, changing the rheological properties of the system, as amply observed in experimental data. Ultimately, more intense changes in any of the external conditions affecting the solubility equilibrium, and also the balance between attractive and repulsion forces, jointly favour the aggregation of the large structural assemblies, eventually giving rise to their phase-precipitation out of the maltenes, with the corresponding generation of an asphaltenic precipitate.

Due to the characteristics of the modern colloidal model, it will mainly be used throughout the present work.

9. Rheology fundamentals

9.1. Introduction

The term 'Rheology' was coined by a Chemistry Professor at Lehigh University, Eugene Bingham, as a way to denote the science dealing with the study of the deformation and flow of matter, since the main root of the word means “to flow” (*rheo* in Greek). This definition was accepted by the American Society of Rheology after its foundation in 1929 (Macosko 1994).

The place of rheology amongst other natural sciences and applied problems is shown in Figure 2.3.

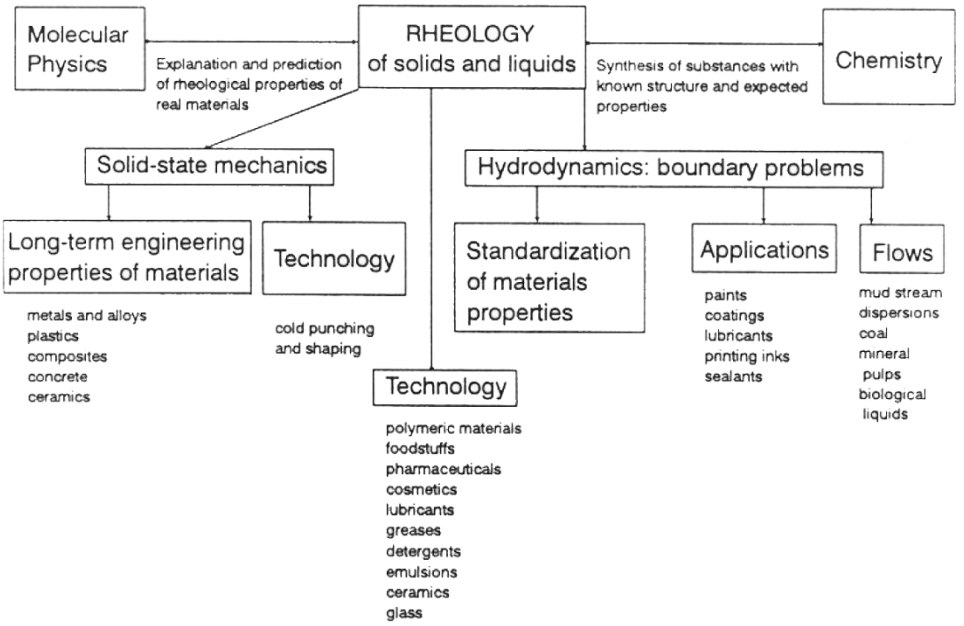

Fig. 2.3. Place of rheology amongst other sciences, considering applied problems.

As illustrated, rheology is a multidisciplinary science having many points of relationship with fundamental physics and chemistry, with applications to real technological and engineering materials in life**,** and focused on mechanical properties of solid-like, liquid-like, and intermediate technological and natural products (materials).

The results of the macroscopic description of behaviour of real engineering and biological media, based on their rheological properties, are used in numerous applications related to technology of synthesis, processing, and shaping of different materials (plastics and ceramics, emulsions and dispersions in the chemical and food industries, pharmaceuticals, cosmetics, transport, oil industry, etc.), their long-term properties, natural phenomena, and biological problems (dynamics of blood circulation, work of bones). The first goal of rheology is then a search for stress versus deformation relationships for various technological and engineering materials in order to solve macroscopic problems related to continuum

mechanics of these materials. The second goal of rheology consists on establishing relationships between rheological properties of a material and its molecular composition content. It is an important independent problem related to estimating quality of materials, understanding laws of molecular movements and intermolecular interactions (Malkin 1994).

9.2. Classification of materials

The concepts of liquid and solid and their formal (mathematical) representation originated from the classical works of Isaac Newton and Robert Hooke, respectively (Malkin 1994).

Newton introduced his ideas in 1687, although it was not until the nineteenth century that Navier and Stokes independently developed a general three-dimensional theory for liquid-like behaviour, resulting in the Navier-Stokes equations.

.One of the most useful types of deformation for rheological measurements is steady simple shearing. In this type of shearing, a material element is placed between two parallel plates, where the bottom plate is stationary and the upper plate is displaced in x-direction by applying a force F tangentially to the surface A (Fig. 2.4). For a similar case, Newton proposed the following statement: "The resistance which arises from the lack of slipperiness of the parts of the liquid, other things being equal, is proportional to the velocity with which the parts of the liquid are separated from one another" (Barnes et al. 1989).

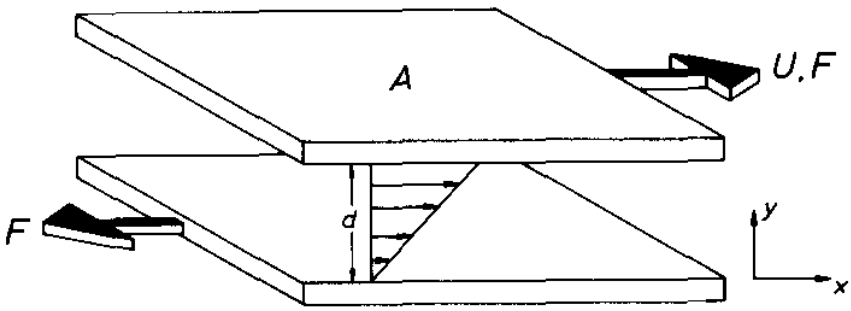

Fig. 2.4. Schematic of steady simple shearing of a material element located between two parallel plates.

According to such ideas, later converted to a more accurate form by Stokes, the force (*F*) applied per unit area (*A*), and the resultant velocity gradient (*U/d*) were related by the so-called Newton-Stokes Law:

$$\sigma = \eta \cdot \dot{\gamma} \qquad \text{(eq. 2.1)}$$

Where σ is the force per unit area, or shear stress, and $\dot{\gamma}$ is the rate of deformation or sear rate. This law hence assumes that a force (or resistance) is proportional to a velocity (of movement), and the coefficient of proportionality, η, is called viscosity (or coefficient of viscosity).

Hooke formulated a similar proposal concerning properties of solids. The law, named after him, was translated to modern form by Bernoulli, giving rise to the Hooke Law, which states that stress, σ_E, is proportional to deformation, ε, and the coefficient of proportionality is called the Young modulus, E:

$$\sigma_E = E \cdot \varepsilon \qquad \text{(eq. 2.2)}$$

The Hooke Law says that the force applied to the surface of a solid is proportional to the deformation provoked on the material. Once the deformed state is reached there is no further movement, but the deformed state persists as long as the stress is applied (Barnes et al. 1989).

Both models represent properties of many real materials and work well in describing their behaviour with considerably high degree of accuracy. However, there are numerous other real materials which are not described by the above-mentioned Newton-Stokes and Hooke laws, and constitute the centre of attention of rheology.

It is also important to note that the rheological behaviour of a material will depend on both time and space scales of observation (experiment). The former is relevant as a measure of the ratio of the rate of inherent processes in a material to the time of experiment and/or observation; whilst the latter determines the necessity to treat a material as homo- or heterogeneous.

Any change in the rheological properties of a material can occur either instantaneously or over a long period of time. Thereby, such a material will behave like a solid or a liquid depending on the time scale of the observation process.

The scaling of time in rheology is achieved by means of the 'Deborah number' (D_e),

$$D_e = {}^{\tau}/_{T} \qquad \text{(eq. 2.3)}$$

where T is a characteristic time of the deformation process being observed and τ is a characteristic time of the material. The time r is infinite for a Hookean elastic solid and zero for a Newtonian viscous liquid.

This number was defined by Professor Marcus Reiner with a reference to the fifth chapter of the book of Judges, in the Old Testament, in which Deborah is reported to have declared "The mountains flowed before the Lord... ", with the idea that everything flows if ones waits long enough.

Then, high Deborah numbers correspond to solid-like behaviour, whereas low Deborah numbers to liquid-like behaviour. A material can therefore appear solid-like either because it has a very long characteristic time or because the deformation process used to study it is very fast. Thus, even mobile liquids with low characteristic times can behave like elastic solids in a very fast deformation process.

Accordingly, a solid can be defined as a material that will not continuously change its shape when subjected to a given stress, i.e. for a given stress there will be a fixed final deformation, which may or may not be reached instantaneously on application of the stress. A liquid, on the other hand, will correspond to a material that will continuously change its shape (i.e. will flow) when subjected to a given stress, irrespective of how small that stress may be (Barnes et al. 1989).

9.3. Newtonian fluid behaviour

In accordance with the Newton law, any liquid characterised by a viscosity that, although varying with temperature and pressure, does not vary with deformation rate or time can be considered as Newtonian. Nevertheless, such a material should not display any elastic properties or extensional anomalies.

A Newtonian liquid is, of course, an idealisation, but in many cases, it is a very good representation of a large number of liquids under normal ‘everyday’ conditions.

9.4. Non-Newtonian fluid behaviour

As indicated, both Newton-Stokes and Hooke laws are linear laws, hence assuming direct proportionality between stress and strain, or strain rate, whatever the stress. Despite this linear framework can accommodate a wide

range of rheological behaviour, it is also very restrictive. The range of stress over which materials behave linearly is invariably limited, and the limit can be quite low. In other words, material properties, such as Young modulus and viscosity, can change with the applied stress, and the stress need not be high. The change can occur either instantaneously or over a long period of time, and it can appear as either an increase or a decrease of the material parameter.

A liquid showing any deviation from the above behaviour is non-Newtonian.

9.4.1. Shear-thinning fluid behaviour

When investigating the influence of shear rate on viscosity, many materials exhibit some departure from Newtonian behaviour, such as dispersions, emulsions and polymer solutions. In the vast majority of cases, the viscosity is found to decrease with increasing shear rates, giving rise to what is generally called 'shear-thinning' behaviour although the terms temporary viscosity loss and 'pseudoplasticity' have also been employed.

For shear-thinning materials, the general shape of the curve representing the variation of viscosity with shear rate in a double logarithmic scale plot is shown in Fig. 2.5.

The curve indicates that in the limit of very low shear rates (or stresses) the viscosity tends to be constant. Then, at a certain shear rate value, the so-called critical shear rate, it begins to decrease, usually entering a straight-line region, which indicates a power-law behaviour. Afterwards, in the limit of high shear rates (or stresses), the viscosity is again constant, but with a lower value. These two extremes are sometimes known as the lower and upper Newtonian regions, respectively, with the lower and upper

referring to the shear rate and not the viscosity. The terms "first Newtonian region" and "second Newtonian region" have also been used to describe the two regions where the viscosity reaches constant values. As for the higher constant value, it is generally called the "zero-shear viscosity".

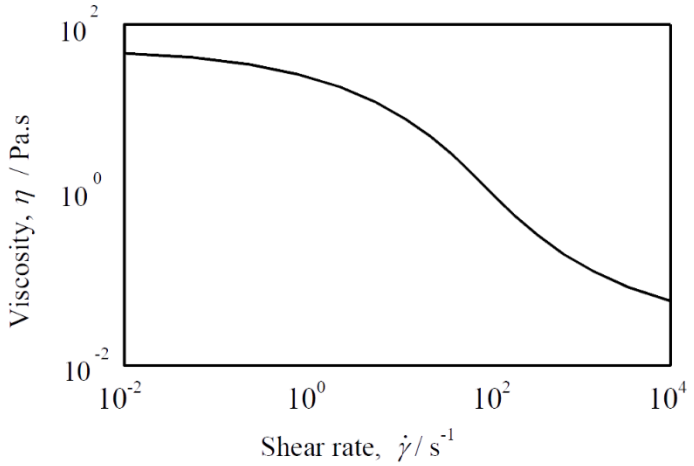

Fig. 2.5. Variation of viscosity with shear rate for a given material.

This decrease of viscosity with shear rate must be distinguished from a decrease of viscosity with time of shearing, which is called thixotropy,

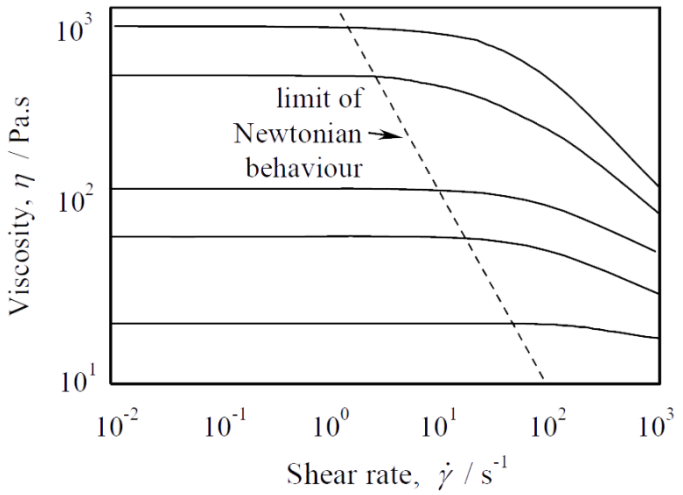

Fig. 2.6. Examples of curves for the evolution of viscosity with shear rate, exhibiting shear-thinning behaviour.

Sometimes, the position of the typical behaviour along the shear-rate axis is such that the particular measurement range used is too low to pick up the higher shear-rate part of the curve, resulting in patterns similar to those included in Fig. 2.6.

9.4.2. Bingham plastic or viscoplastic behaviour

A particular case of shear-thinning behaviour sometimes observed is that related to liquids that do not seemingly flow until a critical yield stress is exceeded, defining the so-called Bingham plastic behaviour, In such liquids, by implication, the viscosity has to be infinite at zero shear rate and there is no question of a first Newtonian region.

Hence, as stated, it has been usually thought that at stresses below the yield stress no flow takes place, and only solid-like behaviour is seen. However, recent advances in rheometry have shown that careful and patient measurements below this stress indicate that viscosity is still finite, and eventually levels off to a constant, but very high value at low stress.

9.4.3. Shear-thickening or dilatant fluid behaviour

Contrarily to the cases presented above, it is also possible that the very act of deforming a material can cause a rearrangement of its microstructure such that the resistance to flow increases with shear rate, as shown in Fig. 2.7. As observed, the shear-thickening region extends over only about a decade of shear rates.

Moreover, in almost all known cases of shear-thickening, there is a region of shear-thinning at lower shear rates.

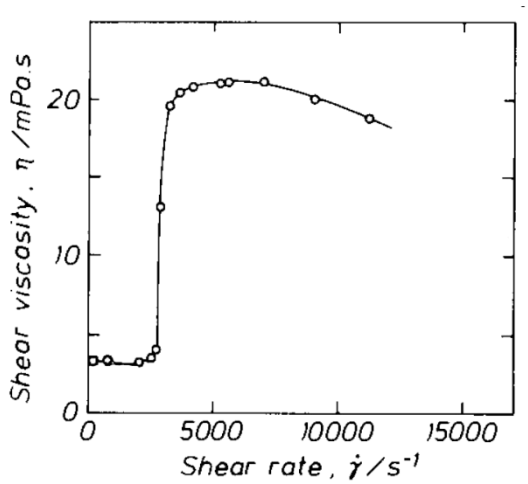

Fig. 2.7. Evolution of viscosity with shear rate for a shear-thickening material.

9.4.4. Time-dependent fluid behaviour-

For most liquids, the step-wise setting of a constant shear rate or shear stress leads to an immediate beginning of flow. Shear stress or shear rate, which maintains the steady flow, remains constant all the time (eliminating inertial effects). After the cessation of flow, stress instantaneously drops to zero. However, there are some liquids for which development and disappearance of stresses is far from the simplest scheme. Fig. 2.8(a) demonstrates the effect of step-wise setting of constant shear rate.

As observed, at low shear rates, there is a very prolonged time interval of slowly developing shear stresses, and this interval becomes shorter if shear rate is increased. At high shear rates, shear stresses pass through a maximum (sometimes several maxima can be observed) before reaching the state of steady flow. Finally, after sudden cessation of flow, shear stress decays (relaxes), and the initial relaxation rate increases with increasing initial shear rate.

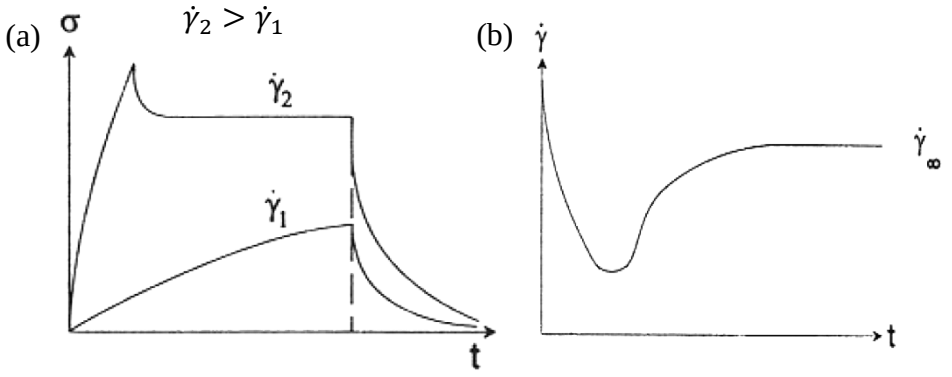

Fig. 2.8. Development of (a) shear stresses at constant shear rates; and (b) shear rate at constant shear stress.

On the other hand, at a constant shear stress (Fig. 2.8(b)), the steady flow regime is reached after a transient range of deformation, when shear rate is changing due to a change of a relative effects of plastic and elastic components, along with deformation rate.

Transient rheological behavior is a very characteristic time effect, leading to a complex relationship between stress and rate of deformation. The reasons for the effects can vary, but the main models of behavior correspond to thixotropic and rheopectic phenomena, as well as to viscoelastic behavior (Malkin 1994), further detailed next.

9.4.4.1.Thixotropy and rheopexy

A gradual decrease of the viscosity under shear stress followed by a gradual recovery of structure when the stress is removed is called thixotropy. The opposite type of behaviour, involving a gradual increase in viscosity, under stress, followed by recovery, is called rheopexy.

Thixotropy invariably occurs in circumstances where the liquid is shear-thinning (in the sense that viscosity levels decrease with increasing shear

rate, other things being equal). In the same way, rheopexy is usually associated with shear-thickening behaviour.

The occurrence of thixotropy implies that the flow history must be taken into account when making predictions of flow behaviour (Barnes et al. 1989).

A typical example of thixotropic behavior of liquid is given in Fig 2.9, showing the relationship of viscosity versus shear rate. The upper part of a curve was measured on increasing shear rate; on reverse measurement (shear rate decreasing from maximum to minimum), viscosity is lower than on ascending shear rate change. The lower part of the curve represents viscosity of a medium with structure changed by previous deformation. Measurements are used to characterize thixotropic properties of material and their quantitative measure is an area of a hysteresis loop between two curves.

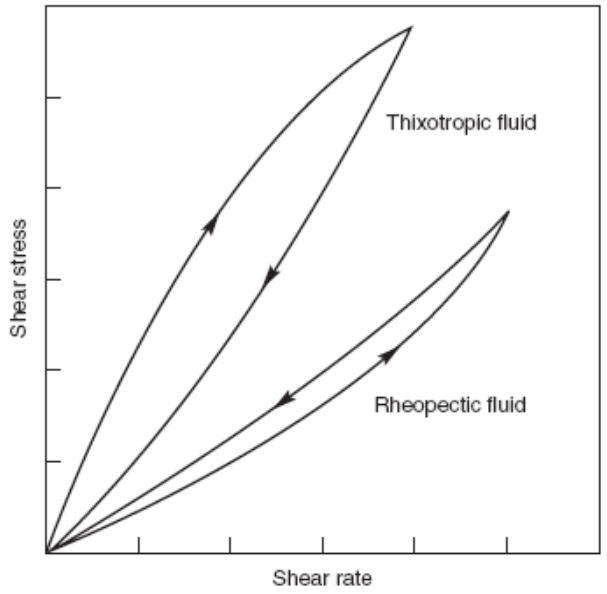

Fig. 2.9. Hysteresis loop in continuous change of shear rate formed due to thixotropic and rheopectic properties of a liquid. An arrow shows the direction of changes of experimental conditions in viscosity measurement.

The change of rheological properties on deformation and rest reflects the structural rearrangement caused by application of external forces. In this sense, thixotropy is a consequence of structure rupture and rheopexy of structure build-up. It can be expected that external forces more likely promote ruptura rather than a build-up of structure, and that is why thixotropic effects are more common than rheopexy, the latter being a very special case in materials with some kind of unusual intermolecular interactions; for example, strong ionic interaction or hydrogen bonding.

It is important to emphasize that in both cases, a new class of phenomena is discussed within the frame of rheology, that is, kinetics of physical or chemical processes in a material related to the effect of stress.

This phenomenon is particularly important for chemical reactions of polymerization, curing of oligomers, chemical transformations in polymeric chains, etc., all of which result in considerable changes of rheological properties (not only viscosity) of a material.

Certainly, this type of phenomena has some major relevancy in applications of polymer technology (synthesis and processing) (Malkin 1994).

9.4.4.2.Viscoelasticity and linear viscoelastic response

The concepts of elasticity and viscosity need to be qualified since real materials can be made to display either property or a combination of both simultaneously. Which property dominates, and what the values of the parameters are, depend on the stress or strain and the duration of its application.

The term 'viscoelasticity' is used to describe behaviour which falls between the classical extremes of Hookean elastic response and Newtonian viscous behaviour. In terms of ideal material response, a solid material with

viscoelasticity is invariably called a 'viscoelastic solid' in the literature. In the case of liquids, there is more ambiguity so far as terminology is concerned. The terms 'viscoelastic liquid', 'elastico-viscous liquid', 'elastic liquid' are all used to describe a liquid showing viscoelastic properties.

There are a number of ways of measuring linear viscoelastic response. One of the simplest is the sudden application of a constant stress to the liquid being tested, and monitoring of the resulting strain thereafter, which is called creep testing.

Another frequently used method is oscillatory testing, i.e. applying an oscillating stress or strain as an input to the liquid and monitoring the resulting oscillatory strain or stress output. The same repetitive sinusoidal straining motion recurs over and over again, with each cycle taking a certain time, and having a frequency that is inversely proportional to that time.

One other method used occasionally is the sudden application of a constant strain, and the monitoring of the consequent stress, which then decays away with time, corresponding to a stress relaxation test. All these tests are schematically summarised in Fig. 2.10.

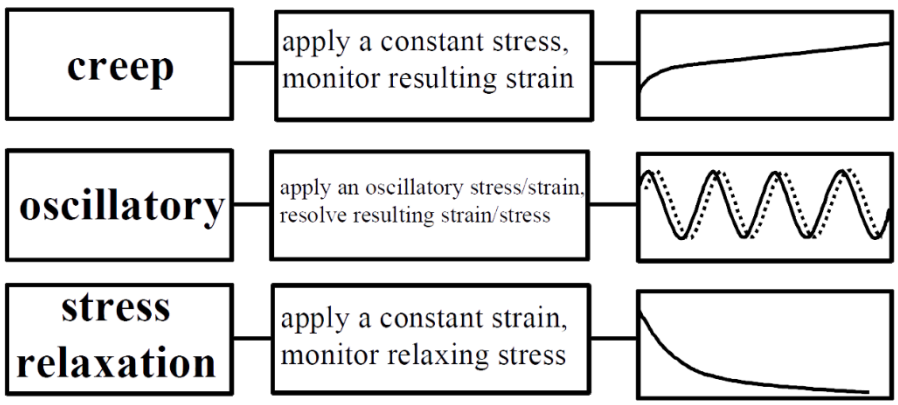

Fig. 2.10. Various tests that measure the time response of a liquid.

Regarding oscillatory tests, these are performed over a range of frequencies, in such a way that short times correspond to high frequencies, and long times relate to low frequencies.

Oscillatory tests involve applying a sine-wave-shaped input of either stress or strain, such that by means of suitable electronic methods, the resulting sinusoidal strain or stress output is separated into a certain amount of solid-like response, which is in phase with the input, and a corresponding amount of liquid-like response which is π/2 (i.e. 90[a]) out of phase with the input, as shown in Fig. 2.11.

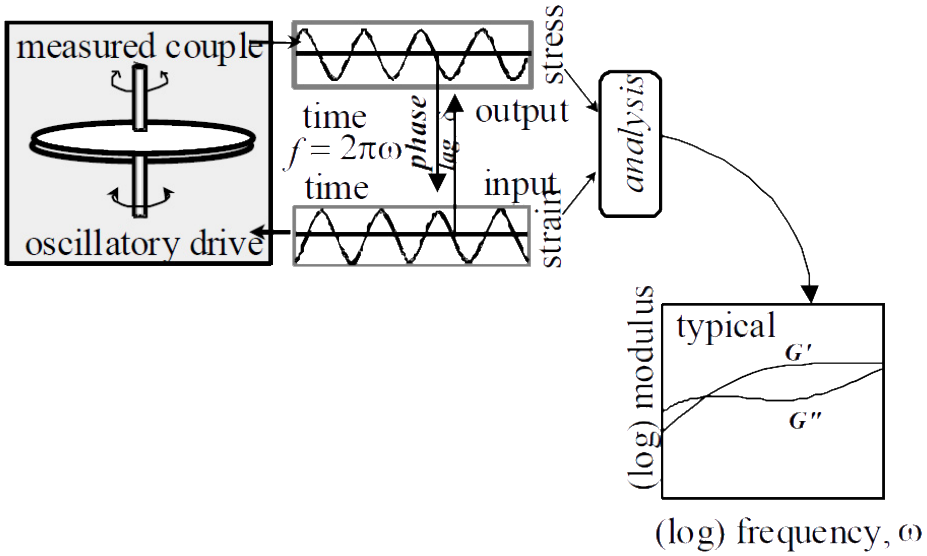

Fig. 2.11. Schematic representation of oscillatory testing.

The solid-like component at any particular frequency is characterised by the storage modulus**,** G', whilst the liquid-like response is described by the complementary loss modulus, G''. The values of both of these parameters vary with applied frequency, ω, which is given by 2πf, where f is the frequency in hertz (Hz).

Accordingly, several mathematical relationships can be established between different rheological parameters:

- Dynamic viscosity: $\eta' = \frac{G''}{\omega}$ (eq 2.4)
- Loss tangent: $\tan\delta = \frac{G''}{G'}$ (eq. 2.5)
- Complex modulus: $G^* = \sqrt{G'^2 + G''^2}$ (eq. 2.6)
- Complex viscosity: $|\eta^*| = \left[\eta' + \frac{G'}{\omega^2}\right]^{\frac{1}{2}}$ (eq. 2.7)

The most general overall *G', G''* response of structured liquids for such a test is shown in Fig. 2.12. The exact values of the moduli and their position in the frequency domain will vary, but the indicated overall qualitative behaviour is usually seen if data is available over a wide-enough frequency range.

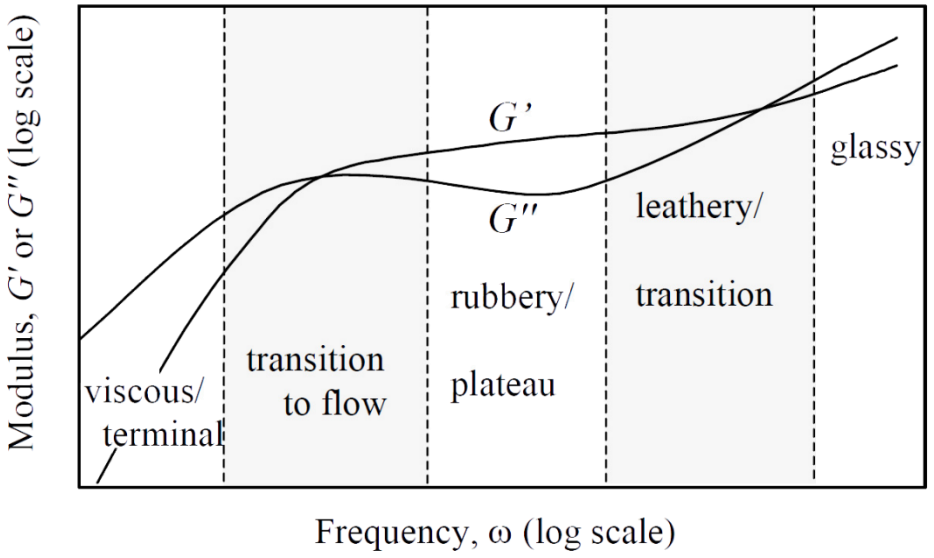

Fig. 2.12. Regions constituting the characteristic viscoelastic spectrum of a non-Newtonian liquid.

A number of specific regions can often be differentiated, namely:

- The viscous or terminal region, where *G'* predominates and viscous (flow) behaviour prevails. All materials have such a region, even solids (because they creep at long times), but the frequency where

this is seen is often so low that most oscillatory instruments cannot detect this part of the curve. At low-enough frequencies, *G''* is linear with increasing frequency and *G'* is quadratic.

- The transition-to-flow region is so called because, when viewed from higher frequencies (where elastic behaviour dominates and *G' > G'')*, the loss modulus *G''*, describing viscous or flow behaviour, becomes significant. The point where the two moduli cross over corresponds to the crossover frequency, indicating the change of prevailing response.
- The rubbery or plateau region is where elastic behaviour dominates. While in many cases there appears to be a flat plateau, there is always a slight increase of *G'* with frequency, but it can be as small as a few percent increase in modulus per decade increase in frequency. The value of *G''* is always lower than that of *G'*, but sometimes it can be considerably so. When the slope of the storage modulus versus frequency curve (G',ω) is small, the value of G'' decreases with increase in frequency, towards a minimum before rising again.
- The leathery or higher transition crossover region is also seen, where, due to high-frequency relaxation and dissipation mechanisms, the value of G'' again rises, this time faster than G'. Once more at G' = G'', a crossover frequency can be defined.
- At the highest frequencies usually encountered in this form of testing, a glassy region is seen, where G'' again predominates and continues to rise faster than G'.

If the range of testing is artificially extended by using different temperaturas (the so-called time/temperature superposition principle), then

for many materials, it is often possible to see all the regions described by superimposing the data using suitable shift factors (Barnes 2000).

10.Rheology of bitumen and structure-property relations

10.1. Steady state shear flow

As described in the previous section, a fundamental test, usually performed for the rheological characterization of any material, corresponds to the evaluation of the steady-state viscous flow behaviour, which accounts for the variation of viscosity with shear rate as a function of temperature.

In the case of bitumen, at high temperatures, it generally exhibits Newtonian behaviour over a relatively wide range of shear rates. Nevertheless, as shear rate is raised, a decrease in viscosity, which corresponds to a shear-thinning behaviour, may also be observed. This viscous behaviour is more apparent at high temperatures, due to the fact that higher shear rates are attained (Martínez-Boza et al. 2001; Stastna et al. 2003), as illustrated in Fig. 2.13.

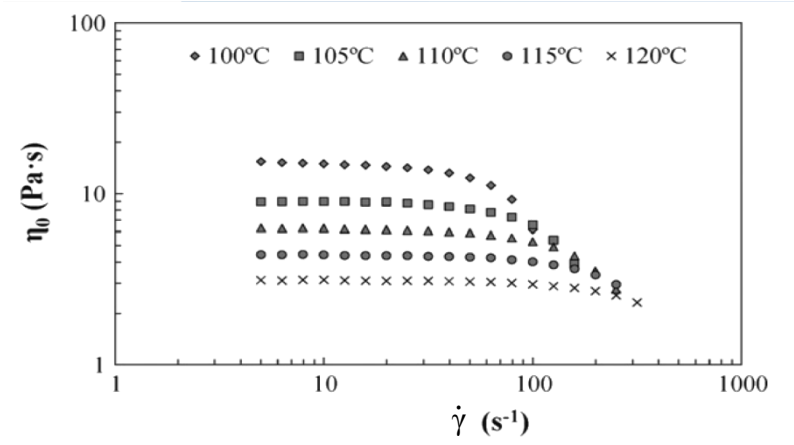

Fig. 2.13. Steady state shear flow tests at different temperatures for a neat bitumen (Baldino et al. 2013).

The transition from a Newtonian to a non-Newtonian flow has been traditionally attributed to the breakage of the weak structure-forming interactions and to the anisometric nature of asphaltenes aggregates, which orient themselves at high shear rates. It is worth noticing that, increasing the temperature, the shear thinning behaviour appears less pronounced, and the Newtonian plateau extends over a wider shear rate range. In this regard, the zero shear viscosity (η_0), well-known for heterogeneous systems, such as suspensions and emulsions, is considered a function of either suspending medium properties (e.g. viscosity) or suspended particles characteristics (e.g. size distribution, volume fraction and potential interactions among particles). Thus, in the case of bitumen, the zero shear viscosity can be related to that of the maltenic phase and to the effective volume of asphaltene aggregates (Baldino et al. 2013).

10.2.Linear viscoelasticity

The principal viscoelastic parameters usually measured for the characterization of bitumen are the complex shear modulus (G*****) and the phase angle (δ). G***** is defined as the ratio of maximum (shear) stress to maximum strain and provides a measure of the total resistance to deformation when the bitumen is subjected to shear loading. It contains elastic and viscous components, which are designated as the storage modulus (G') and loss modulus (G''), respectively. These two components are related to the complex (shear) modulus and to each other through the phase (or loss) angle (δ), which is the phase, or time, lag between the applied shear stress and shear strain responses (Airey and Rahimzadeh 2004), as described in section 9.4.4.2, "*Viscoelasticity and linear viscoelastic response*".

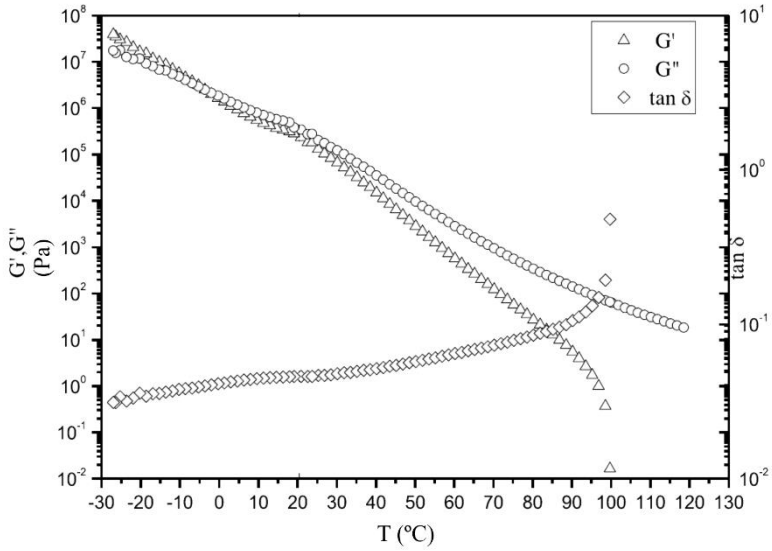

Fig. 2.14. General pattern for the dependency of the viscoelastic functions of a neat bitumen with temperature (Rossi et al. 2015).

Most of bitumen components are of low molecular weight, so that entanglement effects are not significant and, therefore, a continuous transition from the elastic (glassy) to the Newtonian region takes place by decreasing the frequency. Thus, three different regions can be observed in the dynamic mechanical spectrum of bitumen. The transition to the glassy region is mainly observed at low temperatures or in the high frequency region. This region is characterized by an increase in the slope of the storage and loss moduli and tends to disappear as the temperature increases. At intermediate temperatures, a predominantly viscous region with values of G'' higher than those of G' is achieved, transitioning as temperature raises in a continuous feature to the beginning of the Newtonian or terminal region, finally reached at high temperatures or low frequencies, in which the slope of the loss and storage moduli are proportional to 1 and 2, respectively, when represented in double-log scale (Fig. 2.14) (Partal et al. 1999; Martínez-Boza et al. 2001).

The phase angle, δ, or the loss tangent, tan δ, are also paramount parameters for the characterization of the rheological behaviour of bitumen, and those, as stated, are proportional to the ratio of the dissipated and stored energy, i.e. the ratio of the viscous and elastic components of the material. In bitumen, values of tan δ continuously decrease when frequency is raised or temperature is lowered, as depicted in Fig. 2.14 (Airey and Rahimzadeh 2004).

Such a depiction of bitumen's rheological behaviour broaches the additional concept of thermo-rheological simplicity, which constitutes somewhat of a point of contention amongst bitumen researchers. In a thermo-rheologically simple material, all contributing retardation or relaxation mechanisms have the same temperature dependence, and so do stress magnitudes at all times or frequencies. This brings about an equivalence between the effects of increasing the loading time (or decreasing the frequency) on the mechanical properties of a material, and those of raising temperature, hence conforming to the time-temperature superposition principle. This principle allows linear viscoelastic functions (oscillatory shear and creep) obtained at different temperatures, and represented on a double-logarithmic plot, to be shifted either vertically or horizontally, by using a specific constant, in order to give rise to a smooth single master curve that brings together all data over a range of times or frequencies wider than that feasibly attained at a particular temperature. Thus, it is widely accepted that when superposition of the linear viscoelastic functions of a material produces smooth continuous curves, these master curves may be used for comparison, providing useful information about the effects to be analysed, along with a compelling insight into the material's performance in a wider range of frequencies (Cuadri et al. 2013). Nevertheless, for a structurally complex and

heterogeneous material at a submicron scale, like bitumen, a good superposition is only achieved when the dispersed phase undergoes no structural change in the transition from the glassy to the Newtonian zone, which is however not the case of highly crystalline bitumens (wax contents > 7 wt.%), structured bitumen with high asphaltene contents, and highly polymer modified bitumens (Airey 2002; Airey and Rahimzadeh 2004). These could instead be considered thermo-rheologically complex materials. Thus, inconsistency in the applicability of a generalised definition for the thermo-rheological behaviour of all bitumens turns this subject somewhat controversial.

As proposed by some authors (Lesueur 2009), such a variability in the rheological response of bitumen arises as a result of two fundamental transitions: the Brownian/non-Brownian transition of the asphaltenes, which gives rise to a Newtonian/viscoelastic α-relaxation at temperatures around 60 ºC, and the glass transition of the maltenes, with a viscoelastic/elastic β relaxation at temperatures around -20 ºC.

As a consequence, low asphaltene content bitumens have a temperature-dependence close to that of their maltenes (which in turn will be close to that of lighter petroleum products); whilst high asphaltenes content bitumens are less temperature-susceptible. The Newtonian viscosity characterizes bitumen at high temperature (typically higher than 60 °C). At lower temperatures, its behaviour can still be Newtonian at very long loading times, but in most cases, viscoelasticity shows up. The rheology of bitumens can then be separated, as mentioned above, into three regions, corresponding to two distinct relaxation mechanisms, each associated to asphaltenes and maltenes:

- At high temperatures, approximately 60 ºC, a transition from Newtonian flow to viscoelastic flow occurs (α-relaxation), which has been attributed to the solid phase of the bitumen.
- In the low temperature region, at around – 20 ºC, a transition from viscoelastic flow to elastic glassy behaviour occurs (β-relaxation), mainly due to the glass transition of the liquid phase of the bitumen.

10.2.1. Newtonian-to-viscoelastic transition: α-relaxation

As stated, at temperatures slightly below those of the Newtonian region, viscoelastic effects start to show up, arising from α- relaxation mechanisms of bitumen. The switch from Newtonian behaviour to viscoelastic flow is attributed to the disappearance of the Brownian motion of the asphaltene aggregates. Once the viscosity of the bitumen becomes too high, the asphaltenes aggregates are locked in position; whereas at low enough viscosity values, they can freely diffuse within the maltenic matrix. The elasticity in the non-diffusive case would be a consequence of interparticle attraction. The transition from Newtonian to viscoelastic flow hence defines the "so-called" critical shear rate, critical stress or critical relaxation time.

This critical shear rate is essentially a function of asphaltene content and aggregates, and so, it is an intrinsic property of a given bitumen, directly related to its nanostructure, as evidenced by the proportionality between critical stress and viscosity in measurements of the permanent flow of bitumens under constant shear rate.

In summary, the bitumen α-relaxation at which viscoelastic effects start to appear is associated to the Brownian motion of the asphaltenes aggregates, and the associated relaxation time is proportional to the bitumen viscosity.

The maltenic fraction is however also directly involved in the phenomenon through the bitumen viscosity and there is therefore a strong coupling between asphaltenes and maltenes.

10.2.2. Viscoelastic-to-elastic transition: β-relaxation

At temperatures below that of the α-relaxation, the elastic character becomes predominant and the transition to elastic glassy behaviour is observed, represented by the β-relaxation of bitumen. The β-relaxation, transition from the viscoelastic to the elastic regime, is a consequence of the vitrification of the maltenic phase, which defines the glass transition temperature (T_g), in turn, dependent on the specific bitumen source and composition (Baldino et al. 2013; Rossi et al. 2015).

The glass transition temperature defines bitumen properties and its behaviour as temperature changes. Thus, when temperature is lower than T_g, bitumens are glassy, hard and brittle, whereas at temperatures higher than T_g, viscoelastic liquid-like properties are exhibited. The mechanical glass transition is normally detected by using DMA technique, corresponding to the value at which the loss modulus evidences a peak (Rossi et al. 2015).

Asphaltenes still have certain influence on the β-relaxation function, and the higher the asphaltenes content, the smaller the relaxation rate. Thus, analogously to the α-relaxation, there is again a coupling between asphaltenes and maltenes at low temperature as well. The origin of the elastic effects due to the freezing of the Brownian motion of asphaltenes remains still unclear, although it has been suggested that it might be a consequence of either particle-particle interactions or the deformation of asphaltenes aggregates, which can be regarded as supra-molecular

assemblies (Lesueur 2009), in close similarity to those described in the previous section 7.4, *"Supramolecular assembly model*".

11.Bitumen Modification

Bitumen's complex internal structure and composition reflects into its thermo-mechanical properties, characterized by a strong thermal susceptibility. This dependency with temperature becomes manifest in variable rheological behaviour, which at high temperatures corresponds to a viscoelastic liquid; whilst decreasing temperature turns it into a brittle viscoelastic material prone to cracking.

Nevertheless, the properties of bitumen have traditionally made it one of the most widely used materials for waterproofing applications. Currently, it is mainly used in paving industry, constituting a small but crucial part of any paving mix. The remaining part, around 10%, refers to its uses in industry and construction as roofing material, for thermal and acoustic insulation, humidity and corrosion protection components of paints and varnishes, etc.

The performance of bitumen during its in-service life is significantly influenced by its rheological (or mechanical) properties and, to a lesser extent, by its structural and chemical constitution, which might be, in turn, altered by external agents such as air (oxygen), U.V. radiation, temperature and water, hence varying its long-term durability.

Despite the enormous range of applications bitumen may find, most bitumens perform well for a long in-service life. However, sometimes, several problems may arise due to its complex rheological behaviour and the nature of the engineering application bitumen is required for, especially those involving resistance to permanent deformation and cracking, like in

paving applications. Amongst them, fatigue cracking, thermal cracking and high temperature deformation are the most common ones.

- **Fatigue cracking**

This phenomenon results from the repeated application of a stress that is less than the tensile strength of the material. Thus, when subjected to a certain load, the material flexes and a tensile strain is induced at the opposite side of the point of load application. Continuous flexure and relaxation over many years produces the possibility of fatigue cracks appearing in the zone where tensile strain is induced, propagating towards the region where the load is applied. This condition is most commonly observed in pavements, subjected to continuous traffic loads.

- **Thermal cracking**

Process resulting from either extreme cold, which is referred to as low-temperature cracking, or thermal cycling. In both cases, this process takes place when the tensile stress and related strain exceeds the breaking strength of bitumen (Fig. 2.15(a)), which might also be thermally induced, depending on the expansion and relaxation characteristics of the system. These two properties are in turn related to the nature of bitumen, and so, the risk of thermal cracking increases with the age of bitumen, as it hardens as a result of oxidation or time-dependent hardening (Masson et al. 2002), reducing its stress relaxation capability.

This condition, similarly to fatigue cracking, results in cracks appearing on pavement surface, as depicted in Fig. 2.15(b), being more likely to develop at low temperatures, given that stress relaxation at elevated temperatures will prevent stress from reaching levels that may lead to such an event.

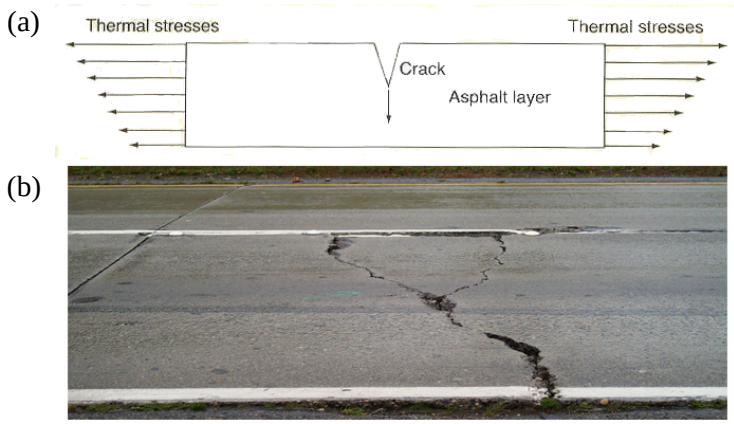

Fig. 2.15. (a)Thermal stresses behind cracking phenomenon in a pavement layer. (b) Cracks arising on a pavement surface.

- **High temperature deformation or rutting**

This process arises from the plastic deformation of the material as a consequence of the cumulative effect of repeated loadings of short duration and high shearing stresses, which most commonly become manifest as a depression or sunken area on pavement surface (Fig. 2.16). This type of problem gains more relevancy at high in-service temperatures, and its effects on bitumen are mainly associated to its viscosity.

Fig. 2.16. Depression appearing on a pavement surface as a consequence of rutting.

It is generally assumed that material response to loads during service corresponds to its linear regime, in which stress and strain are linearly

proportional to each other, so stiffness is independent of stress or strain and the resultant viscosity, the linear viscosity of bitumen, given by the zero-shear viscosity, η_0, also termed "Newtonian viscosity", is independent of the shear rate.

Hence, by measuring bitumen's properties within the linear regime, the likelihood of rutting can be determined, given that the higher the value of the zero-shear viscosity, the lower the influence of the permanent deformation on bitumen.

As a result, in an attempt to overcome or, at least, delay the above-described problems, bitumen properties tend to be improved by the addition of modifying agents. In this regard, any modifying agent for bitumen, in order to be effective enough and both practicable and economic, is desirable to comply with several characteristics (Isacsson and Lu 1995; Read and Whiteoak 2003):

- To be readily available.
- To resist degradation at high mixing temperatures.
- To blend with bitumen.
- To improve resistance to flow at high temperatures without making bitumen too viscous at mixing temperatures or too stiff or brittle at low temperatures.
- To be cost effective.

Furthermore, when blended with bitumen, any modifying agent must be capable of being processed by conventional equipment, as well as physically and chemically stable during storage, application and in service, maintaining its properties.

A wide range of materials, including sulphur, carbon black, maleic anhydride, carboxylic acids, phosphoric acid, posphazenes (Sureshkumar et al. 2010), special fillers, mineral fibres or rubbers (Read and Whiteoak 2003) have been used for the modification of bitumen.

Yet, polymers are the most commonly used modifying agents for bitumen, producing the so-called polymer-modified bitumens (PMBs).

11.1. Polymer-based modification

The addition of one or more compatible polymers to bitumen is aimed at developing a physical network within the bituminous matrix, which generally results in thermodynamically unstable but kinetically stable mixtures (understanding stability as being limited by the maximum time of high temperature storage), accompanied by improvements in performance and properties.

Despite the great variety of polymers used as modifying agents, they can be subdivided into three major categories: thermoplastic elastomers, plastomers, and reactive polymers (Polacco et al. 2006).

- **Thermoplastic block copolymers**

This class of polymers is the most frequently used for bitumen modification, among which poly(styrene-b-butadiene-b-styrene) (SBS) is the preferred one. Styrene-b-isoprene-b-styrene (SIS), belonging to the same copolymer family, is also commonly used.

Modification is normally achieved by simple mechanical dispersion in molten bitumen under high shear.

This type of polymers exhibit great qualities in strength and elasticity, such that when physical crosslinking of their molecules takes place into a three-

dimensional network within bitumen, the elastic recovery capacities and resistance to permanent deformation of the modified bitumen are noticeably enhanced, especially at low temperatures. However, they are quite expensive, and if a high number of unsaturated C=C double bonds are present, they are also prone to undergo degradation phenomena that strongly limit their duration and recyclability (Zhu et al. 2014; Polacco et al. 2015).

- **Plastomers**

Polyolefinic plastomers confer on bitumen high rigidity and resistance to deformation. Polyethylene (PE) and polypropylene (PP) are the two main representatives of this category, although due to their non-polar nature, they are almost completely immiscible with bitumen. Moreover, their high tendency to crystallize further limits the interaction with bitumen, given that rigid domains associated to crystalline molecular areas somehow tend to hamper the swelling process of the polymer molecular chains in the amorphous phase by lighter compounds in bitumen, hence hindering the formation of a physical network.

Nevertheless, their compatibility with bitumen can be enhanced by the insertion of polar groups in their structure, as is the case of ethylene-vinylacetate (EVA) and ethylene-butyl acrylate (EBA), in which the presence of an ester group increases polarity and reduces their crystallization tendency.

- **Reactive polymers**

This category comprises polymers with reactive functional groups in their structures, suitable to react with some bitumen components, rather than physically mix or interact. Amongst them, the most relevant ones are ethylene polymers and isocyanate-based polymers (Zhu et al. 2014). The

latter will be explained in greater detail in section 11.2, "*Isocyanate-based modification*". As for the former, reactive ethylene polymers are mainly reported as ethylene-based copolymers containing epoxy rings, such as the so-called reactive ethylene terpolymers (RETs), which are ethylene-based copolymers containing glycidylmethacrylate (GMA) and an ester group (usually methyl, ethyl or butyl acrylate). This type of reactive polymer has been developed as compatibilizers for blends of polyolefin and other polymers containing a functional group capable of reacting with the epoxy ring. Analogously, the chemical characteristics of these copolymers also make them favourable to react with some groups in bitumen, such as carboxylic, hydroxyl or amine ones, with noticeable improvements in mechanical properties of the material (Polacco et al. 2004). Nevertheless, the high content of reactive groups in RETs may lead to unstable PMBs, due to the tendency of RETs to form chemical polymeric networks instead of physical ones (excessive crosslinking). This might provoke the gelation of modified bitumen, with no significant improvement in performance when used in road applications, as evidenced by some works (Selvavathi et al. 2002; Polacco et al. 2004; Pérez-Lepe et al. 2006).

Other types of reactive polymers would correspond to epoxy resins, which are used for the production of bitumen containing components of a thermoset epoxy resin, in which a chemically crosslinked network entraps bitumen, representing an interesting solution for special applications such as flexible decks or extreme climates.

11.1.1. Polymer modification mechanism

In general, as described in the literature (Polacco et al. 2006; Polacco et al. 2015), obtaining the maximum modification performance for any PMB relies on the formation of a bitumen-dispersed phase in a polymer continuous one upon mixing. In this regard, during the mixing process, the polymer is partially swollen by the lighter bitumen components, and so, the final mixture should ideally consist of a biphasic system with a polymer-rich phase (PRP) coexisting with an asphaltene-rich phase (ARP) in a micro-scale metastable equilibrium, thermodynamically tending to separation, but kinetically impeded if viscosity is high enough (as would be the case of viscosity at ambient temperature). With regard to bitumen for paving applications, some studies (Polacco et al. 2006; Sureshkumar et al. 2010) indicate that the addition of polymers in percentages ranging from 3 to 7 wt.% represents the interval where the so-called "phase inversion" occurs, which refers to a certain morphological state that may be reached when polymer and bitumen are mixed. The mixing process, depending on the swelling ability of bitumen and operating conditions (duration, temperature, shear stress, etc.) may lead to various morphologies, and thus, different degrees of improvement in bitumen properties, as illustrated in Fig. 2.17.

Hence, if polymer is swollen by a small quantity of bitumen molecules (normally at short mixing times), the PRP is dispersed in the continuous ARP, with overall properties not differing from those of the unmodified bitumen. By contrast, if a sufficient degree of swelling is reached, PRP may form a continuous phase, which would correspond to the phase inversion morphology. Moreover, various authors (Polacco et al. 2006; Polacco et al. 2015) point out that in the case of complete swelling, the ARP might

disappear, and if accompanied by the destruction of the polymer network, no improvement in performance can be obtained.

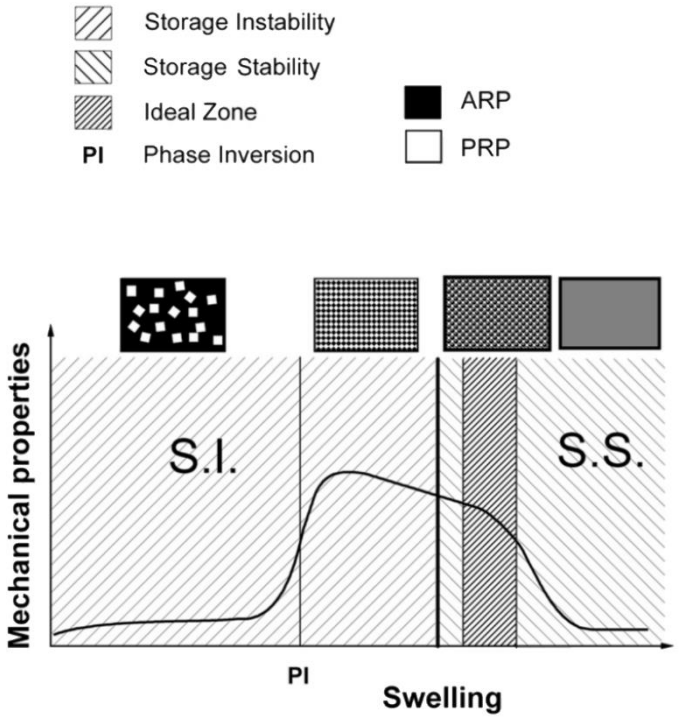

Fig. 2.17. Qualitative behaviour of a generic mechanical property with polymer swelling.

Similarly, it has also been stated by Zhu et al. 2014 that when the phase inversion is reached, the polymer content is high enough so that, due to swelling, its phase forms a continuum or network where the asphaltene-rich phase is dispersed. In these circumstances, the rheological properties of the polymer significantly resemble those of the PMB, which in turn, result improved with respect to those of neat bitumen, showing better overall performance in mechanical properties, storage stability and cost-effectiveness.

Nevertheless, despite the above-mentioned properties for PMBs, it is widely known the low compatibility between polymers and bitumen, and the technical difficulties that may derive from it. Moreover, several other

drawbacks like bitumen oxidation and polymer degradation, and their effects on the applicability of PMBs, including high temperature sensitivity, low ageing resistance, poor storage stability and limited improvements in elasticity also contribute to restrict the applicability of polymers for the modification of bitumen. This is further limited not only by technical aspects, but economic factors are also relevant, and in certain types of modified polymers, their use usually involves a relevant added cost in order to fulfil performance requirements.

11.2. Isocyanate-based modification

This type of modification involves the use of low-molecular weight isocyanate-functionalized compounds that in the presence of groups containing active hydrogen atoms lead to the formation of polymeric networks based on urethane/urea linkages.

These compounds, which generally correspond to polyfunctional isocyanates containing two or more –NCO groups per molecule, can be aliphatic, cycloaliphatic, polycyclic or aromatic in nature. Within such a variety of isocyanate-functionalized compounds, more than 90% of the total world production is accounted for by three products, all of them aromatic: polymeric MDI (pMDI), its co-product 4,4'-diphenylmethane diisocyanate (MDI) and toluene diisocyanate (TDI). However, due to health and safety hazards, TDI tends to be replaced by the less volatile MDI and pMDI, especially by the latter, given its lower cost and liquid state, which facilitates handling tasks.

11.2.1. Manufacture of isocyanates

Aromatic diisocyanates are manufactured by reaction of phosgene ($COCl_2$) with the corresponding amines. Thus, in the case of MDI and pMDI, they

are produced by the acid catalysed condensation of aniline with formaldehyde, resulting in amines that subsequently react with phosgene, yielding a mixture of MDI and pMDI. Then, MDI, containing about 98 wt.% of the 4,4'-isomer, along with 2,4'-isomer and trace amounts of the 2,2'-isomer, is obtained by partial distillation under vacuum of such a mixture, yielding a colourless crystalline solid at room temperature with tendency to dimerize. The residue of such partial distillation is pMDI, a dark brown liquid consisting of around 50 wt.% of remaining MDI, and 50 wt.% of oligomeric isocyanates with a functionality of 3 and higher, although its composition depends on the amount of MDI removed by distillation (Ulrich 1996).

11.2.2. The chemistry of isocyanates

In all these compounds, the reactivity of the isocyanate group is governed by the electron deficiency on the carbon atom, as the cumulated double bond sequence gives rise to resonance structures (Fig. 2.18). Thus, carbon atom results susceptible to be attacked by nucleophiles, whereas oxygen and nitrogen, by electrophiles, with most reactions taking place across the C=N bond (Fig. 2.18(b2)).

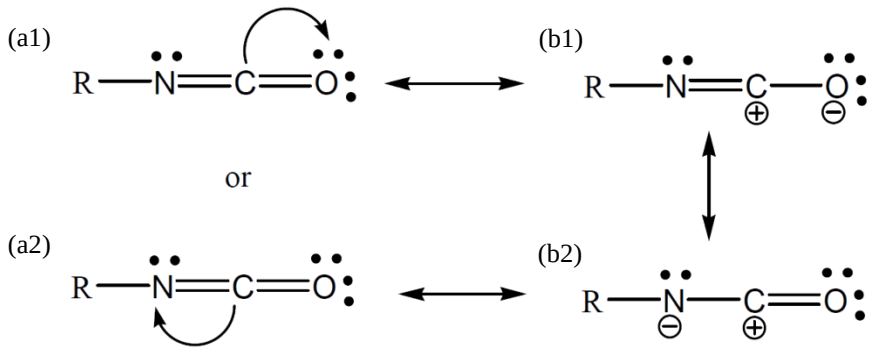

Fig. 2.18. Resonance structures of the isocyanate group.

In case R is an aromatic group, the negative charge on the nitrogen will be delocalized into R (Fig. 2.19), further reducing the electron charge on the central carbon of the isocyanate. This results in higher reactivity of aromatic isocyanates when compared to aliphatic or cycloaliphatic isocyanates, although steric hindrance may reduce the reactivity. In this sense, as a general outline, any electron-withdrawing substituents linked with R in ortho or para position will increase the positive charge on carbon, thereby increasing reactivity of the isocyanate group towards nucleophilic attack. Moreover, the nature of the substituent also determines the reactivity, such that electron-donating substituents decrease the reactivity of isocyanate groups.

In diisocyanates, the presence of the electron-withdrawing second isocyanate increases the reactivity of the first isocyanate. Hence, para substituted aromatic diisocyanates are more reactive than their ortho analogues, primarily attributed to the steric hindrance conferred by the second –NCO functionality.

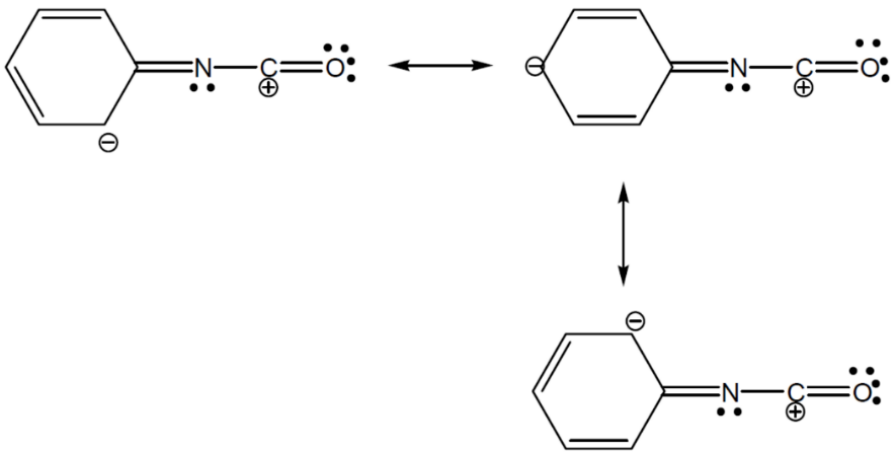

Fig. 2.19. Resonance structures of an aromatic isocyanate.

Isocyanates having the structure R-N=C=O, where R is an alkyl or aryl group, react under mild conditions with compounds containing active

hydrogen atoms, which would correspond to -OH groups (e.g. alcohols, carboxylic acids and water), >NH groups (e.g. amines), or -SH groups (e.g. thioalcohols and thiophenols), giving rise to urea, urethane and amide linkages, according to the following reaction scheme:

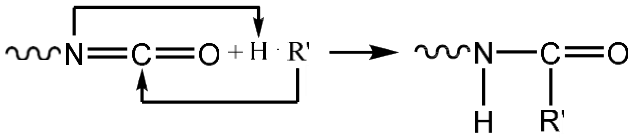

Fig. 2.20. General reaction scheme between an isocyanate group and any functional group containing an active hydrogen atom.

As shown above, the electrophilic carbon of the isocyanate is attacked by the nucleophilic centre of the active hydrogen compound, and hydrogen is added to the isocyanate group.

The order of reactivity of active hydrogen compounds with isocyanates is included in Table 2.1.

Table 2.1. Classification of active hydrogen compound based on their relative reactivity with the isocyanates group.

Active Hydrogen Compound	Typical Structure	Relative Reaction Rate Uncatalyzed at 25C
Primary Aliph. Amine	$R\text{-}NH_2$	100,000
Secondary Aliph. Amine	$R_2\text{-}NH$	20,000-50,000
Primary Aromatic Amine	$Ar\text{-}NH_2$	200-300
Primary Hydroxyl	$R\text{-}CH_2\text{-}OH$	100
Water	H-O-H	100
Carboxylic Acid	$R\text{-}\overset{\overset{O}{\|\|}}{C}\text{-}OH$	40
Secondary Hydroxyl	$R\text{-}\overset{\overset{R}{\|}}{C}H\text{-}OH$	30
Ureas	$R\text{-}NH\text{-}\overset{\overset{O}{\|\|}}{C}\text{-}NH\text{-}R$	15
Tertiary Hydroxyl	$R\text{-}\overset{\overset{R}{\|}}{\underset{\underset{R}{\|}}{C}}\text{-}OH$	0.5
Urethane	$R\text{-}NH\text{-}\overset{\overset{O}{\|\|}}{C}\text{-}O\text{-}R$	0.3
Amide	$R\text{-}\overset{\overset{O}{\|\|}}{C}\text{-}NH_2$	0.1

Generally, isocyanate-involved reactions can be divided into two classes (Sharmin and Zafar 2012): primary and secondary addition reactions with any compound containing active hydrogen atoms, and self-addition reactions. In some of them, CO_2 is released.

11.2.2.1. Primary and secondary addition reactions

The most important addition reaction of isocyanates is between these and hydroxyl groups (Fig. 2.21(c) and (d)), which is exothermic and reversible. Amongst hydroxyl-containing compounds, aliphatic primary alcohols are the most reactive, with faster reaction kinetics than secondary and tertiary alcohols, due to steric factors. Phenols also react with isocyanates, but much slower than alcohols, and result in readily broken urethane groups.

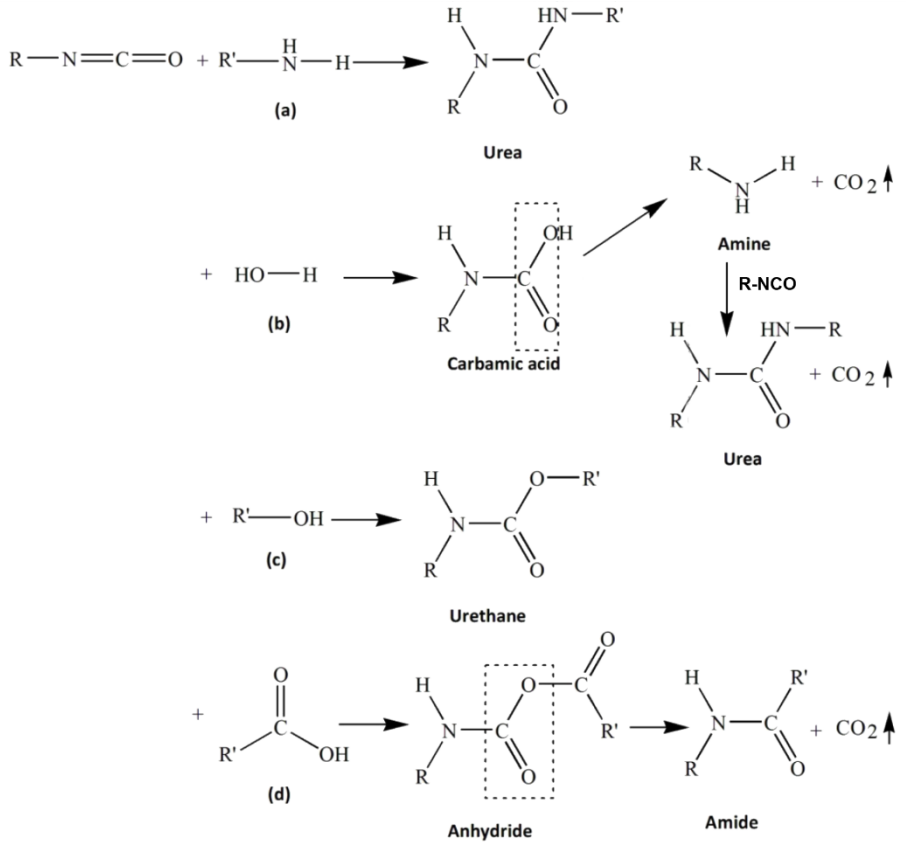

Fig. 2.21. Primary addition reactions of isocyanate with (a) amine, (b) water, (c) alcohol, and (d) carboxylic acid.

Thus, the urethanes formed have variable stability, depending on their structure. In this regard, urethanes formed from tertiary alcohols decompose readily at temperatures as low as 50 ºC; whereas urethanes from many primary and secondary alcohols may undergo changes only slowly at 150 – 200 ºC, also influenced by the presence of other reactants (Saunders 1959).

The reaction of isocyanate with water is also important and produces primary amine and carbon dioxide (Fig. 2.21(b)). The amine will then immediately react with another isocyanate to form symmetric urea.

The next important reaction is the isocyanate-amine reaction (Fig. 2.21(a)). Isocyanate reacts with primary and secondary amines to produce di- and tri-substituted urea.

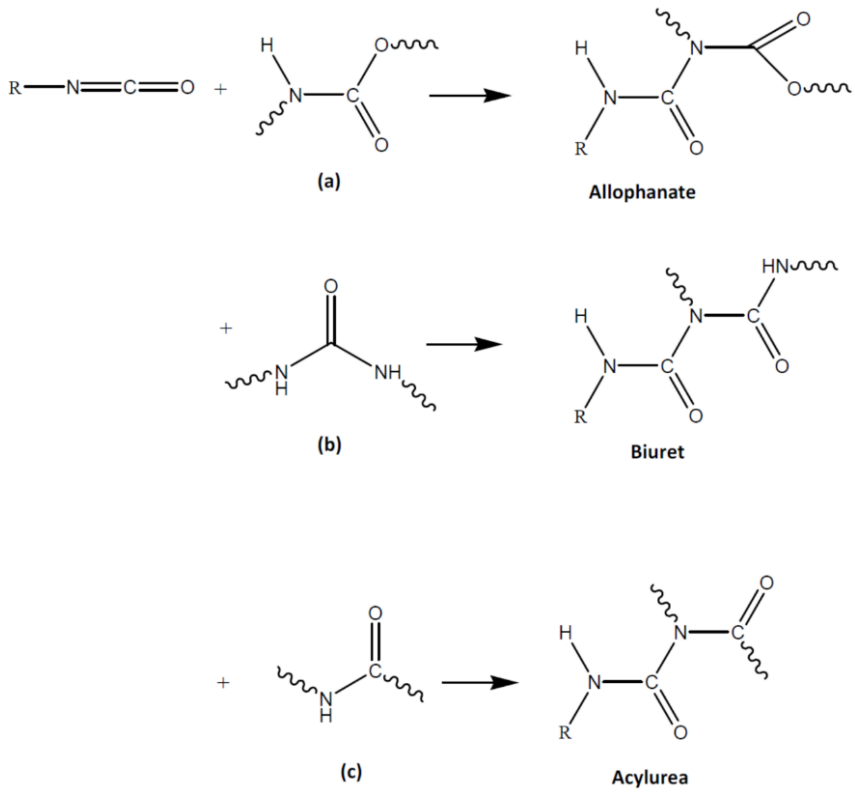

Fig. 2.22. Secondary addition reactions of iscoyanates with (a) urethane, (b) urea, and (c) amide.

The urethane, urea and amide groups formed in the previous reactions contain other "active" hydrogen atoms that can further react with isocyanate groups through secondary addition reactions to form allophanates, biurets and acylureas (Fig. 2.22). These reactions usually become important at 100 ºC and above (Saunders 1959), with biuret reaction proceeding at lower temperatures and significantly faster than the allophonate reaction.

Isoyanate-biuret and isocyanate-urethane reactions usually lead to branching or cross-linking of the polymer chain, with significant effects on the properties of the product.

11.2.2.2. Self-addition reactions

Isocyanates may also react with each other at high temperatures (Saunders 1959), or if special catalysts are used (oligomerization reaction) (Fig. 2.23).

In these reactions, products such as isocyanurates (trimers), uretdiones (dimers) or carbodiimides are formed. Isocyanates undergo a mild exothermic cyclo-addition reaction across two C=N bonds resulting in a four-membered ring called a dimer or uretdiones. Dimer formation mainly arises with aromatic isocyanates, but the reaction is slowed down by ortho substituents. This reaction has low relevancy at elevated temperatures, given that above 150 ºC many dimers tend dissociate to monomers. Moreover, dimers may also react with amines at temperatures around 50 ºC and higher; and with hydroxyl compounds at higher temperatures.

In addition to dimer formation, three isocyanates can undergo a cyclisation reaction across the C=N bond, resulting in a six-membered ring called trimer or isocyanurate. Trimerization reaction is exothermic and continues until all the –NCO groups have reacted. Both aliphatic and aromatic

isocyanates can undergo trimerization, forming trimmers, which are quite stable in the range of 150 – 200 ºC. Similar to dimerization, the presence of ortho substituents greatly reduces the tendency to trimerize. This type of reactions generally takes place in the presence of basic catalysts, such as alkyl metal alkoxides and carboxylic acid salts, and at very high temperatures (180 – 300 ºC), it ultimately leads to the formation of carbodiimides (Saunders 1959).

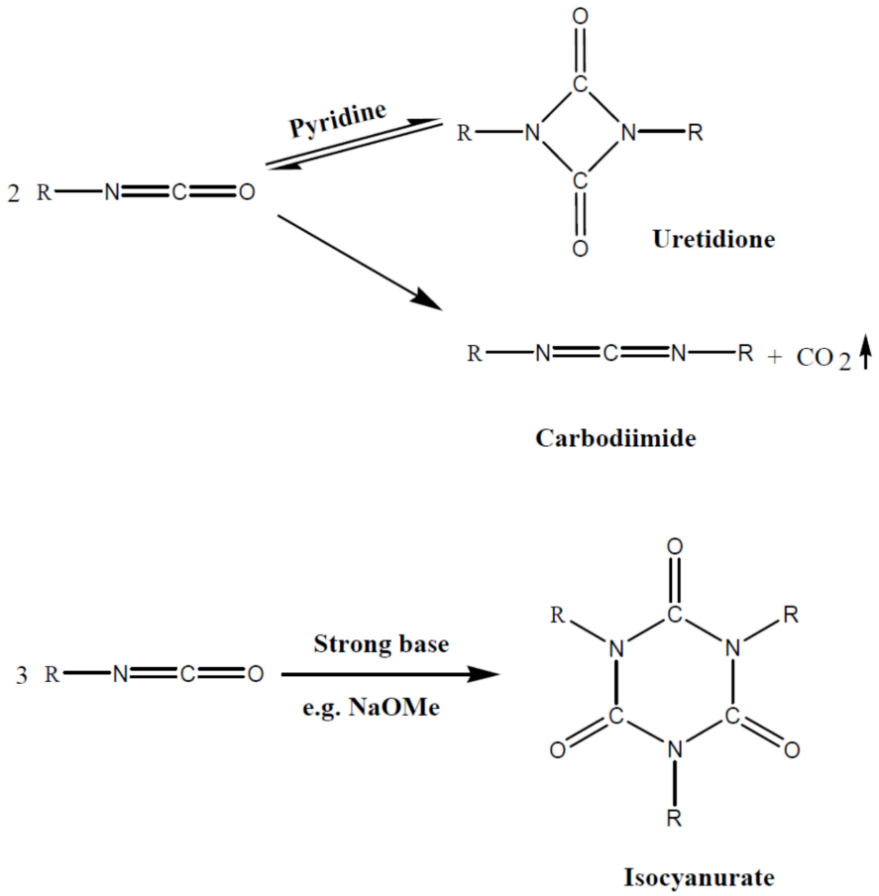

Fig. 2.23. Self-addition reactions of isocyanate.

11.2.3. Isocyanate-bitumen reactive interaction

Isocyanates have been defined as being capable of reacting with any compound containing functional groups with active hydrogen atoms, which correspond to -OH, >NH, and -SH groups. These isocyanate-involved reactions give rise to a wide range of possible linkages between the molecules involved, mainly urethane, urea and amide bonds.

Bitumen exhibits a highly complex composition, including a wealth of heteroatomic species and functional groups, as described above in section 5, "*Bitumen composition*". According to its fractional characterization, bitumen compounds can be grouped into saturates, aromatics, resins and asphaltenes, in increasing order of polarity, although asphaltenes constitute a solubility class, as there are separated based on their solubility properties.

On the basis of this classification and polar properties of each of the fractions, it has been assumed that heteroatoms are mainly to be found as part of both the asphaltenic and resin fractions of bitumen. Principally, in the form of sulphides and thiols and, to a lesser extent, in sulfoxides; pyrrolic and pyridinic structures, ketones, phenols, carboxylic acids and esters (Read and Whiteoak 2003).

Those functional groups in asphaltenes and resins have been shown to react with isocyanate moieties of isocyanate-functionalized compounds under mild conditions (Bukowski and Grętkiewicz 1982), also confirmed by rheological and calorimetric techniques (Singh et al. 2003), mostly resulting in the formation of molecular structures containing urethane and urea linkages, as depicted in Fig. 2.24.

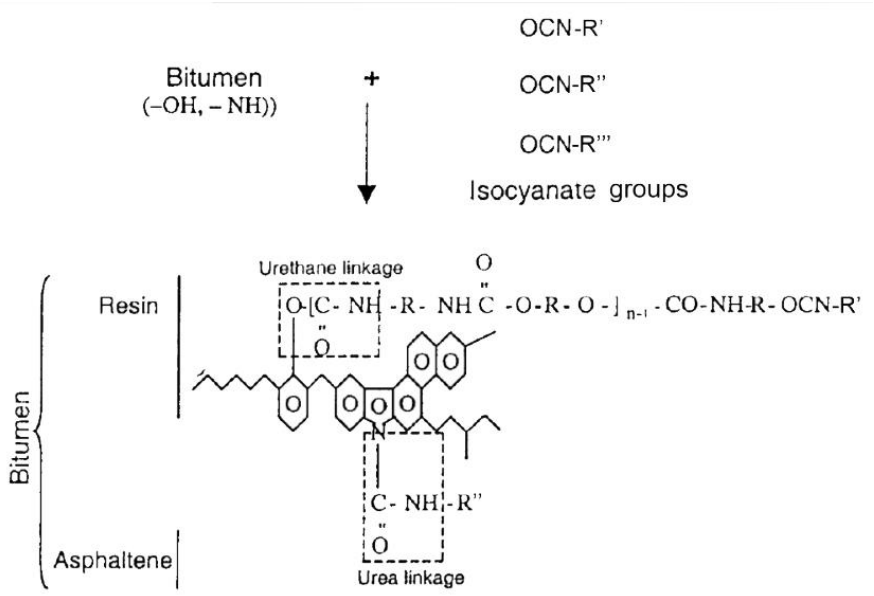

Fig. 2.24. Possible reaction scheme between isocyanate moieties and some bituminous fractions (asphaltenes and resins).

Accordingly, isocyanate-based modification of bitumen with the use of low-molecular-weight isocyanate-functionalized compounds, such as MDI and pMDI, or in the form of prepolymers in combination with polyols, has led to noticeable improvements in the thermo-mechanical properties of modified bitumens (enhanced linear viscoelastic response at high temperatures with greater elastic component). This is evidenced by a wealth of literature (Navarro et al. 2006; Navarro et al. 2007; Carrera et al. 2010; Izquierdo et al. 2013), also including viscosity enhancements and better storage stability at high temperatures (Navarro et al. 2007; Navarro et al. 2009).

However, this type of bitumen modification has failed to enhance low-temperature properties, as compared to the modification with some polymers, like SBS. Furthermore, similarly to the reactive ethylene terpolymers (RETs), the reactions between isocyanate-based compounds

may also lead to gelation of modified bitumen, with no significant effects on end properties of the bituminous system (Navarro et al. 2007).

11.3. Clay-based modification

The search for modifying agents of bitumen has involved, as mentioned above, a wide range of materials other than polymers. As of recently, layered silicates (LS) or clays, which are long known for their use in combination with polymers in polymer/layered silicate nanocomposites (Sinha Ray and Okamoto 2003), have also attracted increasing interest and importance as modifying agents for bitumen.

From a chronological point of view, the study of bitumen/clay interactions started well before the introduction of polymeric nanocomposites, and probably dates back to the use of the so-called oil-sands, which are naturally composed of both components. In this case, the main goal was somehow opposite, because it was necessary to remove the clays from the native oil.

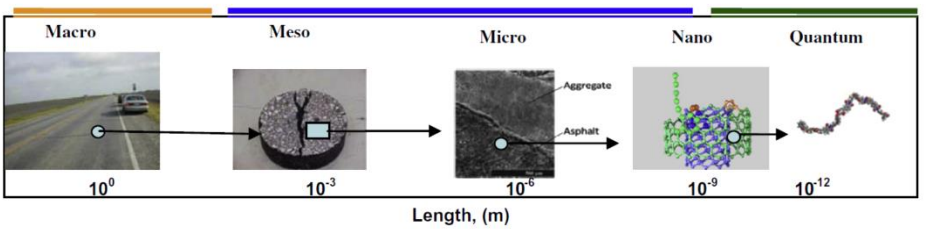

Fig. 2.25. Illustration of the evolution of different bitumen length scales.

In recent years, nanotechnology has gradually been incorporated into the field of modified bitumen with various kinds of nanomaterials, driving a further step in the evolution of the length scales of bitumen modification, from macro to meso, then to micro, and so far, to nano and quantum scales, as Fig. 2.25 illustrates. The microstructure is the sole determinant of macro properties, thus nanomodified bitumen offers a significant improvement

over the fundamental material properties, which is superior to other bitumen modification methods (Fang et al. 2013; Golestani et al. 2015).

Unlike conventional inorganic fillers, the high aspect ratio (e.g. 10 – 1000) (Krishnamoorti and Giannelis 1997) of clays provides a surface area for bitumen/clay interaction much larger than that formed in systems with conventional fillers (Sinha Ray and Okamoto 2003; Jahromi and Khodaii 2009). Thus, whilst those are usually added in percentages varying from 20 to 40 wt.%, typical quantities for nanocomposites range between 2 and 5 wt.% (Polacco et al. 2008; de Paiva et al. 2008; Jahromi and Khodaii 2009; Polacco et al. 2015), resulting in low content requirements, and hence, an economical alternative to polymers, accompanied by several other advantages attributable to their nanoscopic features (e.g. high surface area, strong adsorption, good dispersal ability, high chemical purity, and excellent stability) (Yao et al. 2013).

Moreover, nanoclays are fairly inexpensive, naturally abundant and sustainable materials, so that a significant portion of the current usage of the polymer-modified binder (PMB) can potentially be replaced by nanoclay-modified bitumen for improved mechanical and functional characteristics (Hossain et al.).

11.3.1. Classification and structural properties of clays

Generally, clay minerals, also known as phyllosilicates, or hydrated phyllosilicates (layered clay minerals) are fine-grained fraction of rocks, sediments or soils, which acquire plasticity in water and dry when heated. Clay minerals are normally sourced from clays, which correspond to a naturally occurring material composed of fine-grained minerals (Annabi-Bergaya 2008). As far as nomenclature is concerned, for the sake of

brevity, the term clay will be used in the present work for referring to clay minerals employed for bitumen modification.

In addition to naturally occurring clays, synthetic ones can also be produced, hence broadening the classification to two types: natural and synthetic clays. The former, due to their availability, reduced cost, modifying performance and environmental friendly features, are the most commonly used ones for bitumen modification. The category representing natural clays encompasses several types of clays differing in structure and composition, which establish the bases for their classification, as illustrated in Fig. 2.26.

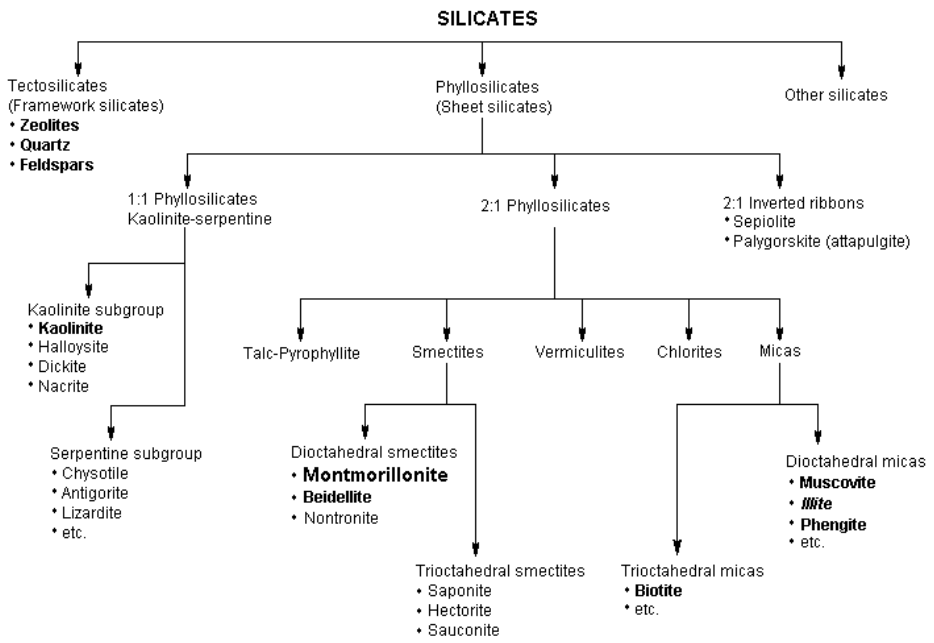

Fig. 2.26. General classification for silicates (clays).

The structure of clays consists of two basic units: an octahedral sheet and a tetrahedral sheet. The octahedral sheet is comprised of closely packed oxygens and hydroxyls in which aluminium, iron, and magnesium atoms

are arranged in octahedral coordination. When aluminium with a positive valence of three is the cation present in the octahedral sheet, only two-thirds of the possible positions are filled in order to balance the charges. When only two-thirds of the positions are filled, the mineral is termed dioctahedral. When magnesium with a positive charge of two is present, all three positions are filled to balance the structure and the mineral is termed trioctahedral. The second structural unit is the silica tetrahedral layer, in which the silicon atom is equidistant from four oxygens, or possibly, hydroxyls arranged in the form of a tetrahedron with the silicon atom in the center. These tetrahedrons are arranged to form a hexagonal network repeated in two horizontal directions to form what is called the silica tetrahedral sheet. The silica tetrahedral sheet and the octahedral sheet are joined by sharing the apical oxygens or hydroxyls to form what is termed the 1:1 clay mineral layer (e.g. kaolinite) or the 2:1 clay mineral layer (e.g. smectite).

Each layer or platelet, separated from its neighbors by a van der Waals gap called gallery or interlayer space, is characterized by a thickness of around 1 nm, and lateral dimensions varying from 30 nm to several microns (Choudalakis and Gotsis 2009). Galleries are usually occupied by cations that counterbalance the negative charge generated by the isomorphic substitution of the tetrahedral or octahedral cations (Mg^{2+} in the place of Al^{3+} in montmorillonite or Li^{+} instead of Mg^{2+} in hectorite). These cations are normally hydrated alkaline and alkaline-earth metal cations (Zanetti et al. 2000; Choudalakis and Gotsis 2009).

The structure and composition of the major industrial clays, i.e. kaolins, smectites, and palygorskite–sepiolite, are very different, even though they are each comprised of octahedral and tetrahedral sheets as their basic

building blocks. The arrangement and composition of these octahedral and tetrahedral sheets account for most of the differences in their physical and chemical properties.

The commonly used layered silicates for bitumen modification belong to the same general family of 2:1 phyllosilicates, more concretely, those included within the group of the smectite minerals (Sinha Ray and Okamoto 2003).

This group of layered silicates includes several hydrated sodium, calcium, magnesium, iron, and lithium-aluminium silicates, as depicted in Fig. 2.26. The major minerals in the smectite group are sodium montmorillonite, calcium montmorillonite, saponite (magnesium montmorillonite), nontronite (iron montmorillonite), hectorite (lithium montmorillonite), and beidellite (aluminium montmorillonite).

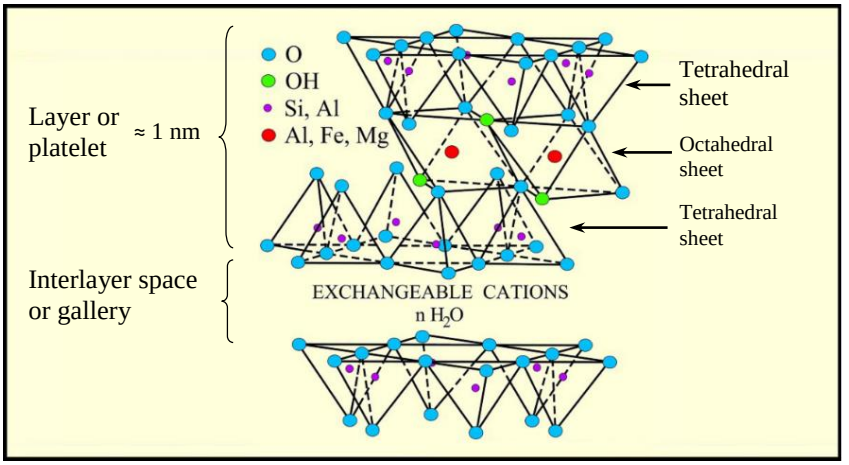

Fig. 2.27. General structure of 2:1 phyllosilicates (Kotal and Bhowmick 2015).

As a 2:1 layered mineral, smectites are composed of two silica tetrahedral sheets with a central octahedral sheet, and water molecules and cations occupying the space between the 2:1 layers (Fig. 2.27). There can be considerable substitution in the octahedral sheet of Fe^{2+} and Mg^{2+} for Al^{3+},

which creates a charge deficiency in the layer, and also, some substitution of silicon by aluminium in the tetrahedral sheets, which again creates a charge imbalance. This affects the total charge of the 2:1 layer as well as the local negative charge at the layer surface, which is balanced by exchangeable cations adsorbed between the unit layers and on the edges. Thus, if the exchangeable cation is sodium, the specific mineral is sodium montmorillonite and if it is calcium, it is a calcium montmorillonite. Substitution within the lattice causes about 80% of the total cation exchange capacity, whilst broken bonds around the edges, about 20%. These events have implications for many physical properties of smectites such as swelling and rheological behaviour.

The most common smectite mineral is calcium montmorillonite, which contains hydrated calcium cations in the interlayer, accompanied by two layers of water molecules; whilst in the case of the sodium montmorillonite, the interlayer space is occupied by sodium ions associated to one layer of water molecules. It is also worth mentioning that the rock term bentonite is commonly used for any clay dominantly comprised of a smectite mineral without regard to its origin. As for industrially used bentonites, these are predominantly comprised of either sodium montmorillonite, calcium montmorillonite, or, to a much lesser extent, hectorite (Murray 2006).

11.3.2. Organo-modification of layered silicates

In order to maximize the performance of nanocomposites, the silicate layers have to be effectively dispersed at the nanometre scale, in this case, within the bituminous matrix, for which a successful delamination and further dispersion of clay layers is required. This involves the separation of the clay layers and insertion of bitumen molecules in-between, which in

turn, establishes a compatibility prerequisite between both the matrix and the clay.

In the case of bitumen, the interactions with clays are slightly favoured by various factors, such as asphaltenes, which guarantee the presence of polar functional groups; and the low molecular weight components of maltenes, which may easily intercalate between the clay platelets owing to their small dimensions (Polacco et al. 2015).

However, pristine smectite layered silicates usually contain hydrated Na^+ or K^+ ions in the gallery, and thus, they are only compatible with hydrophilic materials. Therefore, when bitumen and clay are blended together, mechanical forces alone are not sufficient; rather, there should be a thermodynamic driving force (compatibility) to separate the layers into the primary silicate sheets. This thermodynamic driving force is introduced by inserting molecules of surfactants (which reduces surface tension) on each individual layer (Jahromi and Khodaii 2009). These surfactants or amphiphilic molecules are normally cations of alkylammonium salts (onium salts), including primary, secondary, tertiary, and quaternary alkylammonium cations or phosphonium cations that contain various substituents, which render the hydrophilic layered silicates organophilic, and thus, increase their compatibility with engineering non-polar or organic compounds, such as bitumen.

It is also worth pointing out that at least one of the substituents must be a long carbon chain of 12 carbon atoms or more, in order to make the clay mineral compatible with bitumen or polymers (Choudalakis and Gotsis 2009; Kotal and Bhowmick 2015).

The formation of these organophilic clays, also called organoclays, is achieved due to the property of smectites to exchange cationic species from solution, represented by the cation exchange capacity (CEC), which follows the general reaction equation shown next (Jahromi and Khodaii 2009):

$$M - CLAY + CH_3(CH_2)_nNR_3X \rightarrow CH_3(CH_2)_nNR_3 - CLAY + MX \quad \text{(eq. 2.8)}$$

Where:

$R = -H, -CH_3$; $X = -Cl, -Br, -I$; and $M = Na^+, Ca^+, Mg^+$

CEC values are expressed in centimoles of positive charge per kilogram of dry clay mineral (cmol(+)/kg), which is numerically equal to the traditional unit of milliequivalents per 100 g clay (meq/100 g). Sodium montmorillonite and hectorite have high base-exchange capacities, generally ranging between 80 and 130 meq/100 g. Calcium montmorillonite, on the other hand, has a base-exchange capacity that normally ranges between 40 and 70 meq/100 g (Murray 2000; Tjong 2006).

The high charge on the lattice gives both sodium montmorillonite and hectorite the capacity to exchange the interlayer water and associated cations. Nevertheless, water swelling of the silicate is needed to obtain the exchange of the onium ions with the cations in the galleries. For this reason, alkali cations are preferred in the galleries, since two and higher valent cations prevent water swelling. Indeed, the hydrate formation of monovalent intergallery cations is the driving force for water swelling. Natural clays may contain divalent cations, such as calcium montmorillonite, and those require expensive exchange procedures with sodium prior to further treatment with onium salts (Zanetti et al. 2000). The

process of exchange between cations in silicates, balancing the negative layer charge, and cations in solution, shows the following general features (Brigatti et al. 2006):

- It is reversible;
- It is diffusion-controlled (the rate-limiting step being the diffusion of one charge-balancing ion against another);
- It is stoichiometric;
- In most cases, there is selectivity of one cation over another.

After completion of the ion exchange reactions, the cationic head groups of the alkylammonium molecules preferentially attach at the layer surface via Coulombic interactions (Zanetti et al. 2000), leaving the organic tails radiating away from the surface, as protrayed in Fig. 2.28.

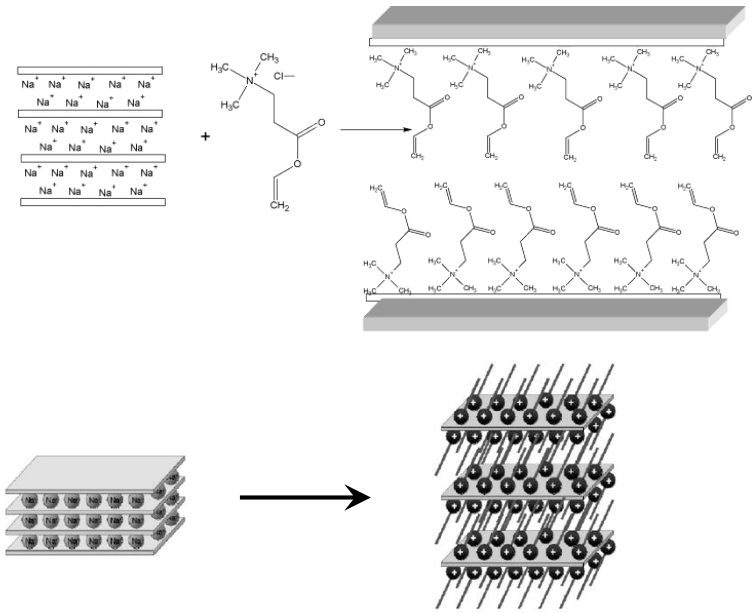

Fig. 2.28. Reaction scheme for surface treatment of a sodium MMT with a surfactant (quaternary alkylammonium salt) from hydrophilic to organophilic (Jahromi and Khodaii 2009; Herrera-Alonso et al. 2010).

In a given temperature range, the spacing of the resulting equilibrium layer mainly depends on both the cation exchange capacity of the layered silicate, which drives the packing of the chains, and the chain length of the organic tail(s), with both parameters affecting the formation of nanocomposites (Alexandre and Dubois 2000).

The number of alkyl chains in the organic cation has also been shown to exert some influence on the interlayer distance. Thus, organic surfactants containing a single alkyl chain lead to interlayer distances markedly lower than those with double alkyl chains. In the case of the chain length, greater interlayer distances are obtained as the alkyl chain length of the surfactant is increased. As for the packing of the chains, a higher content of organic molecules between the clay layers (loading level) generally leads to a larger interlayer spacing, as depicted in Fig. 2.29.

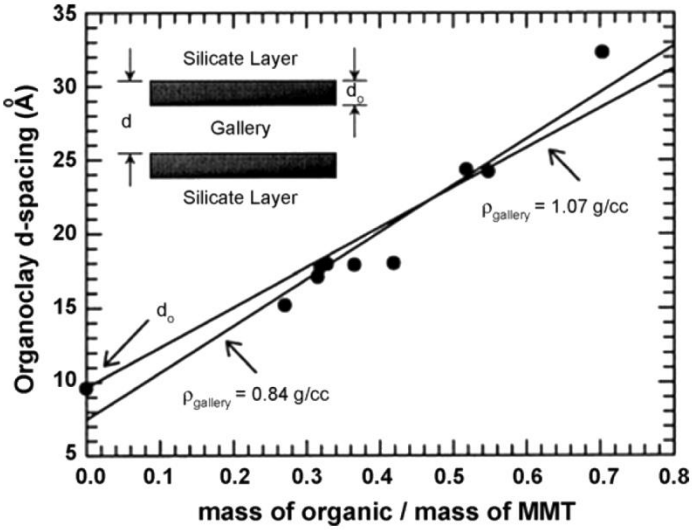

Fig. 2.29. Gallery size (d-spacing) dependence with the ratio of mass of intercalated organic cation to mass of layered silicate (MMT) (Fornes et al. 2002).

However, some authors (He et al. 2010) indicate that beyond a certain loading level of surfactant, no further layer expansion can be achieved, which then results maximal for that specific surfactant/clay pair. This has

been attributed to the surfactant cations/molecules occupying the pores between particles within the aggregates, instead of the interlayer spaces, as supported by DTG data. Nonetheless, it also seems that surfactant configuration has greater influence on interlayer spacing than surfactant loading.

Accordingly, organic cations in the interlayer space may exhibit different types of arrangements depending on both previously mentioned parameters. In general, based on FTIR studies (Vaia et al. 1994; Alexandre and Dubois 2000), as the interlayer packing density or the chain length decreases (or the temperature increases), the intercalated chains adopt a more disordered, liquid-like structure. When the available surface area per molecule is within a certain range, the chains are not completely disordered, but retain some orientational order similar to that in the liquid crystalline state. Hence, the increase of the chain length leads to the evolution of the interlayer structure in a stepwise fashion, from a disordered to a more ordered monolayer, and then, to a more disordered pseudo-bilayer, as depicted in Fig. 2.30.

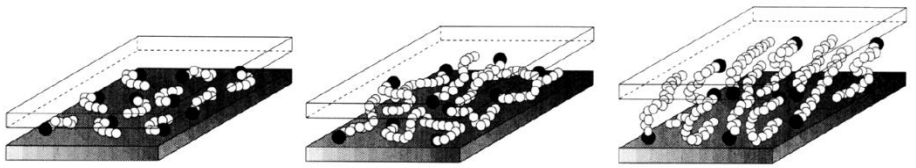

Fig. 2.30. Possible arrangements of alkyl chains in the interlayer space: (a) short alkyl chains: isolated molecules, lateral monolayer; (b) intermediate chain lengths: in-plane disorder and interdigitation to form quasi-bilayers; and (c) longer chain length: increased interlayer order, liquid crystalline-type environment (Vaia et al. 1994; Alexandre and Dubois 2000).

Therefore, by subjecting naturally occurring smectites to ion exchange reactions, they can be tailored to optimize their compatibility with bitumen, resulting in organo-modified clays with lower surface energies, which

improve the wetting characteristics of the bituminous matrix (Barick and Tripathy 2011), and this, in turn, increases the entropy of mixing (Jahromi and Khodaii 2009). All of it accompanied by a larger interlayer spacing (swelling), due to the presence of long aliphatic tails attached to the cationic head of the surfactant, as depicted in Figs. 2.28 and 2.30. Additionally, the alkylammonium or alkylphosphonium cations can provide functional groups that can react with molecules from the environment, or in some cases, initiate the polymerization of monomers to improve the strength of the interface between the inorganic host (silicate layers) and the surrounding matrix (Sinha Ray and Okamoto 2003; Choudalakis and Gotsis 2009; Kotal and Bhowmick 2015).

11.4.Bituminous Composites

Amongst smectite minerals, the easy availability of montmorillonite (MMT), along with its well-known chemistry, high surface area and high surface reactivity (Tjong 2006; Kotal and Bhowmick 2015) have endowed it with the widest acceptability for use in bitumen modification to form nanocomposites (Zare-Shahabadi et al. 2010; You et al. 2011; Fang et al. 2013; Polacco et al. 2015). These constitute a new class of composites, which are particle-reinforced materials, in which at least one dimension of the dispersed particles is in the nanometre range. Depending on how many dimensions of the dispersed particles are in such a range, nanocomposites can be classified in three different types: iso-dimensional nanoparticles, when the three dimensions are in the order of nanometres, such as spherical silica nanoparticles; nanotubes or whiskers, when two dimensions are in the nanometre scale and the third is larger, forming an elongated structure, as for example, carbon nanotubes or cellulose whiskers; and finally, the third type of nanocomposites, characterized by only one dimension in the

nanometre range. In this case, the filler is present in the form of sheets of one to a few nanometres thick and hundreds to thousands nanometres long. This family of composites encompasses those combining polymer and/or bitumen and layered silicates, designated as clay-based nanocomposites, and their study constitutes the main object of this dissertation.

11.4.1. Nanocomposite formation

The use of clays for the formation of bitumen/clay nanocomposites involves two particular characteristics of layered silicates that play a very important role. First, the ability of silicate platelets to disperse into individual layers, and secondly, the possibility to modify their surface chemistry through ion exchange reactions with organic cations. These two characteristics are of course interrelated, since the degree of dispersion of layered silicate in a particular bituminous product depends on the interlayer cation. Eventually, the main goal for the successful development of clay-based nanocomposites is to achieve the complete exfoliation of the layered silicate within the bituminous matrix (Sinha Ray 2006; Choudalakis and Gotsis 2009).

The preparation of bituminous nanocomposites requires both components, i.e. organomodifed clay and bitumen, to be blended in order to make it possible for bitumen molecules to insert between the clay layers. In this regard, several major routes of preparation can be distinguished for polymer/clay nanocomposites:

- In-situ polymerization
- Intercalation of the polymer from a solution
- Direct intercalation of the molten polymer
- Sol/gel technology

However, in the case of bitumen, melting state is required for the adequate dispersion of the clay. Thus, considering the analogy in processing conditions between polymers and bitumen, such a process is generally carried out by means of direct intercalation of the molten polymer, which would instead be bitumen.

11.4.1.1. Direct intercalation of molten bitumen

Direct intercalation of the molten polymer, when applied to bitumen, essentially shares the same application procedure and fundamentals. Hence, it involves annealing the mixture above the glass transition temperature or softening point, in either static or flow conditions (under shear). The polymer or bitumen chains then spread from the molten mass into the silicate galleries to form some type of nanocomposite, as long as both silicate and polymer or bitumen are compatible. Despite differences between polymer and bituminous nanocomposites, basics and fundamentals of polymer nanocomposite formation are both applicable for bituminous homologues. Accordingly, the critical factor that determines which type is obtained has been associated to thermodynamic factors (Vaia and Giannelis 1997b).

- **Thermodynamics of the melt intercalation process**

The thermodynamics that drives the intercalation of a polymer inside a modified layered silicate while the polymer is in the molten state has been approached by Vaia and Giannelis 1997b through the widely accepted "lattice-based mean field" theory. In accordance with this theory, in general, the outcome of polymer intercalation is determined by an interplay of entropic and enthalpic factors. In fact, although the confinement of the polymer chains inside the silicate galleries results in a decrease in the overall entropy of the macromolecular chains, this entropic penalty may be

compensated by the increase in conformational freedom of the tethered alkyl surfactant chains as the inorganic layers separate, due to the less confined environment.

Since small increases in the gallery spacing do not influence strongly the total entropy change, the spontaneity of the process will rather be driven by changes in total enthalpy. In this sense, the enthalpy of mixing has been separated into two components: apolar interactions, generally unfavourable and arising from interactions between polymer and surfactant aliphatic (apolar) chains; and polar interactions, which originate from the Lewis acid/Lewis base character of the layered polar silicates interacting with the polymer chains. In most conventional organo-modified silicates, the tethered surfactant chains are apolar. Hence, dispersion forces dominate polymer-surfactant interactions. On the other hand, a favourable energy decrease is associated with the establishment of many favourable polymer-surface polar interactions.

Thus, a negative change in the enthalpy due to the augmented energy of the interaction between the polymer and the silicate can be reached by the establishment of weak bonds, such as hydrogen bonds, dipole-dipole or van der Waals interactions. The change in enthalpy associated with these interactions is small and, as indicated, many are needed to bring about a substantial total variation. If the variation is sufficient, delamination of the silicate may take place, resulting in both a gain in entropy due to the disorder, and a gain in enthalpy due to increased area of contact between the polymer and the silicate, and so, a greater number of interactions.

The enthalpy of mixing can thus be rendered favourable by maximizing the magnitude and number of favourable polymer-surface interactions, while minimizing the magnitude and number of unfavourable apolar interactions

between the polymer and the aliphatic chains introduced along the modified layer surfaces (Alexandre and Dubois 2000).

In this regard, semiquantitative calculations show that this gain is enough to offset the loss due to confinement of the polymer and make the process isentropic (Zanetti et al. 2000), i.e. the entropy loss associated with the confinement of a polymer molecules is not prohibitive to nanocomposites formation because an entropy gain, associated with layer separation and greater conformational energy of the aliphatic chains of the alkylammonium cations balances the entropy loss of polymeric intercalation, resulting in a net entropy change near zero, as mentioned.

Thus, whether a mixture of polymer and an organo-modified layered silicate produces an exfoliated or an intercalated nanocomposite, or even a conventional microcomposite, depends critically upon the characteristics of the polymer and the layered silicate, including the nature of the polymer, as well as the type, packing density and size of the organic modifiers on the silicate surface.

It is worth mentioning that even when the surfactant chains are miscible with the polymer or bituminous matrix, a complete layer separation depends on the establishment of very favourable bitumen–surface interactions to overcome the penalty of confinement of bitumen molecules. If this is not the case, good dispersion of the particles may be achieved by the help of strong shear forces during the preparation and processing of the nanocomposite materials; nevertheless, the system will remain thermodynamically unstable (Pavlidou and Papaspyrides 2008).

- **Kinetics of melt intercalation process**

In addition to thermodynamic factors, as described above, mass transfer phenomena also plays a relevant role in the formation of composites and its timing. Some authors (Vaia et al. 1995) have shown, by using X-ray diffraction and transmission electronic microscopy (TEM), that mass transport, and so, kinetics of interaction between bitumen or polymer molecules and organoclays are dependent on the size of the clay particles involved in the process of intercalation (Fig. 2.31). Those authors found that the nominal silicate particle consists of smaller oblong-shaped particles, coined as primary particles, forming agglomerates. Those primary particles of 1 – 10 μm length themselves are made up of a compact face-to-face stacking or low angle intergrowth of individual silicate crystallites, also known as tactoids. These crystallites or tactoids are built up as a coherent stacking of individual silicate layers (platelets), with each tactoid containing between 10 and 100 of parallel, equally spaced alumina-silicate layers, which are roughly circular, 0.05 – 0.5 μm in diameter and 1 nm thick, and separated, as indicated in section 11.3.1, "*Classification and structural properties of clays*", by a van der Waals interlayer or gallery containing the alkylammonium cations.

Hence, the accessibility of the interlayer to the polymer chains depends on the location and orientation of the primary particles within the agglomerates, and similarly for the tactoids within the primary particles, meaning that tactoids near the edge will be more accessible to polymer chains than those near the centre. Analogously to polymer molecules, bitumen molecules have then to penetrate the agglomerate and surround the primary particles before any substantial intercalation takes place, given that silicate layers are impenetrable, and the polymer must enter the gallery

from the edges of the tactoids. Therefore, according to those authors, the polymer or bitumen penetration within the agglomerate is not a limiting step for intercalation, which is dependent upon the size of the primary particles. Thus, bigger primary particles will be less intercalated than smaller ones for the same processing time. This size dependence has been explained by the lack of significant difference in the mass transport in between and through the tactoids within a given primary particle, so as bitumen or polymer intercalation could be described as a Fickian process with a single, apparent diffusivity. The diffusion of molecules into the primary particles can therefore be sketched as a mass flow through the curved lateral surface of a cylinder bearing impermeable flat circular faces or area equal to the mean primary particle size.

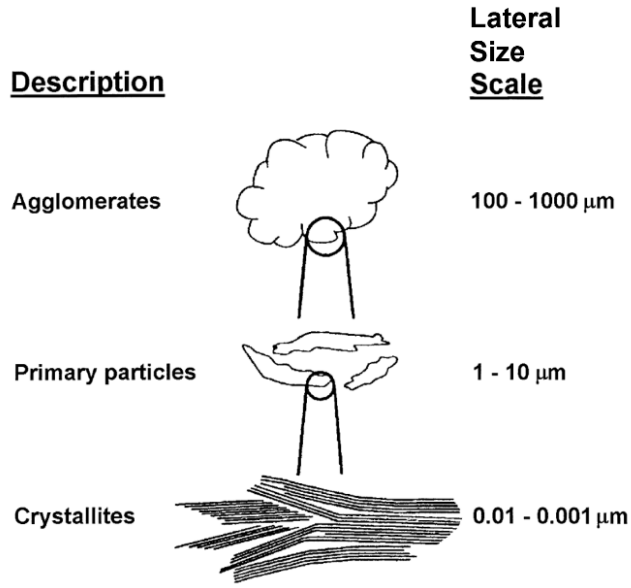

Fig. 2.31. Schematic of the morphology of organo-modified clays (Vaia et al. 1995).

Consequently, the limiting step to achieve intercalation has been assumed to correspond to the mass transport into the primary particle, any dynamic mixing should break down those particles (Yalcin and Cakmak 2004),

increasing the size uniformity of clay particles, and thus, eventually decreasing the intercalation time.

It is also worth mentioning that the accessibility of primary particles and tactoids is a relevant factor to be considered not only for kinetics of bitumen interaction, but also for reactive processes involving silicate layers.

11.4.2. Types of nanocomposite structures

Polymer nanocomposites can exhibit different types of structural arrangements depending on the strength of the interfacial interactions between the polymer matrix and the layered silicate. Those structures, illustrated in Fig. 2.32, are generally deduced from the patterns obtained by X-ray diffraction technique, which can be equally applicable to bitumen/clay nanocomposites (Polacco et al. 2008; Jahromi and Khodaii 2009; You et al. 2011), resulting in three types of thermodynamically achievable structures (Vaia and Giannelis 1997a; Sinha Ray and Okamoto 2003):

- Intercalated: in this arrangement, the insertion of matrix molecules into the layered silicate structure occurs in a crystallographically regular fashion, regardless of the clay to bitumen or polymer ratio. Intercalated nanocomposites are normally interlayered by a few molecular layers of polymer.
- Flocculated nanocomposites: conceptually, this is same as intercalated nanocomposites. However, silicate layers are sometimes flocculated due to hydroxylated edge–edge interaction of the silicate layers, forming large-sized nanoclay aggregates (larger tactoids).
- Exfoliated nanocomposites: in this case, the individual clay layers (platelets) are randomly separated in a continuous polymer or

bituminous matrix by average distances much greater than those of the intercalated structure. Usually, the clay content of an exfoliated nanocomposite is much lower than that of an intercalated nanocomposite.

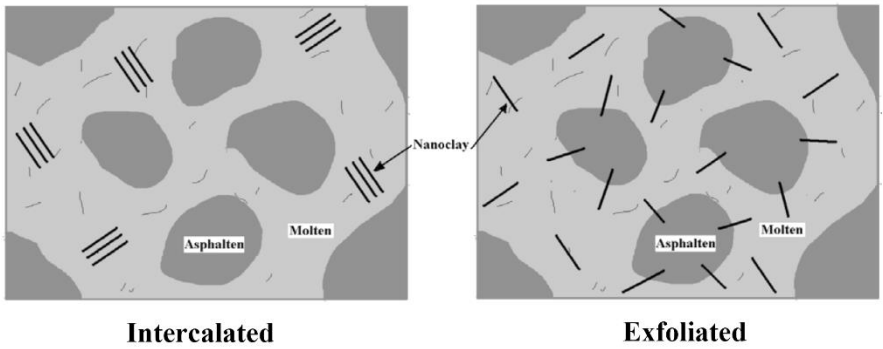

Fig. 2.32. Schematic illustration of the different types of thermodynamically achievable bitumen/layered silicate nanocomposites (Jahromi and Khodaii 2009).

Each of these possible structural arrangements gives rise to a different X-ray diffraction pattern characterised by the position, full-width-at-half-maximum (fwhm), and intensity of the (001) basal reflection appearing on it, if any.

Therefore, as shown in Fig. 2.33(a), for immiscible bitumen/clay mixtures, the structure of the silicate is not affected by the mixing process nor by the presence of a bituminous matrix, and thus, the characteristics of the organically-modified layered silicate (OLS) basal reflection do not change. On the other hand, the finite layer expansion associated with intercalated structures might result in a new basal reflection that corresponds to the larger gallery height of the intercalated hybrid (Fig. 2.33(b)). In contrast, the extensive layer separation associated with exfoliated structures disrupts the coherent layer stacking, resulting in a featureless diffraction pattern (Fig. 2.33(c)). Furthermore, changes in the fwhm and intensity of the basal reflections allows determining the influence of bitumen intercalation on the

order of the OLS layers. An increase in the degree of coherent layer stacking (i.e. a more ordered system) results in a relative decrease in the fwhm of the basal reflections upon hybrid formation (Fig. 2.33(b.1)). On the other hand, a decrease in the degree of coherent layer stacking (i.e. a more disordered system) results in peak broadening and intensity loss (Fig. 2.33(b.2)).

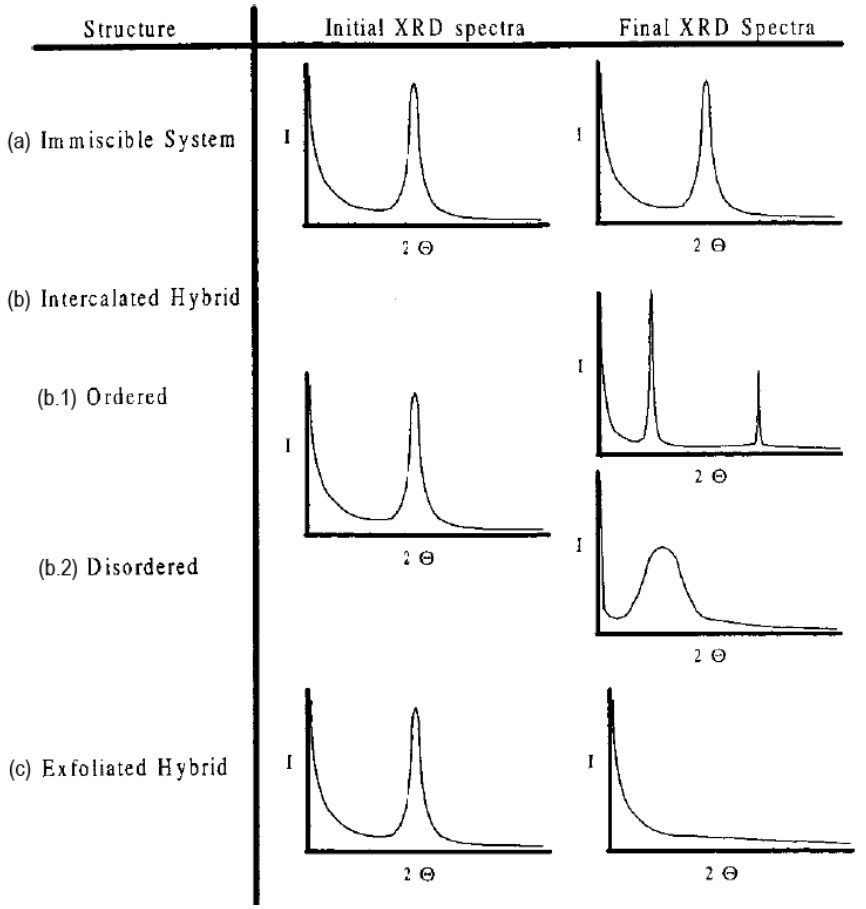

Fig. 2.33. Expected X-ray diffraction patterns for the different types of structural arrangements in clay/bitumen systems.

11.4.3. Rheology of bituminous nanocomposites

As described, the key challenge in designing nanoclay-based materials is the incorporation of clay in a fully dispersed and stable state, as agglomerates typically lead to inferior material performance. Thermodynamics have been shown to be highly relevant in the formation of nanocomposites; nevertheless, the flow during processing must also be considered. In this regard, rheology plays a dual role in nanocomposite formulation and processing. First, microstructure governs flow behaviour during melt processing. Hence, the optimization of the requirements associated to material and processing conditions involves understanding and controlling the non-linear rheological properties. Secondly, both linear and non-linear rheological properties are very sensitive to changes in the clay nanostructure, and inter-particle and bitumen-clay interactions (Jancar et al. 2010). Thus, rheology potentially offers a means to assess the state of dispersion of nanocomposites directly in the melt state. By using rheology, contributions stemming from the effects of particles on the local deformation rate of the surrounding matrix, the effect of particulate orientation, exfoliation, and the interaction between the particles can be characterized (Vermant et al. 2007).

11.4.3.1. Steady state shear flow

In melt rheology of nanocomposites, a first effect of the clay addition is purely hydrodynamic, as in the case of the linear viscoelastic properties, which brings about an increase in the steady-state shear viscosities in a magnitude that depends on volume fraction, particle shape, state of dispersion and degree of intercalation and/or exfoliation. In this regard, higher exfoliation or intercalation of clay involves an increased surface area available for interaction amongst them and with bitumen molecules, which

slows down relaxation dynamics of molecules in the surface vicinity, and may cause some molecular entrapment on the surroundings (increased effective volume), eventually leading to greater viscosities (Jancar et al. 2010). Another feature that might be observed at high shear stress values is a pronounced shear thinning, which has been found to be characteristic of truly nanodispersed composites. In this sense, the flow curve shape of the nanocomposites is somehow associated to the exfoliation and intercalation degree of the silicate platelets in the polymer or bituminous matrix. Hence, a marked shear thinning behaviour is usually associated to more uniformly dispersed clay particles at the micro and nanometre scales, i.e. greater degree of exfoliation and intercalation (Samyn et al. 2008).

11.4.3.2. Linear viscoelastic behaviour

The plateau region of the dynamic strain amplitude sweep experiment where the elastic modulus is independent of shear strain is termed as the linear viscoelastic region of a material.

The transition point at the deviation region from the linear to nonlinear viscoelastic behaviour is defined as critical strain (γ_c), which varies with the clay content and dispersion quality, depending on the nanocomposite composition.

The addition of a small volume fraction of particles to a polymeric or bituminous medium leads to several effects on the structural response of the system. One of them is the enhanced local deformation rates caused by the mere presence of solid particles, given that they provoke the concentration of the global straining motion in the interstitial fluid, accompanied by the corresponding increase in shear stress.

The magnitude of such an increase is determined by the volume of particles and can be expressed as an increased "effective" deformation. This also leads to some general patterns in the linear viscoelastic rheological properties, typically characterised by an increase in the linear viscoelastic dynamic moduli over the whole range of frequencies, along with a decreased linear viscoelastic region, as the effective local strain on the small interstices can result much higher than the bulk deformation imposed. This is known as the "hydrodynamic" effect (Fig. 2.34) (Barick and Tripathy 2011). The dependency of the limiting strain on volume fraction is hence determined by the degree of dispersion and the percolation threshold (Jancar et al. 2010).

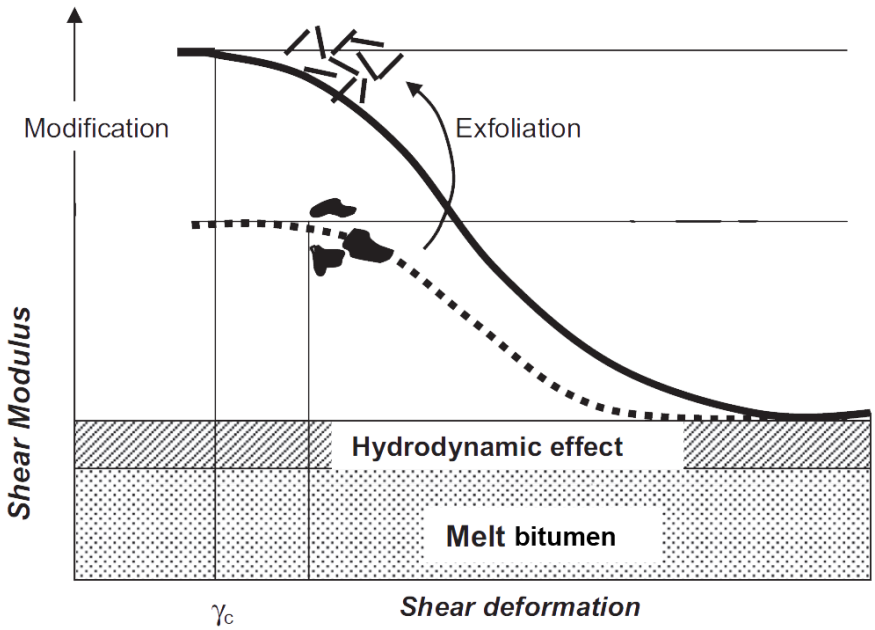

Fig. 2.34. Influence of the degree of intercalation/exfoliation on the evolution of complex shear modulus with shear in a bitumen/clay system.

More importantly, clays used in nanocomposites normally exhibit pronounced colloidal interactions due to their high available surface area. This leads to additional increases in the viscoelastic moduli at low

frequencies, which for aggregated materials and at high volume fractions ultimately tend to a plateau. Such a response has been generally attributed to the presence of a space-filling or "percolating" network, caused by attractive forces between the clay platelets, which results in weak solid behaviour, given that long range motion (low frenquency) of the matrix molecules are constrained by the percolated arrangement of platelets (Hoffmann et al. 2000).

In small amplitude oscillatory shear (SAOS) tests, the effect of clay is especially apparent at low frequencies of the storage modulus or at high temperatures; whilst at high frequencies, the polymer or bituminous matrix contribution to the overall viscoelastic response dominates over the aggregate contribution, because the short range motion of the fluid molecules is not affected.

Thus, liquid-like response is normally observed in the low frequency region ($G' < G''$); whilst inheriting pseudo-solid-like behaviours are obtained in the high frequency region ($G' > G''$). The transition from liquid-like to pseudo-solid-like behaviour occurs at a crossover frequency (ω_c), which shifts toward lower frequencies with the increase in clay content. The so-called pseudo-solid-like behaviour arises due to slower relaxation dynamics of bitumen or polymer molecules in the high frequency range (Barick and Tripathy 2011).

In this regard, the "Van Gurp–Palmen" plot, which shows the variation of the phase angle (δ) with the absolute value of the complex modulus ($|G^*|$), is usually used to detect the clay content at which percolation develops. As clay loading increases, phase angle values at low modulus tend to decrease, so that values lower than 45 ºC suggest a rheological liquid–solid transition (Wu et al. 2008).

Accordingly, much information can be extracted from the measurement of the linear viscoelastic properties, which can be used to assess the microstructure of the bituminous nanocomposites.

11.4.3.3. Non-linear viscoelastic behaviour

Besides the linear viscoelastic properties, the addition of clay particles typically affects the nonlinear and time-dependent properties. In this regard, and similarly to the linear viscoelastic behaviour, interparticle forces also affect the nonlinear properties during flow, this is because of chain orientation or the alignment of microstructures.

Non-linear viscoelastic behaviour arises at large enough strain, beyond the critical strain value. From that point, normally, viscoelastic functions dramatically diminish, leading to strain thinning behaviour in a strain or stress sweep test. For some complex fluids, such as polymer or bitumen composites, the so-called large amplitude oscillatory shear (LAOS) behaviour becomes quite complicated, due to the diverse interactions that may arise between structures at the nano and micrometre scales.

In the non-linear region, the storage and loss moduli lose their mathematical background or physical meaning, as defined in the linear region, and cannot be treated as such. Hence, the linear viscoelasticity theory does not hold anymore, given that higher order terms of strain (the so-called harmonics) become significant, and a more sophisticated analysis, such as a Fourier transformation method, needs to be used.

Even though the moduli measured in the nonlinear region lose their physical meaning as storage or loss modulus, it does not necessarily mean that the measured properties are meaningless or need to be treated as such.

They still provide a great deal of useful information on the microstructure of complex fluids.

With this aim, a network model was developed by Sim et al. 2003. Thus, despite the plethora of network models available, they are all based on a distribution of network junctions that is determined by their creation and loss rates. The main difference between the different models is the functional form of the creation and loss rates of network junctions. As little is known about the creation and loss rates, most network models assume specific functional forms for the creation and loss rates, in such a way that any network model can be regarded as a phenomenological model.

As for the concept of network, it is assumed to consist of segments and junctions, with a segment being a part of a macromolecular chain or a microstructure joining two successive junctions; and the junctions representing the points where the intra- or intermolecular interactions are localized. A junction may be regarded somehow as a crosslinking point, although it is an element defined in the network model for convenience. In this model, two constants are additionally defined: "a" and "b", which are model parameters representing the creation and loss rates, respectively. This approximation is too simplistic and is not adequate for a quantitative analysis. However, it has been shown to work very well for the qualitative analysis of LAOS behaviour of complex fluids (Hyun et al. 2002; Sim et al. 2003).

Therefore, when the shear strain amplitude is large enough, the shear stress response is no longer sinusoidal, but can be represented as a Fourier series containing multiple harmonics of stress contributions. Higher harmonic contributions to the shear stress can be analysed by the spectra in Fourier space with respect to their frequency. However, if those are neglected (they

usually represent less than 20% if compared to the first harmonic contribution), G' and G'' at large strain amplitudes can be named as the effective storage modulus and effective loss modulus, respectively.

Then, those moduli become a useful tool for the definition of the LAOS behaviour of complex fluids, which can hence be classified into at least four types (Hyun et al. 2002), depending on the interactions between the microstructures (Fig. 2.35): type I, strain thinning (G', G'' decreasing); type II, strain hardening (G', G'' increasing); type III, weak strain overshoot (G' decreasing, G'' increasing followed by decreasing); type IV, strong strain overshoot (G', G'' increasing followed by decreasing).

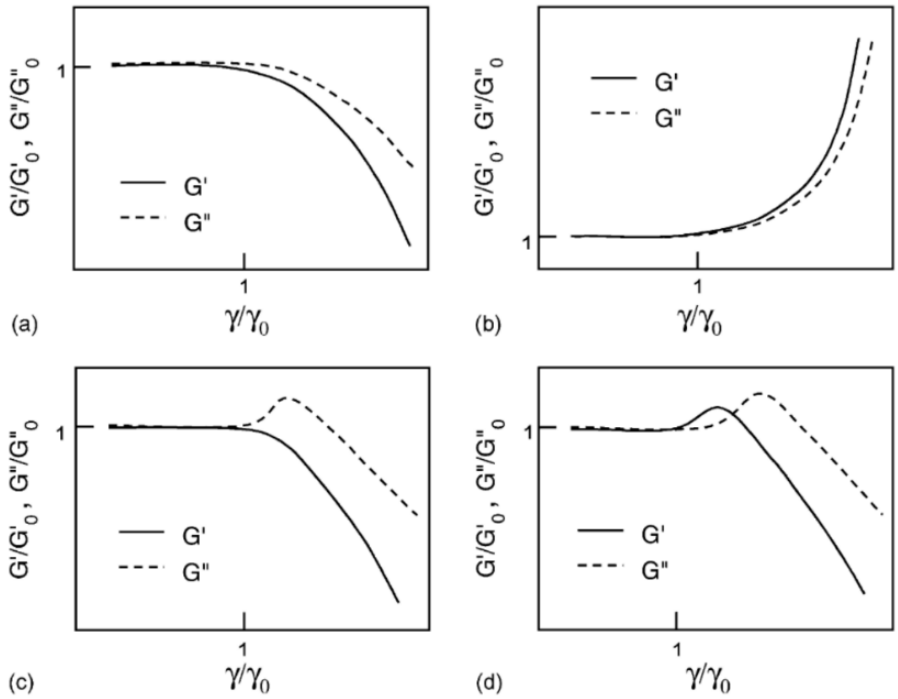

Fig. 2.35. Types of LAOS behaviour: (a) strain thinning; (b) strain hardening; (c) weak strain overshoot; and (d) strong strain overshoot (G'_0 and G''_0 are the moduli in the linear region, and γ_0 is the amplitude at which the moduli begin to deviate).

The two model parameters, "a" and "b", defined previously, can be used as a guide for the classification of complex fluids. Thus, if located on a two-

dimensional plane, as shown in Fig. 2.36, by sweeping the parameters across the plane, the prevalence of each parameter then varies depending on the section of the circle being considered. Hence, according to the creation and loss rates they refer to, the circle can be subdivided into five sections, each corresponding to one type of LAOS behaviour.

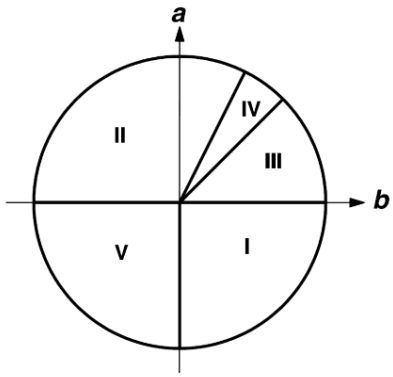

Fig. 2.36. Schematic diagram of representing the types of LAOS behaviour as a function of both the creation rate parameter "a", and the loss rate parameter "b".

- **Type I**

When the creation rate parameter is negative (a< 0) and the loss rate parameter is positive (b> 0), the effective storage modulus and the effective loss modulus decrease as the strain amplitude increases beyond a certain strain amplitude, which henceforth is referred to as a critical strain amplitude, regardless of the imposed frequency as shown in Fig. 2.35(a). This is the typical behaviour of strain sweep tests for most polymer and bitumen melts. In such cases, the molecular chains are in a state of entanglement at small strains, where G' and G'' are constant. When the strain is large, the chain or any microstructure aligns with the flow field, the network junctions are easily lost, and the chain has little chance to retain the network structure. The model parameters specify that the creation rate decreases while the loss rate increases as the strain amplitude becomes larger. When the creation rate parameter a approaches zero, with the loss

rate parameter b fixed, the linear region of G'' expands to higher strain amplitudes. When the loss rate parameter b increases, the critical strain amplitude for G' decreases, while the critical strain amplitude for G'' increases. That is, in the strain sweep test, a higher value of the creation rate parameter gives a higher value of the critical strain amplitude for G'', whereas a higher value of the loss rate parameter results in the lower value of the critical strain amplitude for G'. When the creation rate parameter is greater than zero, a maximum in the G'' curve appears at high frequencies, which corresponds to another type of LAOS behaviour, type III.

- **Type II**

When the creation rate parameter is positive (a> 0) and greater than 2b (a> 2b), both G' and G'' exhibit strain hardening behaviour regardless of the imposed frequency, as shown in Fig. 2.35(b). The parameter set implies that both the creation and loss terms increase with the strain amplitude, and the speed of creation is much larger than that of destruction. Thus, the interaction in this case is the strongest among the cases investigated in the modelling. G' and G'' increase explosively, which is distinct from the gradual increase of G' or G'' in other types. From types I to III, IV, and II, in that order, the creation term becomes more dominant, as evidenced by Fig. 2.36, and the interaction to form a network or a microstructure becomes more pronounced. As the complex or the network resists the deformation, the modulus increases with the strain, and the material behaves like a liquid at small strains but changes to a solid-like material as the strain becomes large, leading to the strain hardening behaviour. The critical strain amplitude after which the hardening is observed decreases as the frequency or the difference between the rate parameters increases.

- **Type III**

When both the creation and loss rate parameters are positive (a> 0, b> 0), and the creation rate parameter is smaller than the loss rate parameter (a<b), there appears a very interesting nonlinear phenomenon. At low frequency, both the effective storage and loss moduli (G' and G'') decrease with the strain amplitude in the nonlinear region. However, at high frequency, the effective loss modulus G'' shows a strain hardening followed by strain thinning; while the effective storage modulus G' shows a typical strain thinning behaviour, as depicted in Fig. 2.35(c). The parameter set means that both the creation and loss terms increase with the strain amplitude, but the destruction rate is faster than that of creation. The creation rate is sufficient to form a network (or any microstructure arising from the interactions, if any) leading to the strain hardening; whilst the loss term becomes dominant at larger strain amplitude, leading to the strain thinning. Thus, the overshoot may be regarded the outcome of the balance between the formation and the destruction of the network junctions. The maximum of G'' increases and shifts to smaller strain amplitudes as the creation rate parameter a increases at a fixed value of the loss rate parameter b. The maximum of G'' depends on the loss rate parameter too, but the effect is much smaller in this case.

- **Type IV**

When both the creation and loss rate parameters are positive (a> 0, b> 0), and the creation rate is greater than b but smaller than 2b (b<a< 2b), another interesting nonlinear phenomenon appears. At low frequencies, the modulus shows the strain thinning behaviour. However at high frequency, both G' and G'' show strain hardening behaviour followed by strain thinning behaviour, as illustrated in Fig. 2.35(d). The parameter set implies

that both the creation and loss terms increase with the strain amplitude, but the speed of creation is a little larger than that of destruction. Thus, the interaction to form a network or a microstructure in this case is stronger than that of type III. When the creation rate parameter a increases, the maximum in G' and G'' becomes more pronounced, shifting to a lower strain amplitude when both a and b increase, with their ratio being fixed, and also increases with frequency. This behaviour is much less often observed than type III. In addition, when oscillations are superimposed to steady shear flow, the maximum in G' and G'' decreases as the applied stress increases, and finally, the LAOS behaviour approaches type III behaviour, in which the overshoot of G' disappears and only G'' shows an overshoot.

This response implies that the material loses its network structure with increasing the shear stress, given that the applied stress causes the disruption of the network, and this corresponds to the situation of decreasing creation rate. As the creation rate decreases, the type IV response turns to type III, and then, to type I.

- **Type V**

When both the creation and loss rate parameters are negative ($a < 0$, $b < 0$), the strain sweep results in a sharp increase of the effective storage modulus G', approaching a plateau value that increases with the creation rate parameter "a"; whilst the effective loss modulus G'' shows strain thinning at high frequencies, but an overshoot at low frequency (Fig. 2.37). In this type of behaviour, the stress signal becomes in phase with the imposed strain at large strain amplitude, largely contradicting the expected absence of sinusoidal character in the time domain of the stress signal, due to the higher harmonic contributions. Thermo-mechanically, this would translate

to a liquid like (or viscoelastic) response at small strain amplitude, but an ideal elastic solid at large strain amplitude, which results inconsistent insofar as it contradicts the nonlinear response prevalence at large strain amplitude. Thereby, such a behaviour is considered unphysical, and generally, not contemplated when classifying the complex fluids.

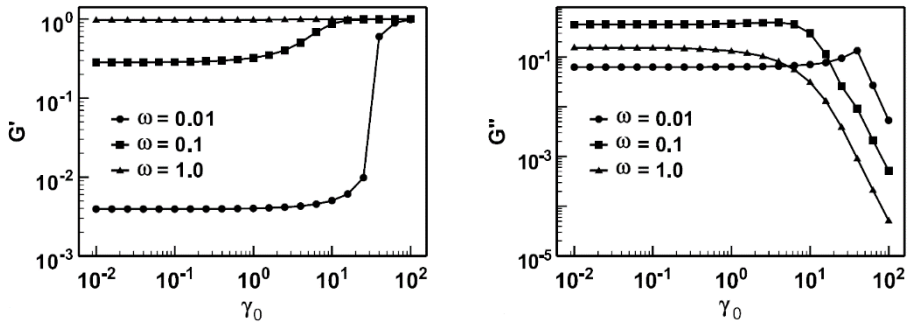

Fig. 2.37. Illustration of the LAOS behaviour type V for (a) effective storage modulus G', and (b) effective loss modulus G''.

In summary, despite that all non-linear constitutive models partially predict some types of LAOS behaviour, especially types I and III, with this model, the entire complexity of LAOS behaviour can be explained in terms of the model parameters, that is, the creation and loss rates of network junctions. In addition, the model parameters reflect the microstructure or any microstructural change, which is in turn reflected on the LAOS behaviour. Therefore, the microstructural evolution or any interaction within the material may well be analysed through the LAOS behaviour, and even though it has been explained on the basis of the model parameters and classified in four types, some complex fluids may show different behaviour, but it may be a variation or a combination of the generic types discussed above.

It is also worth pointing out that the behaviour of types III and IV and the mechanism of strain hardening in LAOS that they represent are not directly

related to shear thickening behaviour (viscosity increasing with shear rate), given that both viscosity and the first normal stress difference show shear thinning behaviour with these parameter sets, while the number of network segments decreases with increasing shear rate for type III and increases for type IV.

In addition to the rheological characteristics previously described, the presence of clay aggregates, and even a particulate network structure may lead to the development of an apparent yield stress and a thixotropic response that adds to the already complex non-linear behaviour. Thixotropy becomes manifest as time-dependent stresses over time, arising due to local spatial rearrangements and aggregation of the particles during flow. Thus, flow affects the nanocomposite structure by both breaking down the aggregate network and by possibly aligning its structural elements, also involving the intrinsic molecular dynamics of bitumen molecules, which results in a highly complex rheological behaviour, accompanied by the mentioned time and shear history dependence of the rheological properties.

11.4.4. Properties of bituminous nanocomposites

An adequate dispersion of clay throughout the bituminous matrix makes it possible to provide noticeable improvements in various characteristics of bitumen, especially in relation to its mechanical behaviour, and thermal and barrier properties, which offer resistance against oxidation (due to lower oxygen diffusion) and heat (Jahromi and Khodaii 2009; Galooyak et al. 2010; Zare-Shahabadi et al. 2010; You et al. 2011; Fang et al. 2013; Yao et al. 2013; Polacco et al. 2015), respectively.

11.4.4.1. Ageing resistance

One of the most relevant problems related to bitumen, resulting from heating operations during its application and from the combined action of thermal oxidation, illumination, precipitation and loads during its in-service life, corresponds to aging. This process is accompanied by bitumen hardening, which makes it gain elasticity, becoming brittle and prone to premature damaging when subjected to loads, as it is not capable of dissipating a part of the energy input associated to vehicle loads. In the case of polymer-modified bitumen, aging also includes the degradation of the polymer. The reduction of the effects of such factors causing aging involves a high compatibility and stability of the phases within a modified bitumen. In this regard, the organic modification of clay has shown to increase compatibility and stability when added to bitumen, as described later. Moreover, the high viscosity of bitumen prevents Brownian motion of nanoclay particles, so that once they are uniformly dispersed, the tendency of nanoparticles to aggregate is considerably reduced.

On the other hand, a major contributor to reduce bitumen ageing corresponds to the distribution pattern of the nanolayered materials in a modified bitumen. Thus, Yu et al. 2009 evaluated the influence of OMMT on the thermo-oxidative aging and UV aging of bitumen by means of its rheological characterization, resulting in a lower degree of variation of the dynamic rheological response in systems containing intercalated or exfoliated OMMT, hinting at some hindrance of both processes due to the presence of clay. Similar results on improved resistance against aging have been obtained by other authors, Li et al. 2010, Zhang et al. 2013, further supported by observations from AFM technique, as evidenced by Zhang et al. 2011a and Zhang et al. 2011b.

Hence, according to the literature, the exfoliated or intercalated structure of nanolayered materials, especially the exfoliated one, can produce an effective barrier to oxygen, water and organic solvents, while preventing the evaporation of the light components of the asphalt, as illustrated in Fig. 2.38. Therefore, OMMT improves the aging resistance of modified bitumen, prolonging its in-service life.

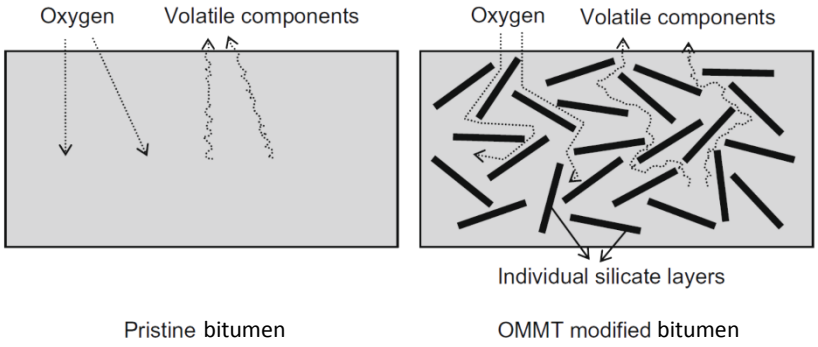

Fig. 2.38. Schematic of the anti-aging mechanism in an OMMT modified bitumen.

11.4.4.2. Thermo-mechanical response and other properties

- **Bitumen/clay binary composites**

Several researches have been conducted on the effects of clay on the rheological behaviour of the bitumen/clay nanocomposites in the viscoelastic linear range. Yu et al. 2007 compared the effects of the addition and content of a pristine and an organo-modified MMT on the rheological properties of bitumen, concluding that both MMT and OMMT greatly improved its dynamic rheological properties, resulting in higher complex modulus and lower phase angle, although effects in the case of OMMT were more pronounced, due to the formation of an exfoliated structure in bitumen. As for concentration, increasing the content of OMMT up to a certain value, corresponding to the "percolation" limit, improved bitumen's rheological properties. Beyond such a value, a progressive deterioration

was obtained, ultimately resulting in a response similar to that of the MMT. Analogous results on the dynamical properties of bitumen after the addition of OMMT have been reported by Zare-Shahabadi et al. 2010, Tao et al. 2010, Liu et al. 2010, You et al. 2011, Muniandy et al. 2013.

- **Bitumen/polymer/clay ternary composites**

In addition to bitumen/clay binary systems, clay has also been used as a third component in polymer modified bitumen (generally containing SBS, SEBS or EVA), either by subsequent addition to the PMB, or by previous preparation of the polymer/clay nanocomposite and addition to bitumen in a later stage. In both cases, investigation on this field has shown that the addition of clay results in the enhancement of the compatibility between the polymer and bitumen phases, attributed to the decrease of the density difference between both (and so, of the buoyant force on the polymer-rich phase), contributing to their stability. Moreover, the joint addition further improved the rheological properties of the ternary system with respect to those of the PMB and clay modified bitumen. In this regard, Ouyang et al. 2005 used a combination of SBS and kaolinite clay (KC) to modify bitumen, concluding that the ratio of SBS to KC had a great effect on the high-temperature storage properties, resulting in stable systems when the ratio of SBS to KC was around 3. Moreover, KC had almost no effect on the mechanical properties of SBS modified asphalts when the content of KC in the modified asphalts was less than 2 wt.%. Those authors also investigated the rheological and high-temperature properties of bitumen modified with SEBS and KC (Ouyang et al. 2006). They concluded that the extent of the influence of KC differed depending on the SEBS content. At low contents (such as 3 or 4 wt.%), high-temperature, mechanical and rheological properties and morphology barely changed. However, at higher

SEBS contents, up to 5 or 6 wt.%, the KC had a dramatic influence on the properties asphalts.

Yu et al. 2007a assessed the properties of clay/SBS modified bitumen composites using different amounts of Na-MMT and OMMT. The XRD results showed that the Na-MMT/SBS modified bitumen composite formed an intercalated structure, whereas the OMMT/SBS modified bitumen composite exhibited an exfoliated one. The addition of MMT to SBS modified bitumen increased viscosity. As for rheological properties, OMMT, when compared with Na-MMT, had greater effects in improving properties of SBS modified bitumen, which indicated that exfoliated structure was more effective than intercalated structure.

Polacco et al. 2008 studied the effect of clay addition as a third component in polymer modified bitumen composed of a soft base bitumen and a radial SBS block copolymer. The order of addition of the components was seen to exert a significant effect on the internal structure of the blends and, therefore, on its rheological behaviour. Generally, the elasticity of the blend prepared by using a master batch was much higher and the dissipation of mechanical energy much lower than in the case of a physical mix. Considering the polymer and bitumen separately, the latter showed a higher compatibility with the clay. Therefore, they concluded that a physical mix of the three components should lead to nanocomposites in which the intercalation in the clay layers would mainly be due to bitumen molecules, while the bitumen/polymer interactions resulting almost not affected by the presence of the clay. They also stated that premixing of the polymer with the clay would probably led to a different morphology, given that the macromolecules would be first intercalated between the clay layers, being then able to maintain this position, at least partially. In this way, the clay,

that was present in a small quantity with respect to the total asphalt content, remained bonded with the polymer and may significantly affect the overall rheological properties.

Sureshkumar et al. 2010 compared the properties of ternary blends of bitumen, EVA and either cloisite or dellite clay, prepared either by the separate additions of clay and polymer to bitumen, or by addition of premixed polymer/clay intercalated nanocomposites, leading to similar conclusions: despite the higher affinity of clays for bitumen than for the polymer, once polymer/clay interactions are established, these are not altered by the bitumen molecules added subsequently. This resulted in systems with better rheological properties (higher elasticity, greater recovery, etc.). Analogous results were obtained by Merusi et al. 2012 on bituminous systems modified with SBS and an OMMT.

Galooyak et al. 2010 assessed the rheological properties of OMMT/SBS modified bitumen prepared by melt intercalated method. Thus, OMMT containing systems exhibited an increase in complex modulus, and a decrease in phase angle, resulting in a predominantly elastic behaviour. The addition of OMMT also enhanced the storage stability of PMB, accompanied by the hindrance of oxygen diffusion to PMB, hence improving its aging resistance. Similarly, results on improved aging resistance have also been reported by Zhang et al. 2012 on bituminous systems containing OMMT and SBS.

12. Bibliography

Agrawala M, Yarranton HW (2001) An Asphaltene Association Model Analogous to Linear Polymerization. Ind Eng Chem Res 40:4664–4672. doi: 10.1021/ie0103963

Airey GD (2002) Use of Black Diagrams to Identify Inconsistencies in Rheological Data. Road Mater Pavement Des 3:403–424. doi: 10.1080/14680629.2002.9689933

Airey GD, Rahimzadeh B (2004) Combined bituminous binder and mixture linear rheological properties. Constr Build Mater 18:535–548. doi: http://dx.doi.org/10.1016/j.conbuildmat.2004.04.008

Alexandre M, Dubois P (2000) Polymer-layered silicate nanocomposites: preparation, properties and uses of a new class of materials. Mater Sci Eng R Reports 28:1–63. doi: http://dx.doi.org/10.1016/S0927-796X(00)00012-7

Andersen SI, Jensen JO, Speight JG (2005) X-ray Diffraction of Subfractions of Petroleum Asphaltenes. Energy & Fuels 19:2371–2377. doi: 10.1021/ef050039v

Andreatta G, Bostrom N, Mullins OC (2005a) High-Q ultrasonic determination of the critical nanoaggregate concentration of asphaltenes and the critical micelle concentration of standard surfactants. Langmuir 21:2728–2736. doi: 10.1021/la048640t

Andreatta G, Goncalves CC, Buffin G, et al (2005b) Nanoaggregates and structure-Function relations in asphaltenes. Energy and Fuels 19:1282–1289. doi: 10.1021/ef0497762

Annabi-Bergaya F (2008) Layered clay minerals. Basic research and

innovative composite applications. Microporous Mesoporous Mater 107:141–148. doi: http://dx.doi.org/10.1016/j.micromeso.2007.05.064

Asphalt Institute, Eurobitume (2015) The Bitumen Industry — A Global Perspective Production, chemistry, use, specification and occupational exposure, Third. Asphalt institute, Eurobitume, U.S.A.

ASTM International (2012) ASTM D3279-12e1 Test method for n-heptane insolubles.

Baldino N, Gabriele D, Lupi FR, et al (2013) Rheological effects on bitumen of polyphosphoric acid (PPA) addition. Constr Build Mater 40:397–404. doi: 10.1016/j.conbuildmat.2012.11.001

Barick AK, Tripathy DK (2011) Effect of organically modified layered silicate nanoclay on the dynamic viscoelastic properties of thermoplastic polyurethane nanocomposites. Appl Clay Sci 52:312–321. doi: 10.1016/j.clay.2011.03.010

Barnes HA (2000) A Handbook of Elementary Rheology. University of Wales, Institute of Non-Newtonian Fluid Mechanics

Barnes HA, Hutton JF, Walters K (1989) An Introduction to Rheology. Elsevier

Brigatti MF, Galan E, Theng BKG (2006) Chapter 2 Structures and Mineralogy of Clay Minerals. In: Faïza Bergaya BKGT and GLBT-D in CS (ed) Handbook of Clay Science. Elsevier, pp 19–86

Buenrostro-gonzalez E, Groenzin H, Lira-galeana C, Mullins OC (2001) Asphaltenes. Energy and Fuels 15:972–978. doi: 10.1021/ef0100449

Bukowski A, Grętkiewicz J (1982) Polyurethane synthesis reactions in asphalts. J Appl Polym Sci 27:1197–1204. doi: 10.1002/app.1982.070270409

Carrera V, Partal P, García-Morales M, et al (2010) Effect of processing on the rheological properties of poly-urethane/urea bituminous products. Fuel Process Technol 91:1139–1145. doi: http://dx.doi.org/10.1016/j.fuproc.2010.03.028

Choudalakis G, Gotsis AD (2009) Permeability of polymer/clay nanocomposites: A review. Eur Polym J 45:967–984. doi: http://dx.doi.org/10.1016/j.eurpolymj.2009.01.027

Connan J (1999) Use and trade of bitumen in antiquity and prehistory: molecular archaeology reveals secrets of past civilizations. Philos Trans R Soc B Biol Sci 354:33–50. doi: 10.1098/rstb.1999.0358

Connan J, de Velde T (2010) An overview of bitumen trade in the Near East from the Neolithic (c.8000 BC) to the early Islamic period. Arab Archaeol Epigr 21:1–19. doi: 10.1111/j.1600-0471.2009.00321.x

Corbett LW (1969) Composition of asphalt based on generic fractionation, using solvent deasphaltening, elution-adsorption chromatography, and densimetric characterization. Anal Chem 41:576–579. doi: 10.1021/ac60273a004

Cuadri AA, García-Morales M, Navarro FJ, et al (2013) End-performance evaluation of thiourea-modified bituminous binders through viscous flow and linear viscoelasticy testing. Rheol Acta 52:145–154. doi: 10.1007/s00397-012-0671-5

de Paiva LB, Morales AR, Valenzuela Díaz FR (2008) Organoclays:

Properties, preparation and applications. Appl Clay Sci 42:8–24. doi: http://dx.doi.org/10.1016/j.clay.2008.02.006

Dickie JP, Yen TF (1967) Macrostructures of the asphaltic fractions by various instrumental methods. Anal Chem 39:1847–1852. doi: 10.1021/ac50157a057

Domin M., Herod A., Kandiyoti R., et al (1999) A comparative study of Bitumen molecular-weight distributions. Energy and Fuels 13:552–557. doi: 10.1021/ef980065b

Eckert A (2001) The application of Iatroscan-technique for analysis of bitumen. Pet Coal 43:51–53.

Evdokimov IN, Fesan AA (2016) Multi-step formation of asphaltene colloids in dilute solutions. Colloids Surfaces A Physicochem Eng Asp 492:170–180. doi: http://dx.doi.org/10.1016/j.colsurfa.2015.11.072

Eyssautier J, Espinat D, Gummel J, et al (2012a) Mesoscale Organization in a Physically Separated Vacuum Residue: Comparison to Asphaltenes in a Simple Solvent. Energy & Fuels 26:2680–2687. doi: 10.1021/ef201411r

Eyssautier J, Frot D, Barré L (2012b) Structure and Dynamic Properties of Colloidal Asphaltene Aggregates. Langmuir 28:11997–12004. doi: 10.1021/la301707h

Eyssautier J, Hénaut I, Levitz P, et al (2012c) Organization of Asphaltenes in a Vacuum Residue : A Small-Angle X-ray Scattering (SAXS) - Viscosity Approach at High Temperatures. Energy & Fuels 26:2696–2704.

Eyssautier J, Levitz P, Espinat D, et al (2011) Insight into asphaltene nanoaggregate structure inferred by small angle neutron and X-ray scattering. J Phys Chem B 115:6827–6837. doi: 10.1021/jp111468d

Fang C, Yu R, Liu S, Li Y (2013) Nanomaterials applied in asphalt modification: A review. J Mater Sci Technol 29:589–594. doi: 10.1016/j.jmst.2013.04.008

Fornes TD, Yoon PJ, Hunter DL, et al (2002) Effect of organoclay structure on nylon 6 nanocomposite morphology and properties. Polymer (Guildf) 43:5915–5933. doi: http://dx.doi.org/10.1016/S0032-3861(02)00400-7

Galooyak SS, Dabir B, Nazarbeygi AE, Moeini A (2010) Rheological properties and storage stability of bitumen/SBS/montmorillonite composites. Constr Build Mater 24:300–307. doi: 10.1016/j.conbuildmat.2009.08.032

Golestani B, Nam BH, Moghadas Nejad F, Fallah S (2015) Nanoclay application to asphalt concrete: Characterization of polymer and linear nanocomposite-modified asphalt binder and mixture. Constr Build Mater 91:32–38. doi: 10.1016/j.conbuildmat.2015.05.019

Goual L (2012) Petroleum Asphaltenes. In: Abdul-Raouf ME-S (ed) Crude Oil Emulsions- Composition Stability and Characterization. InTech,

Goual L, Firoozabadi A (2002) Measuring asphaltenes and resins, and dipole moment in petroleum fluids. AIChE J 48:2646–2663. doi: 10.1002/aic.690481124

Goual L, Sedghi M, Zeng H, et al (2011) On the formation and properties of asphaltene nanoaggregates and clusters by DC-conductivity and

centrifugation. Fuel 90:2480–2490. doi: 10.1016/j.fuel.2011.02.025

Gray MR, Tykwinski RR, Stryker JM, Tan X (2011) Supramolecular assembly model for aggregation of petroleum asphaltenes. Energy and Fuels 25:3125–3134. doi: 10.1021/ef200654p

Grimme S (2008) Do special noncovalent π-π stacking interactions really exist? Angew Chemie - Int Ed 47:3430–3434. doi: 10.1002/anie.200705157

He H, Ma Y, Zhu J, et al (2010) Organoclays prepared from montmorillonites with different cation exchange capacity and surfactant configuration. Appl Clay Sci 48:67–72. doi: http://dx.doi.org/10.1016/j.clay.2009.11.024

Herod AA, Bartle KD, Kandiyoti R (2007) Characterization of Heavy Hydrocarbons by Chromatographic and Mass Spectrometric Methods: An Overview. Energy & Fuels 21:2176–2203. doi: 10.1021/ef060642t

Herrera-Alonso JM, Sedlakova Z, Marand E (2010) Gas barrier properties of nanocomposites based on in situ polymerized poly(n-butyl methacrylate) in the presence of surface modified montmorillonite. J Memb Sci 349:251–257. doi: http://dx.doi.org/10.1016/j.memsci.2009.11.057

Hoffmann B, Kressler J, Stoppelmann G, et al (2000) Rheology of nanocomposites based on layered silicates and polyamide-12. Colloid Polym Sci 278:629–636. doi: 10.1007/s003960000294

Hossain Z, Zaman M, Saha MC Evaluation of Rutting and Moisture Susceptibility of Nanoclay-Modified Asphalt Binders.

Hsu CS, Robinson P (2007) Practical Advances in Petroleum Processing.

Springer New York

Hunter CA, Sanders JKM (1990a) The nature of pi-pi interactions. J Am Chem Soc 112:5525–5534. doi: 10.1021/ja00170a016

Hunter CA, Sanders JKM (1990b) The nature of pi - pi interactions. J Am Chem Soc 112:5525–5534. doi: 10.1021/ja00170a016

Hyun K, Kim SH, Ahn KH, Lee SJ (2002) Large amplitude oscillatory shear as a way to classify the complex fluids. J Nonnewton Fluid Mech 107:51–65. doi: 10.1016/s0377-0257(02)00141-6

Isacsson U, Lu X (1995) Testing and appraisal of polymer modified road bitumens—state of the art. Mater Struct 28:139–159. doi: 10.1007/BF02473221

Izquierdo MA, Navarro FJ, Martínez-Boza FJ, Gallegos C (2013) Effects of MDI-PPG molecular weight on the thermorheological behaviour of MDI-isocyanate based bituminous foams. J Ind Eng Chem 19:704–711. doi: 10.1016/j.jiec.2012.10.025

Jahromi SG, Khodaii A (2009) Effects of nanoclay on rheological properties of bitumen binder. Constr Build Mater 23:2894–2904. doi: 10.1016/j.conbuildmat.2009.02.027

Jancar J, Douglas JF, Starr FW, et al (2010) Current issues in research on structure–property relationships in polymer nanocomposites. Polymer (Guildf) 51:3321–3343. doi: http://dx.doi.org/10.1016/j.polymer.2010.04.074

Koots JA, Speight JG (1975) Relation of petroleum resins to asphaltenes. Fuel 54:179–184. doi: 10.1016/0016-2361(75)90007-1

Kotal M, Bhowmick AK (2015) Polymer nanocomposites from modified clays: Recent advances and challenges. Prog Polym Sci 51:127–187. doi: http://dx.doi.org/10.1016/j.progpolymsci.2015.10.001

Krishnamoorti R, Giannelis EP (1997) Rheology of End-Tethered Polymer Layered Silicate Nanocomposites. Macromolecules 30:4097–4102. doi: 10.1021/ma960550a

Lesueur D (2009) The colloidal structure of bitumen: Consequences on the rheology and on the mechanisms of bitumen modification. Adv Colloid Interface Sci 145:42–82. doi: http://dx.doi.org/10.1016/j.cis.2008.08.011

Li B, Zhang H, Yu J (2010) Effect of organo-montmorillonite on the morphology and aging properties of various bitumens. J Wuhan Univ Technol Sci Ed 25:650–655. doi: 10.1007/s11595-010-0063-6

Liu G, Wu S, van de Ven M, et al (2010) Influence of sodium and organo-montmorillonites on the properties of bitumen. Appl Clay Sci 49:69–73. doi: 10.1016/j.clay.2010.04.005

Lu GW, Li YF, Song H, et al (2008) Micromechanism of petroleum asphaltene aggregation. Pet Explor Dev 35:67–72. doi: 10.1016/S1876-3804(08)60010-5

Macosko CW (1994) Rheology: principles, measurements, and applications. VCH

Malkin AIA (1994) Rheology Fundamentals. Elsevier Science Limited

Martínez-Boza F, Partal P, Navarro FJ, Gallegos C (2001) Rheology and microstructure of asphalt binders. Rheol Acta 40:135–141. doi: 10.1007/s003970000140

Masson JF, Polomark GM, Collins P (2002) Time-dependent microstructure of bitumen and its fractions by modulated differential scanning calorimetry. Energy & Fuels 16:470–476. doi: 10.1021/ef010233r

Masson JF, Price T, Collins P (2001) Dynamics of bitumen fractions by thin-layer chromatography/flame ionization detection. Energy and Fuels 15:955–960. doi: 10.1021/ef0100247

Merusi F, Giuliani F, Polacco G (2012) Linear Viscoelastic Behaviour of Asphalt Binders Modified with Polymer/clay Nanocomposites. Procedia - Soc Behav Sci 53:335–345. doi: 10.1016/j.sbspro.2012.09.885

Moschopedis SE, Fryer JF, Speight JG (1976) Investigation of asphaltene molecular weights. Fuel 55:227–232. doi: http://dx.doi.org/10.1016/0016-2361(76)90093-4

Mousavi M, Abdollahi T, Pahlavan F, Fini EH (2016) The influence of asphaltene-resin molecular interactions on the colloidal stability of crude oil. Fuel 183:262–271. doi: http://dx.doi.org/10.1016/j.fuel.2016.06.100

Mullins OC (2008) Review of the Molecular Structure and Aggregation of Asphaltenes and Petroleomics. Soc Pet Eng 13:48–57. doi: 10.2118/95801-PA

Mullins OC (2010) The Modified Yen Model †. Energy & Fuels 24:2179–2207. doi: 10.1021/ef900975e

Mullins OC, Betancourt SS, Cribbs ME, et al (2007a) The Colloidal Structure of Crude Oil and the Structure of Oil Reservoirs. Energy &

Fuels 21:2785–2794. doi: 10.1021/ef0700883

Mullins OC, Sabbah H, Pomerantz AE, et al (2012) Advances in Asphaltene Science and the Yen − Mullins Model. Energy & Fuels 26:3986−4003. doi: 10.1021/ef300185p

Mullins OC, Sheu EY, Hammami A, Marshall AG (2007b) Asphaltenes, Heavy Oils, and Petroleomics. Springer New York

Muniandy R, Hasham S, Aburkaba E, others (2013) Effect of Organic Montmorillonite Nanoclay Concentration on the Physical and Rheological Properties of Asphalt Binder. Aust J Basic Appl Sci 7:429–437.

Murgich J (2002) INTERMOLECULAR FORCES IN AGGREGATES OF ASPHALTENES AND RESINS. Pet Sci Technol 20:983–997. doi: 10.1081/LFT-120003692

Murgich J, Strausz OP (2001) MOLECULAR MECHANICS OF AGGREGATES OF ASPHALTENES AND RESINS OF THE ATHABASCA OIL. Pet Sci Technol 19:231–243. doi: 10.1081/LFT-100001237

Murray HH (2006) Chapter 2 Structure and Composition of the Clay Minerals and their Physical and Chemical Properties. In: Science HHMBT-D in C (ed) Applied Clay MineralogyOccurrences, Processing and Application of Kaolins, Bentonites, Palygorskite-Sepiolite, and Common Clays. Elsevier, pp 7–31

Murray HH (2000) Traditional and new applications for kaolin, smectite, and palygorskite: a general overview. Appl Clay Sci 17:207–221. doi: http://dx.doi.org/10.1016/S0169-1317(00)00016-8

Navarro FJ, Partal P, García-Morales M, et al (2007) Bitumen modification with a low-molecular-weight reactive isocyanate-terminated polymer. Fuel 86:2291–2299. doi: http://dx.doi.org/10.1016/j.fuel.2007.01.023

Navarro FJ, Partal P, García-Morales M, et al (2009) Bitumen modification with reactive and non-reactive (virgin and recycled) polymers: A comparative analysis. J Ind Eng Chem 15:458–464. doi: 10.1016/j.jiec.2009.01.003

Navarro FJ, Partal P, Martinez-Boza F, et al (2006) Rheology and microstructure of MDI-PEG reactive prepolymer-modified bitumen. Mech Time-Dependent Mater 10:347–359. doi: 10.1007/s11043-007-9029-2

Nellensteyn FJ (1924) The constitution of asphalt. J Inst Pet Technol 10:311–325.

Ouyang C, Wang SF, Zhang Y, Zhang YX (2005) Preparation and properties of styrene-butadiene-styrene copolymer/kaolinite clay compound and asphalt modified with the compound. Polym Degrad Stab 87:309–317. doi: 10.1016/j.polymdegradstab.2004.08.014

Ouyang CF, Wang SF, Zhang Y, Zhang YX (2006) Thermo-rheological properties and storage stability of SEBS/kaolinite clay compound modified asphalts. Eur Polym J 42:446–457. doi: 10.1016/j.eurpolymj.2005.07.004

Painter P, Veytsman B, Youtcheff J (2015) Phase Behavior of Bituminous Materials. Energy & Fuels 29:7048–7057. doi: 10.1021/acs.energyfuels.5b01728

Partal P, Martínez-Boza F, Conde B, Gallegos C (1999) Rheological

characterisation of synthetic binders and unmodified bitumens. Fuel 78:1–10. doi: http://dx.doi.org/10.1016/S0016-2361(98)00121-5

Pavlidou S, Papaspyrides CD (2008) A review on polymer–layered silicate nanocomposites. Prog Polym Sci 33:1119–1198. doi: http://dx.doi.org/10.1016/j.progpolymsci.2008.07.008

Pérez-Lepe A, Martínez-Boza FJ, Attané P, Gallegos C (2006) Destabilization mechanism of polyethylene-modified bitumen. J Appl Polym Sci 100:260–267. doi: 10.1002/app.23091

Petersen JC, Robertson RE, Branthaver JF, et al (1994) Binder Characterization and Evaluation Volume 2 : Chemistry. Strategic Highway Research Program - National Research Council, Washington, D.C.

Pfeiffer JP, Saal RNJ (1940) Asphaltic Bitumen as Colloid System. J Phys Chem 44:139–149. doi: 10.1021/j150398a001

Polacco G, Filippi S, Merusi F, Stastna G (2015) A review of the fundamentals of polymer-modified asphalts: Asphalt/polymer interactions and principles of compatibility. Adv Colloid Interface Sci 224:72–112. doi: 10.1016/j.cis.2015.07.010

Polacco G, Kříž P, Filippi S, et al (2008) Rheological properties of asphalt/SBS/clay blends. Eur Polym J 44:3512–3521. doi: 10.1016/j.eurpolymj.2008.08.032

Polacco G, Stastna J, Biondi D, et al (2004) Rheology of asphalts modified with glycidylmethacrylate functionalized polymers. J Colloid Interface Sci 280:366–373. doi: http://dx.doi.org/10.1016/j.jcis.2004.08.043

Polacco G, Stastna J, Biondi D, Zanzotto L (2006) Relation between polymer architecture and nonlinear viscoelastic behavior of modified asphalts. Curr Opin Colloid Interface Sci 11:230–245. doi: 10.1016/j.cocis.2006.09.001

Read J, Whiteoak D (2003) The Shell Bitumen Handbook, fifth ed. Thomas Telford, London

Redelius P, Soenen H (2015) Relation between bitumen chemistry and performance. Fuel 140:34–43. doi: 10.1016/j.fuel.2014.09.044

Redelius PG (2006) The structure of asphaltenes in bitumen. Road Mater Pavement Des 7:143–162. doi: 10.1080/14680629.2006.9690062

Rogel E (2002) Asphaltene Aggregation: A Molecular Thermodynamic Approach. Langmuir 18:1928–1937. doi: 10.1021/la0109415

Rossi CO, Spadafora A, Teltayev B, et al (2015) Polymer modified bitumen: Rheological properties and structural characterization. Colloids Surfaces A Physicochem Eng Asp 480:390–397. doi: http://dx.doi.org/10.1016/j.colsurfa.2015.02.048

Saal RNJ, Labout JWA (1940) Rheological Properties of Asphaltic Bitumen. J Phys Chem 44:149–165. doi: 10.1021/j150398a002

Samyn F, Bourbigot S, Jama C, et al (2008) Crossed characterisation of polymer-layered silicate (PLS) nanocomposite morphology: TEM, X-ray diffraction, rheology and solid-state nuclear magnetic resonance measurements. Eur Polym J 44:1642–1653. doi: 10.1016/j.eurpolymj.2008.03.021

Saunders JH (1959) The Reactions of Isocyanates and Isocyanate Derivatives at Elevated Temperatures. Rubber Chem Technol

32:337–345. doi: 10.5254/1.3542399

Selvavathi V, Sekar VA, Sriram V, Sairam B (2002) MODIFICATIONS OF BITUMEN BY ELASTOMER AND REACTIVE POLYMER—A COMPARATIVE STUDY. Pet Sci Technol 20:535–547. doi: 10.1081/LFT-120003577

Sharmin E, Zafar F (2012) Polyurethane: An Introduction. In: Zahar F (ed) Polyurethane. New Delhi, pp 3–16

Sim HG, Ahn KH, Lee SJ (2003) Large amplitude oscillatory shear behavior of complex fluids investigated by a network model: a guideline for classification. J Nonnewton Fluid Mech 112:237–250. doi: 10.1016/s0377-0257(03)00102-2

Singh B, Tarannum H, Gupta M (2003) Use of isocyanate production waste in the preparation of improved waterproofing bitumen. J Appl Polym Sci 90:1365–1377. doi: 10.1002/app.12808

Sinha Ray S (2006) Rheology of polymer/layered silicate nanocomposites. J Ind Eng Chem 12:811–842.

Sinha Ray S, Okamoto M (2003) Polymer/layered silicate nanocomposites: A review from preparation to processing. Prog Polym Sci 28:1539–1641. doi: 10.1016/j.progpolymsci.2003.08.002

Speight, J. G., Wernick, D. L., Gould, K. A., et al (1985) Molecular Weight and Association of Asphaltenes: a Critical Review. Rev Inst Fr Pét 40:51–61. doi: 10.2516/ogst:1985004

Speight JG (2004) Petroleum asphaltenes - Part 1: Asphaltenes, resins and the structure of petroleum. Oil Gas Sci Technol 59:467–477. doi: 10.2516/ogst:2004032

Speight JG (2014) The Chemistry and Technology of Petroleum, Fifth Edition. CRC Press

Speight JG (1970) A structural investigation of the constituents of Athabasca bitumen by proton magnetic resonance spectroscopy. Fuel 49:76–90. doi: http://dx.doi.org/10.1016/0016-2361(70)90010-4

Stastna J, Zanzotto L, Vacin OJ (2003) Viscosity function in polymer-modified asphalts. J Colloid Interface Sci 259:200–207. doi: 10.1016/S0021-9797(02)00197-2

Sureshkumar MS, Filippi S, Polacco G, et al (2010) Internal structure and linear viscoelastic properties of EVA/asphalt nanocomposites. Eur Polym J 46:621–633. doi: 10.1016/j.eurpolymj.2009.12.024

Tanaka R, Sato E, Hunt JE, et al (2004) Characterization of asphaltene aggregates using X-ray diffraction and small-angle X-ray scattering. Energy and Fuels 18:1118–1125. doi: 10.1021/ef034082z

Tao Y, Yu J, Li B, Feng P (2010) Effect of different montmorillonites on rheological properties of bitumen/clay nanocomposites. J Cent South Univ Technol 15:172–175. doi: 10.1007/s11771-008-0340-0

Tjong SC (2006) Structural and mechanical properties of polymer nanocomposites. Mater Sci Eng R Reports 53:73–197. doi: http://dx.doi.org/10.1016/j.mser.2006.06.001

Ulrich H (1996) Chemistry and technology of isocyanates. J. Wiley & Sons

Vaia RA, Giannelis EP (1997a) Polymer melt intercalation in organically-modified layered silicates: Model predictions and experiment. Macromolecules 30:8000–8009. doi: 10.1021/ma9603488

Vaia RA, Giannelis EP (1997b) Lattice Model of Polymer Melt Intercalation in Organically-Modified Layered Silicates. Macromolecules 30:7990–7999. doi: 10.1021/ma9514333

Vaia RA, Jandt KD, Kramer EJ, Giannelis EP (1995) Kinetics of Polymer Melt Intercalation. Macromolecules 28:8080–8085. doi: 10.1021/ma00128a016

Vaia RA, Teukolsky RK, Giannelis EP (1994) Interlayer Structure and Molecular Environment of Alkylammonium Layered Silicates. Chem Mater 6:1017–1022. doi: 10.1021/cm00043a025

Vermant J, Ceccia S, Dolgovskij MK, et al (2007) Quantifying dispersion of layered nanocomposites via melt rheology. J Rheol (N Y N Y) 51:429–450. doi: 10.1122/1.2516399

Wallace D, Henry D, Pongar K, Zimmerman D (1987) Evaluation of some open column chromatographic methods for separation of bitumen components. Fuel 66:44–50. doi: 10.1016/0016-2361(87)90210-9

Wei D, Orlandi E, Simon S, et al (2015) Interactions between asphaltenes and alkylbenzene-derived inhibitors investigated by isothermal titration calorimetry. J Therm Anal Calorim 120:1835–1846. doi: 10.1007/s10973-015-4542-z

Wiehe IA, Liang KS (1996) Asphaltenes, resins, and other petroleum macromolecules. Fluid Phase Equilib 117:201–210. doi: 10.1016/0378-3812(95)02954-0

Wu D, Wu L, Gao F, et al (2008) Poly(phenylene sulfide) magnetic composites. I. Relations of percolation between rheology, electrical, and magnetic properties. J Polym Sci Part B Polym Phys 46:233–243.

doi: 10.1002/polb.21360

Wu Q, Pomerantz AE, Mullins OC, Zare RN (2014) Laser-based mass spectrometric determination of aggregation numbers for petroleum- and coal-derived asphaltenes. Energy and Fuels 28:475–482. doi: 10.1021/ef401958n

Yalcin B, Cakmak M (2004) The role of plasticizer on the exfoliation and dispersion and fracture behavior of clay particles in PVC matrix: a comprehensive morphological study. Polymer (Guildf) 45:6623–6638. doi: http://dx.doi.org/10.1016/j.polymer.2004.06.061

Yao H, You Z, Li L, et al (2013) Rheological Properties and Chemical Bonding of Asphalt Modified with Nanosilica. J Mater Civ Eng 25:1619–1630. doi: 10.1061/(ASCE)MT.1943-5533.0000690

Yarranton HW, Fox WA, Svrcek WY (2007) Effect of Resins on Asphaltene Self-Association and Solubility. Can J Chem Eng 85:635–642. doi: 10.1002/cjce.5450850510

You Z, Mills-Beale J, Foley JM, et al (2011) Nanoclay-modified asphalt materials: Preparation and characterization. Constr Build Mater 25:1072–1078. doi: 10.1016/j.conbuildmat.2010.06.070

Yu J, Feng P-C, Zhang H, Wu S-P (2009) Effect of organo-montmorillonite on aging properties of asphalt. Constr Build Mater 23:2636–2640. doi: 10.1016/j.conbuildmat.2009.01.007

Yu J, Wang L, Zeng X, et al (2007a) Effect of montmorillonite on properties of styrene-butadiene-styrene copolymer modified bitumen. Polym Eng Sci 47:1289–1295. doi: 10.1002/pen.20802

Yu J, Zeng X, Wu S, et al (2007b) Preparation and properties of

montmorillonite modified asphalts. Mater Sci Eng A 447:233–238. doi: 10.1016/j.msea.2006.10.037

Zanetti M, Lomakin S, Camino G (2000) Polymer layered silicate nanocomposites. Macromol Mater Eng 279:1–9. doi: 10.1002/1439-2054(20000601)279:1<1::AID-MAME1>3.0.CO;2-Q

Zare-Shahabadi A, Shokuhfar A, Ebrahimi-Nejad S (2010) Preparation and rheological characterization of asphalt binders reinforced with layered silicate nanoparticles. Constr Build Mater 24:1239–1244. doi: 10.1016/j.conbuildmat.2009.12.013

Zhang H, Shi C, Han J, Yu J (2013) Effect of organic layered silicates on flame retardancy and aging properties of bitumen. Constr Build Mater 40:1151–1155. doi: 10.1016/j.conbuildmat.2012.11.097

Zhang H, Wang HC, Yu J (2011a) Effect of aging on morphology of organo-montmorillonite modified bitumen by atomic force microscopy. J Microsc 242:37–45. doi: 10.1111/j.1365-2818.2010.03435.x

Zhang H, Yu J, Wang H, Xue L (2011b) Investigation of microstructures and ultraviolet aging properties of organo-montmorillonite/SBS modified bitumen. Mater Chem Phys 129:769–776. doi: 10.1016/j.matchemphys.2011.04.078

Zhang H, Yu J, Wu S (2012) Effect of montmorillonite organic modification on ultraviolet aging properties of SBS modified bitumen. Constr Build Mater 27:553–559. doi: 10.1016/j.conbuildmat.2011.07.008

Zhu J, Birgisson B, Kringos N (2014) Polymer modification of bitumen:

Advances and challenges. Eur Polym J 54:18–38. doi: 10.1016/j.eurpolymj.2014.02.005

Chapter 3

MATERIALS AND METHODS

Novel organoclay/isocyanate-based modification of bitumen for the development of high-performance composites

1. Materials

1.1. Bitumen

Bitumen provided by REPSOL S.A., with penetration grade within the range 160/220, was used as a base bitumen for the formulations in this work. Bitumen specifications, given by the values of penetration degree (EN 1426:2007), softening temperature (EN 1427:2007) and composition, reported in terms of the "SARAs" fractions, are shown in Table 3.1.

Table 3.1. Penetration, R&B softening temperature and composition (SARAs fractions) values for neat bitumen.

Specifications	Bitumen 160/220
Penetration (1/10 mm)	162
R&B softening point (ºC)	42.4
Saturates (wt.%)	2.91 (0.21)*
Aromatics (wt.%)	23.84 (0.90)*
Resins (wt.%)	66.98 (0.83)*
Asphaltenes (wt.%)	6.27 (0.38)*

*Values given as mean (standard deviation)

1.2. Modifying agents

Bitumen modification was carried out by addition of two different types of modifying agents, polymeric MDI and Cloisite® 20A, which in the present study, and according to the classification for the types of modifications given in chapter 2, section 11, "*Bitumen modification*", are included in the categories of isocyanate-based modification and clay-based modification, respectively.

A description and characterisation of those additives is included next.

1.2.1. Cloisite® 20A

This additive, termed "C20A", hereinafter, was supplied by Southern Clay Products, Inc. (Texas, U.S.A.), and corresponds to an off-white, natural montmorillonite (see Fig. 3.1(a)) modified with N,N-dimethyl di-hydrogenated tallow (C_{14}-C_{18}) quaternary ammonium chloride, whose structural formula is depicted in Fig. 3.1(b).

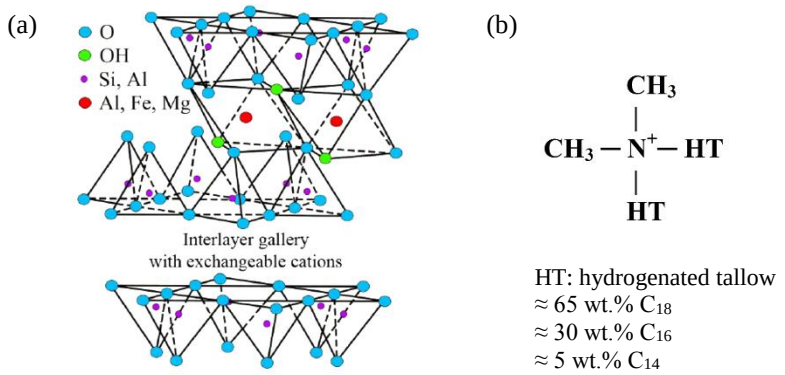

Fig. 3.1. (a) Structure of natural montmorillonite; and (b) Chemical structure of the Cation of dimethyl, dihydrogenated tallow quaternary ammonium chloride.

The cation exchange capacity of this clay is 92.6 meq/100 g clay and the hydrogenated tallow is composed by a combination of octadecyl (65 wt.%), hexadecyl (30 wt.%) and tetradecyl (5 wt.%) groups. Chemically, in addition to the organic cation present between the platelets, clays naturally contain pendant hydroxyl groups on the edge of the platelets, suitable for further interaction with other groups. Regarding particle specifications, the weight loss on ignition is 38 wt.%, with moisture content lower than 2 wt.% and a density of 1.77 g/cm^3. Dry particle sizes range from values lower than 2 µm (10 vol.%), to lower than 13 µm (90 vol.%), with an average value of 8 µm. The platelets are approximately 1 nm in thickness, leading to aspect

ratio values higher than 50, and according to XRD, the interlayer spacing is 2.42 nm.

1.2.2. Polymeric MDI (4,4'-diphenylmethane diisocyanate)

Supplied by T.H. Tecnic (Seville, Spain), it is a dark brown liquid consisting of an olygomeric mixture of 4,4'-diphenylmethane diisocyanate, 2,4' and 2,2' isomers, and condensation products with more than two aromatic rings. The structural formula is given in Fig. 3.2.

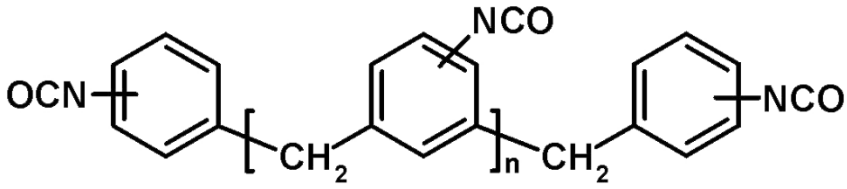

Fig. 3.2. Structural formula of polymeric MDI (n = 1, 2, 3, etc.).

A typical polymeric MDI contains approximately 50 wt.% pure MDI, 30 wt.% tri-isocyanate, 10 wt.% tetra-isocyanate, 5 wt.% penta-isocyanate and 5 wt.% higher homologues, although composition may be subjected to slight variations depending on the production process. The main properties of polymeric MDI are summarized in Table 3.2, being the one used in the present work characterised by an –NCO content of 30 wt.% (ASTM International 2010), and an average functionality of 2.7. Given its high reactivity with hydrogen active groups, it is stored at temperatures comprised between 0 and 8 ºC, and under nitrogen atmosphere.

Table 3.2. Main properties of polymeric MDI.

Property	**pMDI**
Physical form	Liquid
Molecular weight	≈ 450
Functionality	> 2
Flash point (ºC) (Cleveland open cup)	210 – 230
Fire point (ºC) (Cleveland open cup)	220 – 250

2. Processing of samples

2.1. Processing devices for bitumen modification

Samples were processed in metal containers (109 mm diameter and 131 mm height) immersed in a recirculating oil bath "J.P. SELECTA" with digital immersion thermostat "J.P. SELECTA DIGITERM 200", as shown in Fig. 3.3.

Fig. 3.3. J.P. SELECTA recirculating oil bath with DIGITERM 200 digital immersion thermostat.

As for mixing, two different processing devices were used depending upon the nature of the substances to be mixed:

- Polymeric MDI mixing, a low-shear mixer, consisting of a 50 mm four-bladed impeller coupled to the blending device "IKA RW20" (Fig. 3.4), which allowed processing at rotation speeds of 800 – 1000 rpm.

Fig. 3.4. IKA RW20 Stirrer and a 50 mm four-bladed impeller.

- Clay blending, a high-shear mixer, based on the rotor–stator principle, composed of a dispersing accessory with a 25 mm diameter stator coupled to an "Ultraturrax™ T25 digital" (Fig. 3.5), which reached rotation speeds ranging from 16000 to 18000 rpm.

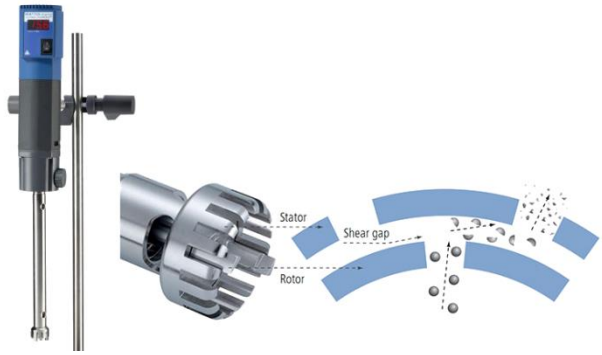

Fig. 3.5. Ultraturrax™ T25 digital high shear mixer and dispersing accessory.

Both devices were purchased from IKA (Germany).

2.2. Processing sequences

2.2.1. Bitumen modification

The modification of bitumen was carried out by applying different orders of addition, in accordance with the two processing sequences below. In any case, a concentration of 10 wt.% was established for C20A, whilst 2 wt.% was selected for MDI, which were correspondingly added depending on the formulation to be prepared. Both concentration values arise from a twofold consideration. On the one hand, purely aiming at producing noticeable effects on bitumen for characterisation purposes, a concentration of 10 wt.% C20A corresponds to the top end of the range of values normally used for bitumen and polymer blends (Choi et al. 2001; Lim et al. 2003; Sinha Ray 2006; Yu et al. 2007; Zare-Shahabadi et al. 2010; Barick and Tripathy 2011; Muniandy et al. 2013). On the other hand, reactivity between –NCO groups in MDI and active hydrogen groups both in bitumen

and in C20A requires the addition of enough MDI to react with them. In this sense, some results (Ortega et al. 2015) have evidenced that the reactive interaction between –NCO in polymeric MDI and –OH in C20A is characterised by a reaction mass ratio of 1.33 g of polymeric MDI per 10 g of C20A, which translates to 1.33 wt.% MDI. The reactivity of MDI with bitumen also had to be considered as an additional contribution to the concentration of the former, which was hence raised up to the value of 2 wt.% applied in the formulation of the composites, providing 2/3 –NCO for C20A and 1/3 –NCO excess for the reactions with the bituminous matrix.

This resulted in the set of systems listed in Table 3.3.

- Sequence A). C20A-MDI modification.

  A.1) C20A pre-dispersion: 10 wt.% C20A was first blended with bitumen at low shear (≈1000 rpm), at 150 °C for 10 min, in order to ensure an initial dispersion at the micrometre scale, favouring subsequent high-shear dispersion. A part of the so-called "bitumen/C20A pre-dispersion" was used as such, whereas the rest of the product was subjected to the following stage, A.2).

  A.2) High shear blending: the previous sample was high-shear blended (18000–20000 rpm) at 150 °C for 20 min, so as to maximize the degree of clay dispersion. Afterwards, the sample ("bitumen/C20A composite") was divided into three parts: a part was used as such; another part was kept under low-shear stirring for 1 h and 24 h, resulting in what are termed the "1 h-bitumen/C20A" and "24 h-bitumen/C20A" composites, respectively; and the remaining part was subjected to stage A.3).

A.3) Reaction with MDI: 2 wt.% polymeric MDI was added to the bitumen/C20A composite and blended at low-shear (≈1000 rpm), at 150 °C, being allowed to cure for 1 h and 24 h, with the resulting systems accordingly termed "1 h-bitumen/C20A/MDI" and "24 h-bitumen/C20A/MDI" composites.

- Sequence B) MDI-C20A modification.

  B.1) Reaction of bitumen with MDI and curing for 1 h and 24 h; followed by B.2) C20A pre-dispersion, for 10 min.; and concluded by B.3) high-shear blending for 20 min, to give the "1 h-bitumen/MDI/C20A" and "24 h-bitumen/MDI/C20A" composites.

Additionally, neat bitumen was also modified with MDI as described in stages A.3) and B.1), resulting in MDI-modified bitumens (1 h and 24 h curing), which were used as control samples.

For the purpose of clarity, note that nomenclature indicates the order of modifier addition.

Curing periods of 1 h and 24 h were evaluated in order to compare the potential benefit of prolonging the reactive stage on the composites' end properties at a short-term temporal scale.

Finally, in order to evaluate the specific effects of every set of processing conditions on the resulting properties, different blank samples of neat bitumen without any modifiers were processed according to each of the sequences above. For the sake of brevity, only selected blank samples, which underwent significant ageing, have been presented in the work.

Table 3.3. Summary of the systems prepared, indicating the stages for each processing sequence and protocol, along with duration and additives used.

				Processing Protocol	
		System	**Additives**	**Stages**[b]	**LSS duration (h)**
Sequence A	A.1	Bitumen/C20A pre-dispersion	C20A	PD	-
	A.2	Bitumen/C20A composite	C20A	PD, HSB	-
	A.2	1h-bitumen/C20A composite	C20A	PD, HSB, LSS	1
	A.2	24h-bitumen/C20A composite	C20A	PD, HSB, LSS	24
	A.2	Blank (24h-bitumen/C20A composite)	-	PD, HSB, LSS	24
	A.3	1h-bitumen/C20A/MDI composite	C20A, MDI	PD, HSB, LSS	1
	A.3	24h-bitumen/C20A/MDI composite	C20A, MDI	PD, HSB, LSS	24
Sequence B	B.1-3	1h-bitumen/MDI/C20A composite	MDI, C20A	LSS, PD, HSB	1
	B.1-3	24h-bitumen/MDI/C20A composite	MDI, C20A	LSS, PD, HSB	24

[b]PD: Pre-dispersion. Carried out by stirring at low shear for 10 min.
HSB: high shear blending
LSS: Low shear stirring

2.2.2. Reactive modification of Cloisite® 20A

With the aim of evaluating the reactivity of nanoclay with MDI, both modifiers were submitted to the following reaction protocol. Cloisite 20A® and polymeric MDI were mixed in a 5:1 mass ratio (same proportion as that used in both bitumen/nanoclay/MDI and bitumen/MDI/nanoclay composites) in toluene and heated under reflux conditions for 24 h. After completion, the solvent was removed under vacuum and the residue stored in N_2 atmosphere in a freezer for subsequent studies.

3. Technological characterization

The tests most widely used for the characterization and classification of the different grades of bitumen are penetration and Ring-and-Ball softening point. Although they are arbitrary empirical tests, they can be used to estimate important engineering properties of bitumen, such as hardness at intermediate in-service temperature, and consistency and thermal susceptibility at high in-service temperature, respectively.

As the penetration and softening point tests are empirically derived, it is essential to carry them out always under exactly the same conditions.

3.1. Penetration Test

This test, as stated above, allows quantifying bitumen hardness at intermediate in-service temperature (25 ºC), according to the standardised procedure found in UNE-EN 1426:2007.

In this test, a needle of specified dimensions is allowed to penetrate into a sample of bitumen, under a specific load (100 g), at a fixed temperature (25 ºC ± 0.1), and for a specific time (5 s). Then, the distance the needle penetrates, in units of decimilimetre, dmm (0.1 mm), is termed the penetration. Therefore, the greater the penetration, the softer bitumen.

Penetrations less than 2 and greater than 500 cannot be determined with accuracy, and even within this range, the specified procedure has to be followed closely to obtain reliable results.

For each test, three individual measurements of penetration are made. Then, the average of them is recorded to the nearest whole unit. The recorded penetration is reported if the difference between the individual three measurements does not exceed a specific limit.

This type of test is performed on a Universal Penetrometer, such as that depicted in Fig. 3.6.

Fig. 3.6. Penetration test device.

3.2. Ring and ball (R&B) softening point test

The R&B softening point test is a method to determine bitumen consistency at high in-service temperatures. By this test, the temperature at which the consistency of bitumen is between solid and liquid state (equi-viscous temperature) is measured. Therefore, regardless of the bitumen grade, the consistency will be the same for different bitumens characterized by the same R&B softening temperature.

The standardized procedure for this test can be found in UNE-EN 1427:2007. Accordingly, two steel balls are each placed on a sample of bitumen contained in a brass ring, which are in turn suspended in a water or glycerol bath under low stirring conditions (100 rpm), as shown in Fig. 3.7. Water is used for bitumens with a softening point of 80 ºC or below, and glycerol is used for softening points greater than 80 ºC. The bath temperature is raised at 5 ºC/min, such that bitumen softens and eventually deforms slowly with the ball through the ring. At the moment at which bitumen and the steel ball touch a base plate set 25 mm below the ring height, the temperature of the surrounding medium is recorded. The test is performed twice and the mean of the two measured temperatures is reported to the nearest 0.5 ºC. If the difference between both results exceeds 1.0 ºC, the test must be repeated. The reported temperature is designated the softening point of that bitumen under study.

This type of measurements was carried out using the Ring and Ball test unit SETA 21000 (Fig. 3.7)

Fig. 3.7. Equipment for R&B softening point measurement.

4. Chemical Characterization

4.1. Thin Layer Chromatography-Flame Ionization Detector analysis

The highly complex chemical composition of bitumen is generally assessed by means of chromatographic techniques, which allows separating bitumen in four different fractions termed saturates, aromatics, resins and asphaltenes (Corbett 1969), according to their chemical affinity for various solvents, thus constituting the so-called SARAs fractions.

The chemical characterization of bitumen is then carried out by a widely used chromatographic experiment set-up, corresponding to the coupling between thin layer liquid chromatography on quartz rods covered by silica gel and a flame ionization detector (Eckert 2001).

This type of measurements were performed using an Iatroscan MK-6 analyser (Iatron Corporation Inc., Japan), depicted in Fig. 3.8(a)

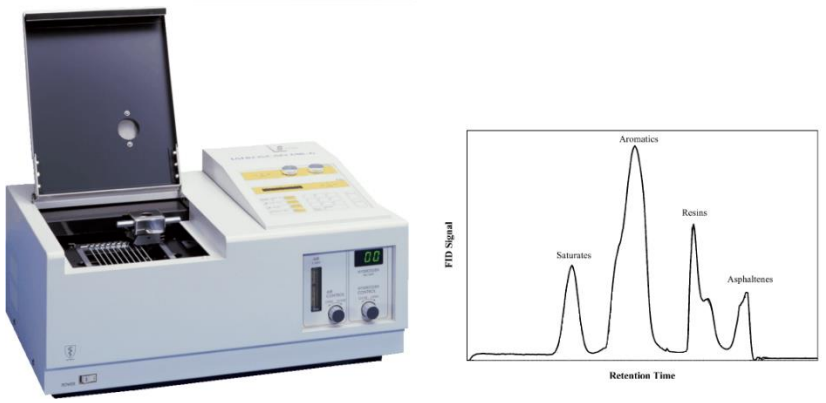

(a) (b)

Fig. 3.8. (a) TLC-FID Iatroscan MK-6 anaalyzer; and (b) General pattern for a chromatogram showing SARAs fractions of bitumen.

Initially, the chromatographic separation of bitumen fractions has to be performed. This is carried out by sequentially applying, by means of a micropipette, 1 µL of sample solution of bitumen in toluene (1 wt./vol.%)

to the lowest part of the silica coating on 10 quartz rods (Chromarods®). Then, those, which are conveniently located in a rod holder, are placed in the development tank containing the corresponding solvent, lined with a wick of chromatographic paper. Fractions are then separated by sequential elution using the following set of solvents as mobile phases: hexane, toluene, and a 95/5 (vol./vol.) blend of methylenedichloride/methanol. This allows the separation of saturates, aromatics and resins, respectively, with the most polar asphaltenes remaining at the original place.

Finally, after completion of the chromatographic separation procedure, the Chromarods® holder is properly inserted into a supporting frame, within the Iatroscan device, which allows the displacement of the holder, such that each Chromarod® is passed through the FID flame at an appropriate rate, ensuring the optimal detection and registration of the corresponding signal. This results in a chromatogram constituted by four well-resolved peaks, each associated to one of the bitumen fractions, as shown in Fig. 3.8(b), which is then used to determine the fractional composition of bitumen.

4.2. Fourier Transform Infrared Spectroscopy (FTIR)

Fourier transform spectroscopy measures the infrared (IR) light absorbed by a material, which will depend on its constituents and particularly, on the chemical functions present in it. Technically, an infrared light beam is charged through the material (either solid form or solution). This energy causes bonds in molecules to vibrate and rotate at distinct frequencies. Then, the energies absorbed at given frequencies are identified with a detector, and a spectrum of absorbance versus wavenumber is obtained.

FTIR spectra were obtained with a Jasco FT/IR-4200 apparatus (JASCO Inc., Japan), portrayed in Fig. 3.9. Different techniques were applied

depending on the type of sample tested. In the case of samples containing Cloisite 20A®, these were prepared as KBr pellets and placed into the appropriate sample holder. For bituminous samples, solutions of each system were prepared by dissolving 0.7 g of sample in 25 mL of dichloromethane, as it does not show any relevant peak within the wavenumber ranges studied (free –NCO, at 2275 cm^{-1}, and urea/urethane –CO bands at 1600 and 2000 cm^{-1}). Then, samples were laid on a potassium bromide (KBr) thin plate and the solvent was allowed to evaporate. Additionally, before any testing process, a blank spectrum was obtained with a clean KBr thin plate.

Fig. 3.9. Jasco FT/IR-4200 spectrometer.

All the spectra were obtained in a wavenumber range of 400 – 4000 cm^{-1}, at 4 cm^{-1} resolution in transmission mode. Furthermore, in order to minimize the influence of sample thickness on the absorption values registered, the peak at 1376 cm^{-1}, corresponding to the –CH symmetric bending vibration in bitumen (barely affected by oxidation and reactivity under the experimental conditions (Marsac et al. 2014)), was taken as a reference to perform the normalization of the curves.

5. Microstructural Characterization

5.1. Atomic Force Microscopy (AFM)

AFM was developed by Binning (Binnig et al. 1986). Its basic working principle is that a sharp tip attached at the end of a cantilever probes the specimen surface, with a laser beam focused at the end of the cantilever reflecting into a photodetector to track the surface topography, as illustrated in Fig. 3.10(a). The Atomic Force Microscope used is the MultiMode™ AFM, connected to a Nanoscope IV scanning probe microscope controller (Digital Instruments, Veeco Metrology Group Inc., Santa Barbara, U.S.A.), shown in Fig. 3.10(b). All the images were acquired in tapping mode at 30 ºC, which simultaneously monitors topography and phase data, in a scan size window of 20 µm x 20 µm.

(a) (b)

Fig. 3.10. (a) Illustration of the AFM working principle; and (b) MultiMode™ AFM, connected to a Nanoscope IV scanning probe microscope controller.

Tapping mode AFM, also called intermittent-contact mode, is a type of dynamic mode, along with non-contact mode, differs from it in that in the latter, the tip does not contact the sample surface. In tapping mode, however, the oscillating cantilever touches the sample surface at the end of its swing and both topographic and phase contrast images (phase-detection

atomic force microscopy) are obtained. This mode hence helps prevent problems of tip pollution by soft and adhesive bitumen, which results in the dragging of material on its surface. Phase contrast image is then generated by recording the phase shift between the oscillation signal sent to the instrument cantilever and its actual oscillation, as affected by tip-sample interactions. Fig. 3.11 illustrates a model oscillator affected by the material surface. The phase lag (δ) is analogous to that obtained during rheological measurements where tan δ = loss modulus/storage modulus, and therefore, provides valuable information about variations of sample rheological or adhesive properties (Masson et al. 2006). As the macroscopic rheological behaviour of bitumen is largely related to its diverse microstructures at the micro and nanometer scales, AFM is a suitable tool for the characterisation of the microscopic morphology of bitumen and its microstructural changes (Yu et al. 2015).

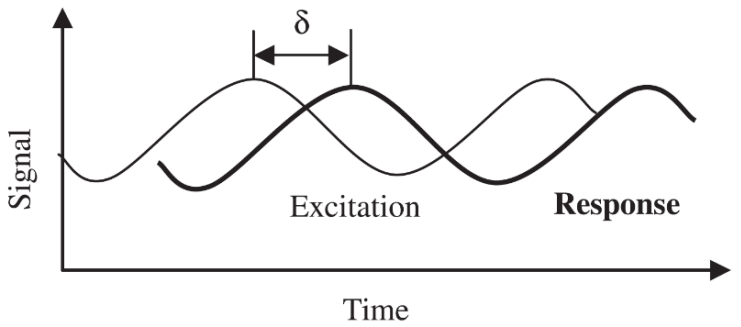

Fig. 3.11. Illustration of the phase lag δ between the set signal (excitation) and the tip response due to sample-tip interaction.

- **Preparation of sample films**

Bitumen films were prepared by heat-casting, a method that causes a negligible effect on the material morphology if compared to solvent-casting, in accordance with the procedure defined by Masson et al. 2006. This consists on the application of a bead of bitumen onto a 12 mm steel disk, which is then heated on a hot plate at around 110 ºC for 1 – 2 min,

which is a temperature high enough to melt bitumen, but not that high to provoke its oxidation. Once bitumen was in a "quasi-liquid" state, it was spread out with a blade to form a round film of about 5 mm in diameter, taking care such that excessive shearing was prevented. This hot film was left on the hot plate undisturbed for an additional 1 min to allow the surface to flow to a smooth and glossy finish. For AFM, the film was then cooled down to room temperature, covered to prevent dust pick-up and annealed for 24 h before imaging. This annealing allowed for the ordering of the asphaltenes responsible for steric hardening (Masson et al. 2002).

5.2. X-ray Diffraction (XRD)

XRD is the most commonly used technique for examining the structure, as well as for occasional study of the kinetics of nanocomposite formation. Either intercalated, including intercalated hybrids, or exfoliated nanostructures can be studied by monitoring the position, shape, and intensity of the basal reflections of XRD patterns of the materials (Jahromi and Khodaii 2009).

In this technique, an X-ray beam impinges on the sample, resulting scattered in all directions by the atoms of that sample. Some waves are then reflected by the atoms in certain directions, giving rise to an increased intensity due to the constructive interference of the scattered waves. Constructive interference between reflected X-rays from different hkl-planes will take place if the path length difference between them is an integer times the wavelength, as depicted in Fig. 3.12. This condition is summarized in the Bragg's law, as shown next.

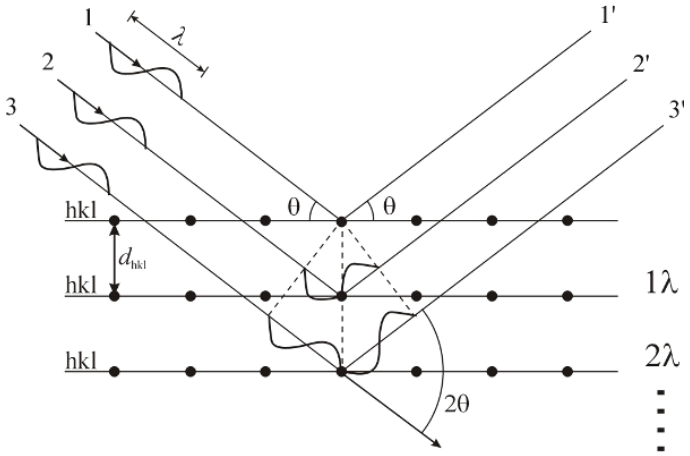

Fig. 3.12. Scattering of an X-ray beam by planes of atoms in a clay crystal lattice.

Thus, XRD allows measuring the distance (d-spacing) between clay layers (interlayer spacing or gallery) in intercalated structures by means of the 2θ angle value at which the (001) basal reflection peak is observed, according to the Bragg's law:

$$n\lambda = 2d \sin\theta \qquad \text{(eq. 3.1)}$$

Where λ is the X-ray wavelength of the incident beam (Cu used in the equipment has a λ value of 0.15418 nm), d is the interlayer distance, n is the order of diffraction, corresponding to an integral multiple of the wavelength, and θ is the angle of incident radiation.

Thus, the observation of changes in the diffraction angle corresponding to the plane d_{001} of the clay enables the structurl arrangement to be characterised.

X-ray diffraction tests were carried out at 25 ºC in a D8 Advance X-ray diffractometer (Bruker-AXS, Germany), shown in Fig. 3.13, with Cu-Kα radiation at a generator voltage of 40 kV, a current of 30 mA, and a wavelength of 0.15406 nm. The scan rate used was 0.475º min^{-1} in the 2θ

range from 1.5 to 10º. Pure C20A was tested as a powder, whereas bituminous samples were prepared by placing a small amount on a supporting glass slide of 25 × 25 mm^2, which was subsequently flattened to approximately 1 mm thick by applying a slight pressure at 70 °C for 0.5 min, followed by annealing at room temperature. Afterwards, the sample-containing slide was located at the centre of a metal holder, externally shaped to be allocated in the instrument.

Fig. 3.13. Bruker D8 Advance X-ray diffractometer.

5.3. Optical Microscopy

This technique uses visible light and a system of lenses to magnify images of small samples, and thus, it can be used to determine the shape, size and size distribution of microscopically dispersed particles, droplets or aggregates, reaching resolutions in the order of 0.5 μm.

In optical microscopy, light from an incandescent source is aimed toward a lens beneath the stage, called condenser, and then follows the path through the specimen, an objective lens, and to the eye, through a second magnifying lens, the ocular or eyepiece. In such an arrangement, the condenser is used to focus light on the specimen through an opening in the

stage. After passing through the specimen, the light is displayed to the eye with an apparent field that is much larger than that of the area illuminated, hence producing the magnifying effect.

Fig. 3.14. Olympus BX51 microscope.

In this case, microphotographs for microstructural characterisation were taken by means of a standard Olympus BX51 microscope (Olympus Optical, Japan) (Fig. 3.14), which can operate both in transmission and reflection mode, and coupled with a LTS-350 Heating-Freezing Stage, manufactured by Linkam Scientific Instruments (UK). This microscope possesses a built-in transmitted Koehler illumination that uses a 100W halogen bulb as a light source. Complementing the set-up is an Olympus C5050Z camera, along with several objectives from 4X to 50X magnification, which allow reaching resolutions of up to 0.37 μm.

As for testing, before proceeding, samples were prepared by setting very thin films of modified bitumen on standard microscope slides (76 × 26 mm). Then, microstructural observation was performed at room temperature (25 °C).

6. Thermal analysis

6.1. Modulated Differential Scanning Calorimetry (MDSC)

Conventional Differential Scanning Calorimetry (DSC) is a thermal analysis technique that allows the detection of transitions such as melts, glass transitions, phase changes, and curing by measuring the difference in heat flow rate between a sample and an inert reference with temperature. Hence, this technique provides quantitative and qualitative data on endothermic (heat absorption) and exothermic (heat evolution) processes.

In this work, a developed extension of DSC was used, namely modulated differential scanning calorimetry (MDSC), which adds a new dimension to the conventional DSC. In MDSC, the linear temperature programme is modulated by a sine wave, and thus, a mathematical treatment is applied to the resultant data to deconvolute the sample response to that sine wave from its response to the underlying heating programme. In this way, it allows distinguishing between reversing and non-reversing thermal behaviours in materials. The former include those that can be brought to equilibrium during the period of the modulated temperature signal used in the MDSC experiment, with the atomic motions responsible for the heat capacity as the most important one. As a result, this is the major contributor to the reversing curve. Effects that cannot be modulated and brought to equilibrium are excluded from the reversing curve and are shown as non-reversing, e.g. oxidation, evaporation, decomposition, relaxation, reaction. The melting of crystals can include both reversing and non-reversing contributions (Masson and Polomark 2001).

Hence, advantages with respect to conventional DSC include the capability of deconvoluting overlapping phenomena, improved resolution and enhanced sensitivity.

Fig. 3.15. TA Q-100 modulated differential scanning calorimeter.

Modulated differential scanning calorimetry (MDSC) was performed using a TA Q-100 (TA Instruments, USA) (Fig. 3.15) on 5 – 10 mg of sample inside hermetic pans. Every sample was submitted to the following procedure before testing, so that all of them were characterised by the same thermal history. Hence, before running the tests, samples were heated up to 150 ºC and left at that temperature for 30 min. Then, after a cooling period from the melt, they were annealed at room temperature for 24 h. Once annealed, a two-stage testing procedure was applied as follows, under nitrogen atmosphere. The first stage consisted on quenching to a temperature of 70 ºC, keeping the sample at that thermal condition for 5 min. In the second stage, the temperature was risen at a rate of 5 K/min up to 150 ºC in modulated mode, with a period of 60 s and an amplitude of 0.5 ºC.

6.2. Thermogravimetric Analysis (TGA)

Thermogravimetric analysis is a technique in which the mass of a substance is monitored as a function of temperature or time as the sample specimen is subjected to a controlled temperature program in a controlled atmosphere. It is widely used to characterize any material that exhibits

weight loss due to decomposition, dehydration or oxidation. Two different modes can be used for investigating thermal stability behaviour in controlled atmosphere:

- Temperature ramp, in which temperature is increased at a linear rate.
- Isothermal, in which temperature is kept constant.

Any TGA consists of a sample pan that is supported by a precision balance. That pan resides in a furnace and is heated or cooled during the experiment, and so, the mass of the sample is monitored, while a sample purge gas controls its environment. This gas, which may be inert or a reactive gas, flows over the sample and exits through an exhaust.

In the present work, thermogravimetric analysis tests were conducted using a TA Q-50 (TA Instruments, USA) (Fig. 3.16), under nitrogen atmosphere, on 5 – 10 mg of sample placed in aluminium pans, which were first heated up to 50 ºC and equilibrated at that temperature for 5 min., to be subsequently subjected to a continuous heating ramp at 10 K/min up to 600 ºC.

Fig. 3.16. TA Q-50 Thermogravimetric analyser.

7. Rheological Characterization

7.1. Rheometers

The study of the steady-state viscous properties of the systems and their viscoelastic characterization were performed by using a Physica MCR 301 rheometer. In addition to it, a Haake RheoStress RS-150 rheometer was complementarily used to assess the effects of shearing time. Both devices correspond to rheometers of controlled-stress rotational typology.

- **Physica MCR 301 rheometer** (Anton Paar, Austria) (Fig. 3.17).
  In this rheometer, temperature control is performed by a CTD-600 (Anton Paar, Austria), applying a combination of both convection and radiation. The device CTD-600 consists of two half-shells in which a convection gas, normally air, is heated, flowing completely symmetric in the sample chamber, and thus, ensuring perfect temperature distribution in the sample across the entire temperature range. Rheometer's testing specifications include ranges of torque between 0.1 μNm and 200 mN·m; speed from 10^{-6} to 3000 min^{-1}; and frequency from 0.0001 to 100 Hz.

Fig. 3.17. Physica MCR-301 rheometer.

- **RS-150 rheometer** (ThermoHaake, Germany) (Fig. 3.18).
  In this rheometer, sample temperature is controlled by an electric temperature control system (UTC), which consists of separately-controlled hybrid base and top plates, with electric heating systems and connectors for air or thermal liquid cooling (ThermoHaake, Germany). Testing specifications comprise a range of torque between 0.0005 and 150 mN·m, rotational speed from 10^{-7} to 1000 rpm, and frequency from 0.0001 to 100 Hz, with a strain resolution of $6 \cdot 10^{-7}$ rad.

Fig. 3.18. Rheostress RS-150 rheometer.

The geometry used for the entire set of samples corresponds to smooth parallel-plate with 25 mm in diameter, applying 1 – 2 mm gap. Before testing, in every case, samples were equilibrated at the test temperature for at least 20 min.

Moreover, every sample was subjected to testing at least three times in order to ensure the accuracy of the results obtained, which are shown as the average of the data gathered in each set of tests.

7.2. Rheological tests

7.2.1. Steady-state viscous flow tests

Viscosity curves, accounting for the variation of viscosity with shear rate, were performed at 60 ºC in controlled-strain mode, applying different shear rate intervals depending upon the type of system subjected to study. Such a temperature is usually taken as maximum expected temperature for a pavement exposed to the ambient in warm climate countries. As for shear rates applied, clay-containing materials were subjected to values from 10^{-3} s^{-1} up to the maximum value allowing obtaining reliable results, generally around 10 s^{-1}; whilst for the rest of systems, shear rates were comprised between 10^{-2} s^{-1} and the maximum value ensuring reliability, mainly located within the interval of 10 and 10^2 s^{-1}. In any case, smooth parallel-plate geometry with 25 mm diameter and 1 mm gap was used to perform the tests.

Time sweep tests under steady shear, at 10 s^{-1} and 150 °C, were performed aiming at assessing the effects of shearing time on the system response. For this purpose, a measuring device consisting of a cylindrical vessel with a four-bladed impeller was installed in the controlled-stress RS-150 rheometer, such that mixing conditions were simulated.

7.2.2. Oscillatory shear tests

The linear viscoelastic ranges, in which viscoelastic functions are independent on the stress or strain applied, were determined by means of stress sweeps at 1 Hz, which were carried out at the highest and lowest testing temperatures, corresponding to 30 and 150 ºC, respectively, for clay-containing systems; and 30 and 90 ºC, for the rest of them. Along with the tests performed at such temperature bounds, additional stress sweeps were carried out at several temperatures in-between, in order to obtain

stress values that ensured the continuity in the linear viscoelastic response when varying temperature throughout the entire thermal range studied for each system.

Temperature sweep tests in oscillatory shear, at a frequency of 10 rad/s, were conducted using a continuous heating ramp rate of 1 K/min, from 30 ºC up to the maximum possible temperature for reliable measurements. In each case, stress values were specifically selected in order to ensure a linear viscoelastic response within the entire range of temperatures tested.

Oscillatory-shear frequency sweep tests between 0.03 and 10^2 rad/s were carried out at different temperatures, ranging from 30 ºC up to the maximum possible value that allowed obtaining reliable measurements. At each temperature, values of stress within the linear viscoelastic response were correspondingly selected.

8. Bibliography

ASTM International (2010) ASTM D2572 – 97(2010) Test method for isocyanate groups in urethane materials or prepolymers.

Barick AK, Tripathy DK (2011) Effect of organically modified layered silicate nanoclay on the dynamic viscoelastic properties of thermoplastic polyurethane nanocomposites. Appl Clay Sci 52:312–321. doi: 10.1016/j.clay.2011.03.010

Binnig G, Quate CF, Gerber C (1986) Atomic Force Microscope. Phys Rev Lett 56:930–933. doi: 10.1103/PhysRevLett.56.930

Choi HJ, Kim SG, Hyun YH, Jhon MS (2001) Preparation and rheological characteristics of solvent-cast poly(ethylene oxide)/montmorillonite nanocomposites. Macromol Rapid Commun 22:320–325. doi: 10.1002/1521-3927(20010301)22:5<320::aid-marc320>3.0.co;2-3

Corbett LW (1969) Composition of asphalt based on generic fractionation, using solvent deasphaltening, elution-adsorption chromatography, and densimetric characterization. Anal Chem 41:576–579. doi: 10.1021/ac60273a004

Eckert A (2001) The application of Iatroscan-technique for analysis of bitumen. Pet Coal 43:51–53.

Jahromi SG, Khodaii A (2009) Effects of nanoclay on rheological properties of bitumen binder. Constr Build Mater 23:2894–2904. doi: 10.1016/j.conbuildmat.2009.02.027

Lim ST, Lee CH, Choi HJ, Jhon MS (2003) Solidlike transition of melt-intercalated biodegradable polymer/clay nanocomposites. J Polym Sci Part B-Polymer Phys 41:2052–2061. doi: 10.1002/polb.10570

Marsac P, Piérard N, Porot L, et al (2014) Potential and limits of FTIR methods for reclaimed asphalt characterisation. Mater Struct 47:1273–1286. doi: 10.1617/s11527-014-0248-0

Masson JF, Leblond V, Margeson J (2006) Bitumen morphologies by phase-detection atomic force microscopy. J Microsc 221:17–29. doi: 10.1111/j.1365-2818.2006.01540.x

Masson JF, Polomark GM (2001) Bitumen microstructure by modulated differential scanning calorimetry. Thermochim Acta 374:105–114. doi: http://dx.doi.org/10.1016/S0040-6031(01)00478-6

Masson JF, Polomark GM, Collins P (2002) Time-dependent microstructure of bitumen and its fractions by modulated differential scanning calorimetry. Energy & Fuels 16:470–476. doi: 10.1021/ef010233r

Muniandy R, Hasham S, Aburkaba E, others (2013) Effect of Organic Montmorillonite Nanoclay Concentration on the Physical and Rheological Properties of Asphalt Binder. Aust J Basic Appl Sci 7:429–437.

Ortega FJ, Navarro FJ, García-Morales M, McNally T (2015) Thermo-mechanical behaviour and structure of novel bitumen/nanoclay/MDI composites. Compos Part B Eng 76:192–200. doi: http://dx.doi.org/10.1016/j.compositesb.2015.02.030

Sinha Ray S (2006) Rheology of polymer/layered silicate nanocomposites. J Ind Eng Chem 12:811–842.

Yu J, Zeng X, Wu S, et al (2007) Preparation and properties of montmorillonite modified asphalts. Mater Sci Eng A 447:233–238.

doi: 10.1016/j.msea.2006.10.037

Yu X, Burnham NA, Tao M (2015) Surface microstructure of bitumen characterized by atomic force microscopy. Adv Colloid Interface Sci 218:17–33. doi: 10.1016/j.cis.2015.01.003

Zare-Shahabadi A, Shokuhfar A, Ebrahimi-Nejad S (2010) Preparation and rheological characterization of asphalt binders reinforced with layered silicate nanoparticles. Constr Build Mater 24:1239–1244. doi: 10.1016/j.conbuildmat.2009.12.013

Chapter 4

RESULTS AND DISCUSSION

Novel organoclay/isocyanate-based modification of bitumen for the development of high-performance composites

Chapter 4. Results and discussion

Los artículos que forman parte del apartado “Chapter 4”, han sido retirados de la tesis debido a restricciones relativas a derechos de autor. En sustitución de los artículos ofrecemos la siguiente información: referencia bibliográfica, enlace a la revista, y resumen.

- Ortega, F.J., Navarro, F.J., García Morales, M., McNally, T. : “Therma-mechanical behaviour and structure of novel bitumen/nanoclay/MDI composites”. Composites Part B: Engineering. Vol. 76, págs. 192-200 (2015).
DOI: 10.1016/j.compositesb.2015.02.030

Enlace al texto completo: https://doi.org/10.1016/j.compositesb.2015.02.030

RESUMEN:
Novel ternary bituminous composites have been prepared by mixing neat bitumen with an organically modified montmorillonite (Cloisite 20A®) and polymeric MDI (diphenylmethane diisocyanate). Rheological measurements (flow curves and temperature sweeps in oscillatory shear), X-Ray diffraction, Atomic Force Microscopy (AFM) and Fourier Transform Infrared Spectroscopy (FTIR) were used to analyse the individual and joint effects of both modifiers. The results obtained show that the addition of 10 wt.% nanoclay provokes a very remarkable enhancement in the bitumen rheological response. The addition of 2 wt.% MDI and subsequent curing at 150 °C, resulting from the chemical interaction between the bitumen/clay composite and MDI, improves the composite properties at low-to-intermediate temperatures but deteriorates them when temperature is further increased.

- Ortega, F.J., Navarro, F.J., García Morales, M., McNally, M.: “Effect of shear processing on the linear viscoelastic behaviour and microstructure of bitumen/montmorillonite/MDI ternary composites”. Journal of Industrial and Engineering Chemistry. Vol. 48, págs. 212-223, (2017). DOI: 10.1016/j.jiec.2017.01.004

Enlace al texto completo: https://doi.org/10.1016/j.jiec.2017.01.004

RESUMEN:
Polymer modified bitumens (PMBs) have largely been utilized as a construction material. However, lack of affinity between bitumen and polymer leads to phase separation, and eventually, performance depletion. In this paper, alternative formulations of bitumen with an organically-modified montmorillonite (OMMT) Cloisite 20A® and polymeric methylene diphenyl diisocyanate (MDI) were prepared by melt blending. Their comprehensive rheological characterisation evidenced improved linear viscoelastic properties when OMMT is added, revealing a noticeable structural reinforcement and thermal stability. Rheological data also showed that MDI-involved reactions control the composite end properties, being greatly influenced by the shear conditions applied.

- Ortega, F.J., Roman, C., Navarro, F.J., García Morales, M., McNally, M.: "Physico-chemistry control of the linear viscoelastic behaviour of bitumen/montmorillonite/MDI ternary composites: Effect of the modification sequence". Fuel Processing Technology. Vol. 143, págs. 195-203, (2016). DOI: 10.1016/j.fuproc.2015.11.011

Enlace al texto completo: https://doi.org/10.1016/j.fuproc.2015.11.011

RESUMEN:
Binary bituminous composites consisting of asphaltic bitumen and 10 wt.% organically modified montmorillonite (OMMT) Cloisite 20A®, and ternary composites, also containing 2 wt.% polymeric MDI (diphenylmethane diisocyanate), were prepared by melt blending. In order to appraise the effect that the order of addition of bitumen modifiers has on the composites rheological properties, dynamic shear temperature sweep measurements were conducted. If the MDI curing was prolonged for up to 24 h, quite notable differences were observed between ternary blends at which the OMMT was added before and after MDI modification. On the one hand, a later MDI addition increased the binary composite linear viscoelastic (LVE) moduli at low-to-intermediate temperatures, but provoked a marked reduction at the highest temperatures studied. By contrast, an inversion in the order of addition showed to enhance the rheological response in the entire range of temperature studied. Optical microscopy observations and, mainly, atomic force microscopy (AFM) scans suggest the reactive agglomeration of OMMT into large domains if MDI is added in a second step. However, if MDI is firstly added, the reactive modification is mainly targeted at the bitumen matrix and then at the interaction between that and the hydroxyl groups located in the MMT.

Chapter 5

CONCLUSIONS

Novel organoclay/isocyanate-based modification of bitumen for the development of high-performance composites

The ample variety of studies performed in the present work have allowed drawing several major highlights, encompassing the most relevant facts inferred from the entirety of experimental results obtained, as outlined next:

- ✓ The single addition of 2 wt.% MDI to bitumen yields an improvement in both viscous and viscoelastic responses, especially after curing for 24 h, but does not change it, prevailing the viscous contribution to the overall response at that concentration. This well-known effect arises from isocyanate-involved reactions that lead to the formation of urethane and urea bonds, jointly developing a new microstructure composed of larger and more complex molecules.

- ✓ The addition of Cloisite 20A® to bitumen, in this case in a concentration of 10 wt.%, gives rise to a considerable alteration of the thermo-rheological behaviour with respect to that of neat bitumen, resulting in a marked shear thinning drop of the viscosity over the entire shear rate interval tested, as measured at 60 ºC, along with a clear solid-like behaviour of the linear viscoelastic functions ("rubbery" plateau-like zone) at temperatures above 100 ºC. This reveals a more complex multiphasic structural arrangement that acts as a reinforcing clay-based network, contributing to the retention of the structural stability at temperatures at which bitumen normally softens. The intercalation of clay tactoids by bitumen molecules and the corresponding formation of a hybrid intercalated structure, as inferred from X-ray scans, and AFM and optical microscopy imaging, seems to be the main process behind such a structural reinforcement.

- ✓ The type of shear applied during the preparation procedure of the bitumen/C20A binary system greatly influences the degree of dispersion clay tactoids within the bituminous matrix and the end

properties of such a system. Thus, if high shear stresses are applied, intercalation/exfoliation processes of clay tactoids are favoured, leading to the formation of composites in which clay tactoids/platelets act as a structural reinforcement, markedly improving material's thermo-mechanical properties. However, use of mere low shear stirring of bitumen/C20A composites tends to promote the association/re-aggregation of clay platelets/tactoids, as a consequence of edge-to-edge hydroxyl interactions in C20A. This results in the disruption of the clay-based structural reinforcing network and a marked decay in the LVE response at the highest temperatures studied in this work, further intensified at longer stirring times.

- ✓ Isocyanate groups in MDI are prone to interact reactively with groups containing active hydrogen atoms both in bitumen and in C20A, although a preferential reactivity is observed in relation to those present in the latter. This has paramount implications regarding the constitution of an adequate processing procedure that allows obtaining and optimising the beneficial effects of –NCO-involved reactions on the composite's end properties.

- ✓ The addition of 2 wt.% MDI to the bitumen/C20A composite results in material's end properties controlled by curing time, in turn associated to -NCO-involved reactions and their effects on dispersion state of the clay platelets/tactoids, as evidenced by microstructural and morphological studies. Thus, at short curing times (1 h), neither all -NCO groups have reacted nor dispersion condition of clay platelets/tactoids has been significantly modified, leading to a somewhat improved rheological behaviour, as long as the testing temperature is low enough so that the continuous bitumen phase still

exerts the overall control of the response. By contrast, longer curing times up to 24 h bring about the progressive formation of larger and more complex compounds containing urea/urethane linkages, which promote the clustering of clay platelets/tactoids, causing the disruption of the clay-based network, and thus, the destabilisation of its reinforcing effect when the bituminous matrix softens, despite properties at intermediate in-service temperatures (30 – 40 ºC) are improved.

- ✓ The processing sequence in which MDI is initially added to bitumen, followed by curing and further incorporation of C20A to the MDI-modified bitumen yields a composite with a dramatically improved rheological response. A marked enhancement in G' and G'' and a prevailing solid-like behaviour are found in the entire temperature range studied in this work. Evidence for this has also been obtained from optical and atomic force microscopy investigations, revealing a better degree of dispersion of clay platelets/tactoids. In this case, the -NCO groups are first attached to the compounds in the bitumen matrix, whereas the remaining -NCO groups are available to link to C20A at a later step, consequently hindering the disruption of the clay-based structural reinforcement.

- ✓ The type of shear processing applied during curing greatly affects the composites' end properties, with clay intercalation/exfoliation processes being favoured in the absence of stirring, leading to a greater reinforcement of the system structure. Contrarily, shear processing promotes the agglomeration/re-aggregation of clay platelets/tactoids, diminishing their degree of dispersion, and therefore, the structural reinforcement they provide. In the presence of MDI, processing shear

effects are even more pronounced, as the -NCO-involved reactions determine whether new larger and more complex molecules contribute to a better nanoclay dispersion, if not stirred, or tend to destabilise the system, under shear processing.

Conclusiones

La variedad de estudios efectuados en el presente trabajo ha posibilitado determinar diversas relaciones causales de importancia, englobando los hechos de mayor relevancia procedentes de los resultados experimentales obtenidos, según se describe seguidamente:

- ✓ La adición de un 2 % (p/p) de MDI al betún genera una mejora de las respuestas viscosa y viscoelástica, especialmente tras un proceso de curado de 24 h, aunque sin modificarla, manteniéndose el carácter prevalente de la contribución viscosa a la respuesta total del sistema para dicha concentración. Tal efecto es consecuencia de las reacciones con los isocianatos, que conllevan la formación de enlaces urea y uretano, y dan lugar en conjunto al desarrollo de una nueva microestructura constituida por molecular de mayor tamaño y complejidad.

- ✓ La adición de Cloisite 20A® al betún, en este caso en una concentración del 10 % (p/p), da lugar a una considerable modificación del comportamiento termo-reológico con respecto al del betún original, resultando en un marcado carácter pseudoplástico de la viscosidad en la totalidad del intervalo de velocidades de cizalla estudiado, según las medidas realizadas a 60 ºC, junto con un comportamiento de las funciones viscoelásticas principalmente elástico (zona plateau) a temperaturas superiores a los 100 ºC. Ello revela una organización estructural multifásica de mayor complejidad, que actúa como red de refuerzo con base de nanoarcilla, contribuyendo a mantener la estabilidad estructural a aquellas temperaturas a las que el betún se reblandece. La intercalación de las láminas de nanoarcillas por las moléculas de betún y la consiguiente formación de una

estructura híbrida intercalada, según se deduce de los datos de rayos X, AFM y microscopía óptica, parecen ser los principales procesos que generan dicho nivel de refuerzo estructural.

- ✓ El tipo de cizalla aplicada durante el procedimiento de preparación del sistema binario betún/C20A presenta una gran influencia sobre el grado de dispersión de la nanoarcilla en la matriz bituminosa y las propiedades finales del sistema. De esta forma, la aplicación de alta cizalla favorece los procesos de intercalación/exfoliación de las nanoarcillas, dando lugar a la formación de composites en los que la láminas de nanoarcillas actúan como refuerzo estructural, mejorando notablemente las propiedades termo-mecánicas del material. En cambio, el uso de agitación a baja cizalla de los composites de betún/C20A tiende a promover la asociación/re-agregación de las láminas de nanoarcilla, como consecuencia de la interacción entre los hidroxilos localizados en las aristas de las láminas de aluminosilicatos de la C20A. Esto resulta en la desestabilización de la red de refuerzo estructural proporcionada por la nanoarcilla, y en un marcado descenso de la respuesta viscoelástica lineal a las temperaturas más altas estudiadas en este trabajo, lo que se intensifica al incrementarse el tiempo de agitación.

- ✓ Los grupos isocianato del MDI tienden a interaccionar reactivamente con los grupos que contienen átomos activos de hidrógeno tanto en el betún como en la C20A, distinguiéndose una reactividad preferencial con respecto a aquellos presentes en esta última. Dicha preferencia presenta implicaciones de gran importancia en lo que concierne al establecimiento de un procedimiento de procesado tal que permita

obtener y optimizar los efectos beneficiosos de las reacciones de los isocianatos sobre las propiedades finales del composite.

- ✓ La adición del 2 % (p/p) de MDI al composite de betún/C20A resulta en un material cuyas propiedades finales dependen del tiempo de curado, asociado a su vez a las reacciones de los isocianatos y sus efectos sobre el estado de dispersión de las láminas de nanoarcilla, según los datos de los estudios morfológicos y microestructurales. Por lo tanto, a tiempos cortos de curado (1h) no reaccionan la totalidad de grupos isocianatos, ni se modifica el estado de dispersión de la nanoarcilla, lo que produce una mejora del comportamiento reológico a temperaturas suficientemente bajas como para que la fase bituminosa controle la respuesta reológica. Por el contrario, tiempos de curado superiores, de hasta 24 h, dan lugar a la progresiva formación de compuestos de mayor tamaño y complejidad, con enlaces ure/uretano, que promueven la agregación de las láminas de nanoarcilla, provocando la desestabilización de la red estructural que ésta genera, así como el deterioro su efecto de refuerzo a las temperaturas a las que el betún se reblandece, a pesar de que se mejoran las propiedades a temperaturas intermedias de servicio (30 – 40 ºC).

- ✓ La secuencia de procesado en la que el MDI se añade en primer lugar al betún, seguido por la etapa de curado y la posterior adición de C20A, da lugar a un composite con una respuesta reológica considerablemente mejorada. En este sentido, se distinguen un marcado incremento en G’ y G’’ y un comportamiento eminentemente elástico en la totalidad del rango de temperatura estudiado en el presente trabajo. Los resultados procedentes de la microscopía óptica y de fuerza atómica también evidencian tal efecto, revelando un mayor

grado de dispersión de las láminas de aluminosilicatos. Así, en este caso, los grupos isocianato reaccionan en primer lugar con los compuestos de la matriz bituminosa, mientras que los isocianatos restantes estarían disponibles para interaccionar posteriormente con la C20A, evitándose de esta forma la desestabilización del refuerzo estructural proporcionado por la nanoarcilla.

- ✓ El tipo de cizalla aplicada durante el curado afecta considerablemente a las propiedades finales de los composites, de tal forma que los procesos de intercalación/exfoliación resultan favorecidos en ausencia de agitación, dando lugar a un mayor grado de refuerzo de la estructura del sistema. En cambio, la aplicación de cizalla promueve la aglomeración/re-agregación de las láminas de nanoarcilla, reduciendo su grado de dispersión y, por tanto, el refuerzo estructural que éstas proporcionan. En presencia de MDI, los efectos de la cizalla durante el procesado se acrecientan, dado que las reacciones de los isocianatos determinan si las nuevas moléculas de mayor tamaño y complejidad contribuyen a una mejor dispersión de la nanoarcilla, en el caso de ausencia de agitación; o tienden a desestabilizar el sistema, en condiciones de procesado con cizalla.

Annexe I

LIST OF PUBLICATIONS

Novel organoclay/isocyanate-based modification of bitumen for the development of high-performance composites

Thermo-mechanical behaviour and structure of novel bitumen/nanoclay/MDI composites

F.J. Ortega[a], F.J. Navarro[a], M. García-Morales[a], T. McNally[b]

[a]*Departamento de Ingeniería Química, Centro de Investigación en Tecnología de Productos y Procesos Químicos (Pro^{2}TecS), Campus de 'El Carmen', Universidad de Huelva, 21071, Huelva (Spain)*

[b]*International Institute for Nanocomposites Manufacturing (IINM), WMG, The University of Warwick, CV4 7AL, Coventry (United Kingdom)*

Published in: ***Composites Part B: Engineering***

ISSN: 1359-8368

Publisher: Elsevier

Editor-in-Chief and Editor for North America and Asia: David Hui

JCR Impact Factor (2014): 2.983

JCR Category	Quartile
Engineering, Multidisciplinary	Q1
Materials Science, Composites	Q1

Effect of shear processing on the linear viscoelastic behaviour and microstructure of bitumen/montmorillonite/MDI ternary composites

Francisco J. Ortega[a], Francisco J. Navarro[a,✉], Moisés García-Morales[a], Tony McNally[b]

[a]*Departamento de Ingeniería Química, Centro de Investigación en Tecnología de Productos y Procesos Químicos (Pro^{2}TecS), Campus de 'El Carmen', Universidad de Huelva, 21071, Huelva (Spain)*

[b]*International Institute for Nanocomposites Manufacturing (IINM), WMG, University of Warwick, CV4 7AL, Coventry (United Kingdom)*

Published in: ***Journal of Industrial and Engineering Chemistry***

ISSN: 1226-086X

Publisher: Elsevier

Editor-in-Chief: Bok Ryul Yoo

JCR Impact Factor (2015): 4.179

JCR Category	Quartile
Chemistry, Multidisciplinary	Q1
Engineering, Chemical	Q1

Physico-chemistry control of the linear viscoelastic behaviour of bitumen/montmorillonite/MDI ternary composites: effect of the modification sequence

F.J. Ortega[a], C. Roman[a], F.J. Navarro[a], M. García-Morales[a], T. McNally[b]

[a]*Departamento de Ingeniería Química, Centro de Investigación en Tecnología de Productos y Procesos Químicos (Pro^{2}TecS), Campus de 'El Carmen', Universidad de Huelva, 21071, Huelva (Spain)*

[b]*International Institute for Nanocomposites Manufacturing (IINM), WMG, The University of Warwick, CV4 7AL, Coventry (United Kingdom)*

Published in: ***Fuel Processing Technology***

ISSN: 0378-3820

Publisher: Elsevier

Editor-in-Chief: Chun-Zhu Li

JCR Impact Factor (2015): 3.847

JCR Category	Quartile
Chemistry, Applied	Q1
Energy & Fuels	Q1
Engineering, Chemical	Q1

Appendix I

LIST OF TABLES

Novel organoclay/isocyanate-based modification of bitumen for the development of high-performance composites

INTRODUCTION

–

LITERATURE REVIEW

Table 2.1. Classification of active hydrogen compound based on their relative reactivity with the isocyanates group. 87

MATERIALS AND METHODS

Table 3.1. Penetration, R&B softening temperature and composition (SARAs fractions) values for neat bitumen. 155

Table 3.2. Main properties of polymeric MDI 157

Table 3.3. Summary of the systems prepared, indicating the stages for each processing sequence and protocol, along with duration and additives used. 162

RESULTS AND DISCUSSION

Block 1

Table 1. Penetration, R&B softening temperature and composition (SARAs fractions) values for base bitumen. 192

Table 2. Diffraction angle and interlayer spacing at the (001) basal reflection for pure C20A, and for bitumen/C20A and bitumen/C20A/MDI composites. 206

Block 2

Table 1. Penetration, R&B softening temperature and composition (SARAs fractions) values for neat bitumen. 226

Table 2. Bitumen SARAs fraction values for neat bitumen, and for Bitumen/C20A and Bitumen/C20A/MDI composites. Data for the corresponding blanks are also included. 254

Block 3

Table 1. Penetration, R&B softening temperature and composition (SARAs fractions) values for base bitumen. 268

Table 2. Summary of the systems prepared, indicating the stages for each processing sequence and protocol, along with duration and additives used. 271

Appendix II

LIST OF FIGURES

Novel organoclay/isocyanate-based modification of bitumen for the development of high-performance composites

INTRODUCTION

–

LITERATURE REVIEW

Fig. 2.1. Bitumen manufacturing process 24

Fig. 2.2. Schematic representation of the molecular organization in (a) SOL type bitumen and; (b) GEL type bitumen (Read and Whiteoak 2003) 46

Fig. 2.3. Place of rheology amongst other sciences, considering applied problems. 52

Fig. 2.4. Schematic of steady simple shearing of a material element located between two parallel plates. 54

Fig. 2.5. Variation of viscosity with shear rate for a given material. 58

Fig. 2.6. Examples of curves for the evolution of viscosity with shear rate, exhibiting shear-thinning behaviour. 58

Fig. 2.7. Evolution of viscosity with shear rate for a shear-thickening material. 60

Fig. 2.8. Development of (a) shear stresses at constant shear rates; and (b) shear rate at constant shear stress. 61

Fig. 2.9. Hysteresis loop in continuous change of shear rate formed due to thixotropic and rheopectic properties of a liquid. An arrow shows the direction of changes of experimental conditions in viscosity measurement. 62

Fig. 2.10. Various tests that measure the time response of a liquid. 64

Fig. 2.11. Schematic representation of oscillatory testing. 65

Fig. 2.12. Regions constituting the characteristic viscoelastic spectrum of a non-Newtonian liquid. 66

Fig. 2.13. Steady state shear flow tests at different temperatures for a neat bitumen (Baldino et al. 2013). 68

Fig. 2.14. General pattern for the dependency of the viscoelastic functions of a neat bitumen with temperature (Rossi et al. 2015). 70

Fig. 2.15. (a)Thermal stresses behind cracking phenomenon in a pavement layer. (b) Cracks arising on a pavement surface. 77

Fig. 2.16. Depression appearing on a pavement surface as a consequence of rutting. 77

Fig. 2.17. Qualitative behaviour of a generic mechanical property with polymer swelling. 83

Fig. 2.18. Resonance structures of the isocyanate group. 85

Fig. 2.19. Resonance structures of an aromatic isocyanate. 86

Fig. 2.20. General reaction scheme between an isocyanate group and any functional group containing an active hydrogen atom. 87

Fig. 2.21. Primary addition reactions of isocyanate with (a) amine, (b) water, (c) alcohol, and (d) carboxylic acid. 88

Fig. 2.22. Secondary addition reactions of iscoyanates with (a) urethane, (b) urea, and (c) amide. 89

Fig. 2.23. Self-addition reactions of isocyanate. 91

Fig. 2.24. Possible reaction scheme between isocyanate moieties and some bituminous fractions (asphaltenes and resins). 93

Fig. 2.25. Illustration of the evolution of different bitumen length scales. 94

Fig. 2.26. General classification for silicates (clays). 96

Fig. 2.27. General structure of 2:1 phyllosilicates (Kotal and Bhowmick 2015). 98

Fig. 2.28. Reaction scheme for surface treatment of a sodium MMT with a surfactant (quaternary alkylammonium salt) from hydrophilic to organophilic (Jahromi and Khodaii 2009; Herrera-Alonso et al. 2010). 102

Fig. 2.29. Gallery size (d-spacing) dependence with the ratio of mass of intercalated organic cation to mass of layered silicate (MMT) (Fornes et al. 2002). 103

Fig. 2.30. Possible arrangements of alkyl chains in the interlayer space: (a) short alkyl chains: isolated molecules, lateral monolayer; (b) intermediate chain lengths: in-plane disorder and interdigitation to form quasi-bilayers; and (c) longer chain length: increased interlayer order, liquid crystalline-type environment (Vaia et al. 1994; Alexandre and Dubois 2000). 104

Fig. 2.31. Schematic of the morphology of organo-modified clays (Vaia et al. 1995). 111

Fig. 2.32. Schematic illustration of the different types of thermodynamically achievable bitumen/layered silicate nanocomposites (Jahromi and Khodaii 2009). 113

Fig. 2.33. Expected X-ray diffraction patterns for the different types of structural arrangements in clay/bitumen systems. 114

Fig. 2.34. Influence of the degree of intercalation/exfoliation on the evolution of complex shear modulus with shear in a bitumen/clay system. 116

Fig. 2.35. Types of LAOS behaviour: (a) strain thinning; (b) strain hardening; (c) weak strain overshoot; and (d) strong strain overshoot (G'_0 and G''_0 are the moduli in the linear region, and γ_0 is the amplitude at which the moduli begin to deviate). 121

Fig. 2.36. Schematic diagram of representing the types of LAOS behaviour as a function of both the creation rate parameter "a", and the loss rate parameter "b". 122

Fig. 2.37. Illustration of the LAOS behaviour type V for (a) effective storage modulus G', and (b) effective loss modulus G''. 126

Fig. 2.38. Schematic of the anti-aging mechanism in an OMMT modified bitumen. 129

MATERIALS AND METHODS

Fig. 3.1. (a) Structure of natural montmorillonite; and (b) Chemical structure of the Cation of dimethyl, dihydrogenated tallow quaternary ammonium chloride. 156

Fig. 3.2. Structural formula of polymeric MDI (n = 1, 2, 3, etc.) 157

Fig. 3.3. J.P. SELECTA recirculating oil bath with DIGITERM 200 digital immersion thermostat. 158

Fig. 3.4. IKA RW20 Stirrer and a 50 mm four-bladed impeller. 158

Fig. 3.5. Ultraturrax™ T25 digital high shear mixer and dispersing accessory. 159

Fig. 3.6. Penetration test device. 164

Fig. 3.7. Equipment for R&B softening point measurement. 165

Fig. 3.8. (a) TLC-FID Iatroscan MK-6 anaalyzer; and (b) General pattern for a chromatogram showing SARAs fractions of bitumen. 166

Fig. 3.9. Jasco FT/IR-4200 spectrometer. 168

Fig. 3.10. (a) Illustration of the AFM working principle; and (b) MultiMode^{TM} AFM, connected to a Nanoscope IV scanning probe microscope controller. 169

Fig. 3.11. Illustration of the phase lag δ between the set signal (excitation) and the tip response due to sample-tip interaction. 170

Fig. 3.12. Scattering of an X-ray beam by planes of atoms in a clay crystal lattice. 172

Fig. 3.13. Bruker D8 Advance X-ray diffractometer. 173

Fig. 3.14. Olympus BX51 microscope. 174

Fig. 3.15. TA Q-100 modulated differential scanning calorimeter. 176

Fig. 3.16. TA Q-50 Thermogravimetric analyser 177

Fig. 3.17. Physica MCR-301 rheometer. 178

Fig. 3.18. Rheostress RS-150 rheometer. 179

RESULTS AND DISCUSSION

Block 1

Fig. 1. Viscous flow curves, at 60 ºC, for neat bitumen, MDI-modified bitumens and bitumen/C20A composite. Their corresponding blanks are also included. 198

Fig. 2. Modification indexes at 0.01 and 0.1 s^{-1} for MDI-modified bitumens, and for bitumen/C20A and bitumen/C20A/MDI composites. 199

Fig. 3. Temperature sweep tests in oscillatory shear, at 10 rad/s, for neat bitumen, MDI-modified bitumens, and bitumen/C20A composite. Blank after 24 h curing is also included. 201

Fig. 4. Viscous flow curves, at 60 ºC, for neat bitumen, and for bitumen/C20A and bitumen/C20A/MDI composites. Blanks after 1 and 24 h curing are also included. 203

Fig. 5. Temperature sweep tests in oscillatory shear, at 10 rad/s, for neat bitumen, and for bitumen/C20A and bitumen/C20A/MDI composites. Blank for high shear blending, followed by 24 h curing, is also included. 204

Fig. 6. XRD intensity profiles for pure C20A and neat bitumen, and for bitumen/C20A and bitumen/C20A/MDI composites. 207

Fig. 7. AFM micrographs (20 x 20 µm2), at 25 ºC: (A) neat bitumen; (B) bitumen/C20A composite; (C) 24h-cured bitumen/C20A/MDI composite. 209

Fig. 8. FTIR spectra focused on –NCO (polymeric MDI), –CO (urethane/urea) and >NH (urethane/urea) bands for neat bitumen and MDI-modified binders, after 1 and 24 h curing. 211

Fig. 9. FTIR spectra for pure C20A and MDI-modified C20A. 213

Block 2

Fig. 1. (a) Evolution of the complex modulus with temperature, and (b) evolution of the loss tangent with temperature, at 10 rad/s, for neat bitumen, and for bitumen/C20A and bitumen/C20A/MDI composites. Blank for high shear blending, followed by 24h stirring, is also included. 232

Fig. 2. Frequency sweep tests, at 10 rad/s, in the temperature range from 30 ºC to 75 ºC, with a step size of 15 ºC between data series, for (a) neat bitumen; and from 30 ºC to 150 ºC, with a step size of 30 ºC between data series, for (b) bitumen/C20A, and (c) 24h-bitumen/C20A/MDI composites. 234

Fig 3. Black diagrams, at 10 rad/s, with a step size of 15 ºC between data series, for (a) neat bitumen, within the range of temperature from 30 ºC to 75 ºC; (b) bitumen/C20A composite, from 30 ºC to 150 ºC; and (c), (d) bitumen/C20A/MDI composites, from 30 ºC to 150 ºC. 236

Fig. 4. Stress sweep tests, at 1 rad/s, for (a) bitumen/C20A composite, at 30 and 150 ºC; and (b) bitumen/C20A/MDI composites at several temperatures between 30 and 150 ºC. 239

Fig. 5. Temperature sweep tests for bitumen/C20A composites: (a) dynamic oscillatory shear testing protocol within the linear viscoelastic range, with an intermediate isothermal stage at 150 ºC for 24 h; and (b) temperature sweep patterns after shear processing at 150 ºC for 24 h (diamonds), and after the isothermal small-amplitude-oscillatory-shear (ISAOS) stage (circles). Arrows point out the temperature ramp applied on each test. 243

Fig. 6. Temperature sweep tests for bitumen/C20A/MDI composites: (a) dynamic oscillatory shear testing protocol within the linear viscoelastic range, with an intermediate isothermal stage at 150 ºC for 24 h; and (b) temperature sweep patterns after shear processing at 150 ºC for 24 h (diamonds), and after the isothermal small-amplitude-oscillatory-shear (ISAOS) stage (circles). Arrows point out the temperature ramp applied on each test. 245

Fig. 7. Isothermal small-amplitude-oscillatory-shear (ISAOS) test at 150 ºC for 24 h, for bitumen/C20A and bitumen/C20A/MDI composites. 246

Fig. 8. (a) Typical pattern and thermal events for the non-reversing heat flow of the systems studied. (b) Enthalpy values of the non-reversing heat flow thermal events for neat bitumen, and for bitumen/C20A and bitumen/C20A/MDI composites. 248

Fig. 9. (a) Characteristic pattern for the derivative of the heat capacity versus temperature for the systems studied, displaying the peaks corresponding to the different T_g's found. (b) T_g values for neat bitumen, and for bitumen/C20A and bitumen/C20A/MDI composites in the range of temperature from –60 ºC to 150 ºC. 251

Fig. 10. Bitumen SARAs fractions for neat bitumen, and for bitumen/C20A and bitumen/C20A/MDI composites. Data for the corresponding blanks are also included. 253

Block 3

Fig. 1. Temperature sweeps, at 10rad/s, for neat bitumen, bitumen/C20A pre-dispersion, and bitumen/C20A composites. Blank for 24h-bitumen/C20A composite is also included. Transient sweep test, at 10 s^{-1} and 150 ºC, for bitumen/C20A composite is portrayed in inset graph. 274

Fig. 2. Temperature sweep tests, at 10 rad/s, for A) neat bitumen and bitumen/C20A/MDI composites; and B) neat bitumen and bitumen/MDI/C20A composites. Blank for 24h stirring is also included. 276

Fig. 3. XRD intensity profiles for neat bitumen, pure C20A and bitumen/C20A pre-dispersion and composites. 280

Fig. 4. X-Ray diffractograms for A) bitumen/C20A and bitumen/C20A/MDI composites; and B) bitumen/MDI/C20A composites. Neat bitumen and pure C20A intensity profiles are also included for reference. 281

Fig. 5. Interlayer spacing at the (001) basal reflection for pure C20A, bitumen/C20A pre-dispersion and composites, and bitumen/C20A/MDI and bitumen/MDI/C20A composites. 282

Fig. 6. Optical microscopy images, at 25 ºC, of A) neat bitumen; B) bitumen/C20A pre-dispersion; C) bitumen/C20A composite; D) 1h-bitumen/C20A/MDI composite; E) 24h-bitumen/C20A/MDI composite; F) 1h-bitumen/MDI/C20A composite; and G) 24h-bitumen/MDI/C20A composite. 284

Fig. 7. AFM micrographs (window sizes of 20 x 20 μm^2 and 5 x 5 μm^2), at 25 ºC, corresponding to: (N) neat bitumen; (A1) and (A2) bitumen/C20A composite; (B1) and (B2) 1h-bitumen/C20A composite; and (C1) and (C2) 24h-bitumen/C20A composite. 286

Fig. 8. AFM micrographs (window sizes of 20 x 20 μm^2 and 5 x 5 μm^2), at 25 ºC, for (N) neat bitumen; (D1) and (D2) bitumen/C20A composite; (E1) and (E2) 24h-bitumen/C20A/MDI composite; (F1) and (F2) 24h-bitumen/MDI/C20A composite. 289